Effects of Stromal Cell-derived Factor-1 and its Peptide Analog on Cord Blood Hematopoietic Stem Cell Trafficking and Homing

LEUNG, Kam Tong

A Thesis Submitted in Partial Fulfillment

of the Requirements for the Degree of

Doctor of Philosophy

in

Medical Sciences

The Chinese University of Hong Kong

July 2010

ProQuest LLC.
789 East Eisenhower Parkway
P.O. Box 1346
Ann Arbor, MI 48106 - 1346

Thesis Committee

Professor Francis Ka Leung CHAN (Chair)

Professor Karen Kwai Har LI (Thesis Supervisor)

Professor Pak Cheung NG (Committee Member)

Professor Andy Peng XIANG (External Examiner)

Abstract of thesis entitled:

Effects of Stromal Cell-derived Factor-1 and its Peptide Analog on Cord Blood Hematopoietic Stem Cell Trafficking and Homing

Submitted by LEUNG Kam Tong

for the degree of Doctor of Philosophy in Medical Sciences

at The Chinese University of Hong Kong in July 2010

Homing of hematopoietic stem cells (HSC) to their bone marrow (BM) niches is crucial to clinical stem cell transplantation. However, the molecular mechanism controlling this process remains not fully understood. In this study, we aimed to explore novel regulators of HSC homing through investigating downstream signals and effector molecules of the stromal cell-derived factor-1 (SDF-1)/CXCR4 axis. We further characterized specific functions of targeted regulators by *in vitro* and *in vivo* migration/homing assays on human cord blood (CB) $CD34^+$ hematopoietic stem/progenitor cells.

We first investigated the effects of SDF-1 and its analog, CTCE-0214 (a small cyclized peptide analog of the SDF-1 terminal regions), on homing-related properties

(chemotaxis, transwell migration, adhesion and actin polymerization) of CB $CD34^+$ cells. Our results demonstrated that both SDF-1 and CTCE-0214 induced a robust actin polymerization response and improved adhesion of $CD34^+$ cells to fibronectin. Unlike SDF-1, CTCE-0214 did not induce a chemotactic response when added to the lower chamber of the transwell system. Addition of CTCE-0214 to the upper chamber significantly improved migration of $CD34^+$ cells to a SDF-1 gradient, but there was no preferential enhancement in the migration of specific colony-forming unit (CFU) progenitors or the more primitive $CD34^+CD38^{-/lo}$ subpopulation. Pre-exposure of $CD34^+$ cells to CTCE-0214 for 4 hours promoted cell migration, whereas SDF-1 pretreatment retarded migration. To dissect the molecular mechanisms leading to the observed functional differences mediated by SDF-1 and CTCE-0214, we investigated whether the two compounds differentially regulated the expression of several known regulators of HSC migration. Flow cytometric analysis revealed that the cell surface expression of CD26, CD44, CD49d, CD49e and CD164 was not changed by either compounds. Exposure to SDF-1, but not CTCE-0214, decreased membrane expression of CXCR4 on $CD34^+$ cells. Addition of CTCE-0214 to the upper chamber inhibited the SDF-1-induced CXCR4 downregulation in both migrated and non-migrated cell population in the transwell setting. Notably, SDF-1 and CTCE-0214 had an opposite effect on the expression level of regulator of

G-protein signaling 13 (RGS13), a negative regulator of chemokine-induced responses. Treatment of $CD34^+$ with SDF-1 for 4 hours resulted in a significant increase in RGS13 expression, whereas CTCE-0214 induced a time-dependent decrease in RGS13 expression. Our results provide the first evidence that SDF-1 and CTCE-0214 differentially regulate migration of $CD34^+$ cells, and we speculate that this might be attributed to their differential regulation of CXCR4 and RGS13 expression.

To investigate the transcriptional regulation provided by the SDF-1/CXCR4 axis, we performed the first differential transcriptome profiling of human CB $CD34^+$ cells in response to a short-term exposure of SDF-1, and identified a panel of genes with putative homing functions. We demonstrated that CD9, a member of the tetraspanin family proteins, was expressed in $CD34^+CD38^{-/lo}$ and $CD34^+CD38^+$ cells. CD9 levels were enhanced by SDF-1, which simultaneously downregulated CXCR4 membrane expression. Using specific inhibitors and activators, we demonstrated that CD9 expressions were modulated via the CXCR4, G-protein, PKC, PLC, ERK and JAK2 signals. Pretreatment of $CD34^+$ cells with anti-CD9 mAb ALB6 significantly inhibited SDF-1-mediated transendothelial migration and calcium mobilization, whereas adhesion to fibronectin and endothelial cells were enhanced. Infusion of

$CD34^+$ cells pretreated with ALB6 significantly impaired their homing to bone marrow and spleen of sublethally irradiated NOD/SCID mice. There also appeared a preferential homing/retaining of untreated $CD34^+CD9^+$ cells to these niches. Our results indicate that CD9, as a downstream member of SDF-1/CXCR4 signals might possess specific and important functions in HSC homing.

In summary, we have provided the first transcriptome profile of CB $CD34^+$ cells downstream of the SDF-1/CXCR4 axis. We also reported the first evidence that HSC homing was regulated by the tetraspanin CD9. By comparing the homing-related responses of $CD34^+$ to SDF-1 and CTCE-0214, we identified RGS13 as another potential regulator of HSC homing. It is anticipated that strategies for modulating the expressions and functions of CD9 and RGS13 might improve HSC homing to their hematopoietic niches.

中文摘要

基質細胞衍生因子-1 及其肽類似物對臍血造血幹細胞歸巢和販運的影響

造血幹細胞(HSC)歸巢到骨髓(BM)中造血微環境的龕位是臨床幹細胞移植上一個重要的過程。然而，控制這過程的分子機制仍然未完全被理解。我們希望透過研究基質細胞衍生因子-1(SDF-1)/CXCR4 軸的下游信號和效應分子，從而發掘出新的 HSC 歸巢調節者。我們利用人類臍血(CB)的 $CD34^+$造血幹 /祖細胞遷移/歸巢的體外和體內實驗，進一步了解當中調節者的具體功用和特點。

CTCE-0214 是 SDF-1 終端位的小環化肽類似物，我們首先研究 SDF-1 及 CTCE-0214 對臍血 $CD34^+$細胞歸巢相關屬性的影響，當中包括趨化、微孔隔離小室(Transwell)遷移、黏附和肌動蛋白聚合的能力研究。研究結果顯示，$CD34^+$細胞分別在 SDF-1 和 CTCE-0214 影響下引發強大的肌動蛋白聚合反應，而對其纖維連接蛋白的黏附力亦同樣被提升；然而，當將 CTCE-0214 與 SDF-1 分別加在 transwell 系統的下室時，細胞只會在加入 SDF-1 的環境下引起趨化反應，而在 CTCE-0214 的情況下則沒有此反應。另一方面，將 CTCE-0214 加入 transwell 系統的上室顯著改善了 $CD34^+$細胞向 SDF-1 濃度梯度的遷移，但沒有增加特定一種集落形成單位(CFU)的祖/更原始的 $CD34^+CD38^{-/lo}$ 亞群細胞的遷移。將

$CD34^+$細胞預先暴露於 CTCE-0214 四小時會促進其遷移，然而 SDF-1 則會妨礙其遷移。我們研究 SDF-1 和 CTCE-0214 是否不同地影響著某幾個已知的 HSC 遷移調節者而導致功能差異。流式細胞儀分析顯示，SDF-1 和 CTCE- 0214 沒有改變細胞表面的 CD26、CD44、CD49d、CD49e 或 CD164 表達。$CD34^+$細胞膜上的 CXCR4 表達會因爲暴露在 SDF-1 而降低，但 CTCE-0214 則沒有影響。在 transwell 系統中，無論遷移或非遷移群，其細胞膜上的 CXCR4 下調都會在 CTCE-0214 加進系統上室後而被抑制。值得注意的是，SDF-1 和 CTCE-0214 在調節 G 蛋白信號 13(RGS13；一個趨化因子引起反應的負調節者)的表達水平有著相反的作用。$CD34^+$的 RGS13 表達因爲暴露於 SDF-1 四小時後而顯著增加，而其表達則隨著暴露於 CTCE-0214 的時間增加而減少。研究結果首次提供證據證明 SDF-1 和 CTCE-0214 能用不同的機制去調節 $CD34^+$細胞的遷移，我們推測這可能是由於它們在調控 CXCR4 和 RGS13 表達上的差別。

我們進行了首次人類臍血 $CD34^+$細胞的轉錄譜分析，透過將細胞短時間暴露在 SDF-1 中，去探討及分析細胞在 SDF-1/CXCR4 軸下的轉錄調控，並發現了一系列與歸巢功能有關的基因。我們證明了 $CD34^+CD38^{-/lo}$ 和 $CD34^+CD38^+$ 細胞均表達 CD9 (四旋蛋白的家庭成員之一)。SDF-1 提高了 CD9 的水平，同時降低了細胞表面 CXCR4 的表達。我們使用特定的抑製劑和激活劑，發現了 CD9 的表達須要透過 CXCR4，G-蛋白，PKC, PLC，ERK 和 JAK2 的信號。用 CD9 單抗

ALB6 預先處理過的 $CD34^+$細胞在通過血管內皮細胞遷移和鈣活動的能力都明顯減少，而其黏附於纖維連接蛋白和血管內皮細胞的能力則增強。經亞致死劑量照射的 NOD/SCID 小鼠在輸注 ALB6 預先處理過的 $CD34^+$細胞後，其細胞歸巢到骨髓和脾臟的能力被大幅削弱。此外，未經處理的 $CD34^+CD9^+$細胞會傾向歸巢至/保留他們的龕位。我們的研究結果顯示，作爲 SDF-1/CXCR4 信號下游成員的 CD9，可能於 HSC 歸巢上發揮著重要的功能。

總括而言，我們提供了第一個臍血 $CD34^+$細胞在 SDF-1/CXCR4 軸下游的轉錄譜。我們還報導了第一個證據證明 HSC 的歸巢是受四旋蛋白 CD9 調節。通過比較 $CD34^+$細胞對 SDF-1 和 CTCE-0214 在歸巢反應，我們發現 RGS13 有可能是一個 HSC 的歸巢的調節者。根據研究結果，我們可以透過調控 CD9 和 RGS13 的表達和功能，從而改善 HSC 歸巢至其龕位的能力。

Acknowledgements

I would like to deliver my heartful thanks with gratitude to my supervisor, Professor Karen Li for her continuous teachings, guidance and support throughout the study over the past three years. Her inspirational advice on experimental design, data analysis, and preparation of thesis, manuscript and presentations has been very precious. Without her support, it would have been impossible to write up this thesis.

I would also like to make sincere appreciations for Professor Pak-Cheung Ng for his support on my project.

Heartful gratitude is expressed to Dr. Kathy Chan and Dr. Kent Tsang, for their expertise advice on research design and thesis writing.

I would like to thank every member of the cord blood collection team, including Dr. Kathy Chan, Dr. Joanna Ho, Ruby Chiu, Hanna Fong, Fiona Leung, Yolanda Chu, Laura Ng, Eve Choi, Carmen Chuen, Goldie Gu and Michelle Lum. Without their efforts, every single experiment would not have been done.

I appreciate Dr. King-Yiu Lee, Benny Fong and Carmen Chuen for their assistance in

cell culture and fluorescence imaging, Ruby Chiu and Carrie Kong for NOD/SCID mice experiments, Dr. Kathy Chan, Hanna Fong, Eve Choi, and Carol Szeto for the microarray study, Dr. Joanna Ho, Henry Pong and Raymond Wong for flow cytometry.

Additional thanks must go to colleagues and friends, including Venus Liu, Siu-To Ma, Fung and Victor for their help and support during my course of work.

Last but not least, I would also like to express my deepest gratitude to my beloved parents, my wife Apple Yeung and my lovely daughter Kola Leung, for their patience, everlasting love and unfailing support.

Publications

Refereed journal:

Leung KT, Chan KYY, Ng PC, Lau TZ, Chiu RWM, Tsang KS, Li CK and Li K. The tetraspanin CD9 regulates migration, adhesion and homing of human cord blood $CD34^+$ hematopoietic stem/progenitor cells. (Submitted to *Blood* for publication)

Abstract presented in conferences:

Leung KT, Chan KYY, Lee KY, Lau TK, Tsang KS, Law P, Wong D and Li K. Differential effects of stromal cell-derived factor-1 (SDF-1) and its peptide analog (CTCE-0214) on homing-related responses and gene expression profile of human cord blood $CD34^+$ hematopoietic stem/progenitor cells. *Seventh Annual Meeting of the International Society of Stem Cell Research*. 8 July 2009, Barcelona, Spain.

List of Abbreviations

7-AAD	7-amino-actinomycin D
ANXA3	annexin A3
APC	allophycocyanin
BFU/CFU-E	burst-forming unit/colony-forming unit-erythroid
BM	bone marrow
BSA	bovine serum albumin
CB	cord blood
CFSE	5-(6)-carboxyfluorescein diacetate succinimidyl ester
CFU	colony-forming unit
CFU-GEMM	colony-forming unit-granulocyte, erythroid, macrophage, megakaryocyte
CFU-GM	colony-forming unit-granulocyte macrophage
CKLF	chemokine-like factor
CMTM2	CKLF-like MARVEL transmembrane domain containing 2
DAPI	4',6-diamidino-2-phenylindole
DIXDC1	DIX containing domain 1
DUSP6	dual specificity phosphatase 6
ECM	extracellular matrix
EMP1	epithelial membrane protein 1
EPHA4	EPH receptor A4
ERK	extracellular signal-regulated kinase
FCS	fetal calf serum
FITC	fluorescein isothiocyanate
FL	Flt-3 ligand

FMLP	formyl-methionyl-leucyl-phenylalanine
GAPDH	glyceraldehyde 3-phosphate dehydrogenase
GCOS	GeneChip Operating Software
G-CSF	granulocyte colony-stimulating factor
GDP	guanosine diphosphate
GO	gene ontogeny
GRK	G-protein coupled receptor kinase
GTP	guanosine triphosphate
GTPase	guanosine triphosphatase
GVHD	graft-versus-host disease
Gα	G-protein α subunit
HLA	human leukocyte antigen
HPC	hematopoietic progenitor cell
HSC	hematopoietic stem cell
HUVEC	human umbilical vein endothelial cell
ICAM-1	intercellular vascular adhesion molecule-1
IDB	ingenol 3,20-dibenzoate
IL-6	interleukin-6
IL-8	interleukin-8
IL-16	interleukin-16
IMDM	Iscove's Modified Dulbecco's medium
ITGAX	integrin alpha X
ITGB1	integrin beta 1
ITGB5	integin beta 5
ITPR3	Inositol 1,4,5-triphosphate receptor, type 3

JAK2	Janus kinase 2
LEL	large extracellular loop
LFA-1	lymphocyte function associated antigen-1
LMNA	lamin A/C
LTC-IC	long-term culture initiating cell
mAb	monoclonal antibodies
MCP-1	monocyte chemoattractant protein-1
ME1	malic enzyme 1, NADP (+) - dependent, cytosolic
MEK	MAP kinase kinase
MEZ	mezerein
MFI	mean fluorescence intensity
MIIA	myosin heavy chain IIA
MMP-2	matrix metalloproteinase-2
MMP-9	matrix metalloproteinase-9
MNC	mononuclear cells
MPB	mobilized peripheral blood
MT-MMP	membrane type-MMP
MYO10	myosin X
NOD/SCID	non-obese diabetic/severe combined immunodeficient
PBS	phosphate buffered saline
PC-PLC	phosphatidylcholine-specific phospholipase C
PE	phycoerythrin
PerCP-Cy5.5	peridin chlorophyll protein-cyanin 5.5
p-ERK	phosphorylated ERK
PI3K	phosphatidylinositol 3-kinase

PI-PLC	phosphatidylinositol-specific phospholipase C
PKC	protein kinase C
PLC	phospholipase C
PMA	phorbol 12-myristate 13-acetate
PSGL-1	P-selectin glycoprotein ligand-1
RGS1	regulator of G-protein signaling 1
RGS2	regulator of G-protein signaling 2
RGS3	regulator of G-protein signaling 3
RGS4	regulator of G-protein signaling 4
RGS5	regulator of G-protein signaling 5
RGS8	regulator of G-protein signaling 8
RGS13	regulator of G-protein signaling 13
RGS16	regulator of G-protein signaling 16
RGS18	regulator of G-protein signaling 18
RGS21	regulator of G-protein signaling 21
RIN	RNA integrity number
SCF	stem cell factor
SDF-1	stromal cell-derived factor-1
ST6GALNAC3	ST6 (alpha-N-acetyl-neuraminyl- 2,3-beta-galactosyl-1,3)-N-acetylgalactosaminide alpha-2,6-sialytransferase 3
SYNJ2	synaptojanin 2
TEM	tetraspanin-enriched microdomain
TNC	total nucleated cells
TNF-α	tumor necrosis factor-α
TPO	thrombopoietin

UTP	uridine triphosphate
VCAM-1	vascular cellular adhesion molecule-1
VLA-4	very late activation antigen-4
VLA-5	very late activation antigen-5

List of Tables

Table 1.1 CD9-regulated homing-related functions…… …25

Table 1.2 A list of CD9-associated molecules…….....27

Table 1.3 R4 RGS proteins-regulated homing-related functions……. 30

Table 3.1 Taqman assays used for detection of R4 RGS subfamily members……...…. 51

Table 3.2 RNA quality of the 4 CB cases used in microarray experiments……....52

Table 3.3 Taqman Gene Expression Assays used in validation experiments……53

Table 5.1 GO categories significantly modulated by SDF-1…….....96

Table 5.2 SDF-modulated genes associated with cell motility…….....100

Table 5.3 SDF-modulated genes associated with cell adhesion……...102

Table 5.4 SDF-modulated genes associated with actin cytoskeleton organization and biogenesis……..104

Table 5.5 SDF-modulated genes associated with small GTPase mediated signal transduction……105

Table 5.6 Expression data of 19 selected target genes in microarray and qPCR experiments……..……..106

List of Figures

Figure 1.1 Structural features of CD9……..…..31

Figure 1.2 Classification of mammalian RGS proteins……..…32

Figure 3.1 Purity of enriched CB $CD34^+$ cells……..……..54

Figure 3.2 Colonies derived from CB $CD34^+$ cells…….55

Figure 4.1 Amino acid sequences of SDF-1 and CTCE-0214……72

Figure 4.2 Effects of SDF-1 and CTCE-0214 on migration of *ex vivo* expanded cells……..……...…73

Figure 4.3 Effects of SDF-1 and CTCE-0214 on transwell migration of freshly isolated CB $CD34^+$ cells…….74

Figure 4.4 Lineage analysis of the migrated $CD34^+$ cells……76

Figure 4.5 Effects of SDF-1 and CTCE-0214 on actin polymerization and adhesion of CB $CD34^+$ cells…….…...…77

Figure 4.6 Effects of SDF-1 and CTCE-0214 on CXCR4 expression of freshly isolated $CD34^+$ cells……..….79

Figure 4.7 Effects of SDF-1 and CTCE-0214 on CXCR4 expression of *ex vivo* expanded cells……81

Figure 4.8 CXCR4 expression in non-migrated and migrated $CD34^+$ cells…...82

Figure 4.9 Effects of SDF-1 and CTCE-0214 on expression of several known regulators of HSC homing……..83

Figure 4.10 Basal mRNA expression of R4 RGS subfamily members…….84

Figure 4.11 Effects of SDF-1 and CTCE-0214 on mRNA expression of R4 RGS subfamily members……...85

Figure 4.12 Protein expression of RGS13 on CB CD34$^+$ cells……...…86

Figure 4.13 Proposed mechanisms of the differential effect of SDF-1 and CTCE-0214 on migration of CD34$^+$ cells…….…..…..87

Figure 5.1 Workflow of microarray data analysis……108

Figure 5.2 Hierarchical clustering analysis……..……109

Figure 5.3 Functional classification of the SDF-1-modulated genes……110

Figure 5.4 qPCR validation of the microarray data……...111

Figure 6.1 Basal CD9 and CXCR4 membrane expression on subpopulations of CB CD34$^+$ cells…….…....126

Figure 6.2 Cell surface expressions of CD9 and CXCR4 on CB CD34$^+$ cells and their subpopulations in response to SDF-1……...127

Figure 6.3 Kinetics of SDF-1-regulated CD9 and CXCR4 expressions……...128

Figure 6.4 Effects of specific inhibitors of selected signal transducers on SDF-1-modulated CD9 and CXCR4 membrane expressions…129

Figure 6.5 Effects of SDF-1 on Akt and ERK activation……...…...130

Figure 6.6 Effects of specific inhibitors of selected signal transducers on SDF-1-induced ERK activation…….……131

Figure 6.7 Effects of PKC activators on membrane expression of CD9 and CXCR4……..…..……..132

Figure 6.8 Effects of the anti-CD9 antibody, ALB6, on membrane expression of CD9 and CXCR4…….……133

Figure 6.9 Effects of ALB6 on migration of CB CD34$^+$ cells……...……..134

Figure 6.10 Effects of ALB6 on actin polymerization, calcium flux and

Akt activation……..……..……..135

Figure 6.11 Effects of ALB6 on adhesion of CB $CD34^+$ cells to fibronectin……...……137

Figure 6.12 Effects of ALB6 on adhesion of CB $CD34^+$ cells to HUVEC……138

Figure 6.13 Effects of ALB6 on homing of CB $CD34^+$ cells in NOD/SCID mice…..……....139

Figure 6.14 Comparison of CD9 expression on injected with homed $CD34^+$ cells……..……...…....140

Figure 6.15 Proposed signaling pathways of SDF-1-induced CD9 expression in CB $CD34^+$ cells…….....141

Table of Contents

	Page
Abstract (English)	**i**
(Chinese)	**v**
Acknowledgements	**viii**
Publications	**x**
List of Abbreviations	**xi**
List of Tables	**xvi**
List of Figures	**xvii**
Table of Contents	**xx**

CHAPTER ONE: Introduction..... 1

1.1 Hematopoietic stem cells..... 1
1.1.1 Properties..... 1
1.1.2 Functions and sources..... 2
1.2 Cord blood transplantation..... 2
1.3 Strategies to improve cord blood transplantation..... 4
1.3.1 *Ex vivo* expansion..... 4
1.3.2 Double cord blood transplantation..... 6
1.3.3 Intraosseous transplantation..... 7
1.3.4 Enhancing homing/engrafting capability by small molecules..... 7
1.4 Hematopoietic stem cell homing..... 8
1.4.1 Processes involved in HSC homing..... 8
1.4.2 *In vitro* and *in vivo* models of HSC homing..... 9
1.4.3 HSC homing efficiency..... 10
1.4.4 Molecular mediators of HSC homing..... 12
1.4.4.1 SDF-1/CXCR4 axis..... 12
1.4.4.2 Adhesion molecules..... 14
1.4.4.3 Proteolytic enzymes..... 16
1.5 CD9..... 17
1.5.1 Structure and expression..... 17
1.5.2 Roles in homing-related functions..... 18
1.5.3 Mechanisms of action..... 20
1.5.4 Known functions in hematopoietic stem/progenitor cells..... 21

1.6 R4 RGS proteins.....21
1.6.1 Structure and expression.....21
1.6.2 Roles in homing-related functions.....22
1.6.3 Mechanisms of action.....23
1.6.4 Known functions in hematopoietic stem/progenitor cells.....24

CHAPTER TWO: Objectives.....33

CHAPTER THREE: Materials and Methods.....34

3.1 Homing-related responses of cord blood $CD34^+$ cells to SDF-1 and CTCE-0214.....34
3.1.1 Cord blood collection.....34
3.1.2 Enrichment of cord blood $CD34^+$ cells.....34
3.1.3 *Ex vivo* expansion.....35
3.1.4 Flow cytometry.....36
3.1.5 Immunofluorescence microscopy.....37
3.1.6 Migration assay.....38
3.1.7 Clonogenic colony-forming unit assay.....39
3.1.8 Actin polymerization assay.....39
3.1.9 Adhesion assay.....40
3.1.10 Quantitative polymerase chain reaction (qPCR).....40
3.1.11 Statistics.....42
3.2 Transcriptional responses of cord blood $CD34^+$ cells to SDF-1.....42
3.2.1 RNA quality assessment.....42
3.2.2 Expression profiling.....43
3.2.3 Microarray data analysis.....44
3.2.4 Validation of target genes.....45
3.3 Homing functions of CD9 in cord blood $CD34^+$ cells.....45
3.3.1 Characterization of CD9 and CXCR4 membrane expression.....45
3.3.2 Quantitative polymerase chain reaction (qPCR).....46
3.3.3 Detection of phosphorylated ERK and Akt.....46
3.3.4 Migration assay.....47
3.3.5 Adhesion assay.....47
3.3.6 Calcium flux assay.....48
3.3.7 Actin polymerization assay.....49
3.3.8 *In vivo* homing assay.....49

CHAPTER FOUR: Effects of Stromal Cell-derived Factor-1 (SDF-1) and its Peptide Analog on Homing-related Responses of Human Cord Blood CD34$^+$ Hematopoietic Stem/progenitorCells..... .56

4.1 Background and objectives.....56
4.2 Results.....58
4.2.1 CTCE-0214 enhances the migratory responses of *ex vivo* expanded cells.....58
4.2.2 Differential effects of SDF-1 and CTCE-0214 on migration of freshly isolated cord blood CD34$^+$ cells.....59
4.2.3 Effects of SDF-1 and CTCE-0214 on actin polymerization and adhesion of CD34$^+$ cells.....61
4.2.4 SDF-1 and CTCE-0214 differentially regulates CXCR4 expression.....62
4.2.5 Differential effects of SDF-1 and CTCE-0214 on the expression of regulator of G-protein signaling 13.....64
4.3 Discussion.....66

CHAPTER FIVE: Expression Profiling of Human Cord Blood CD34$^+$ Hematopoietic Stem/progenitor Cells in Response to SDF-1.....88

5.1 Background and objectives.....88
5.2 Results.....90
5.2.1 Effects of SDF-1 on the transcriptome of CB CD34$^+$ cells.....90
5.2.2 Functional annotation of the SDF-1 modulated genes.....90
5.2.3 Quantitative PCR validation of selected SDF-1 modulated genes.....92
5.3 Discussion.....93

CHAPTER SIX: Role of the Tetraspanin CD9 in Homing of Human Cord Blood CD34$^+$ Hematopoietic Stem/progenitorCells.....113

6.1 Background and objectives.....113
6.2 Results.....114
6.2.1 CD9 is expressed in cord blood CD34+ cells and is regulated by SDF-1 via specific signaling pathways.....114
6.2.2 Anti-CD9 antibody alters migratory and adhesive functions of cord blood CD34$^+$ cells.....117
6.2.3 CD9 neutralization impairs homing of transplanted CD34$^+$ cells in NOD/SCID mice.....119
6.3 Discussion.....121

CHAPTER SEVEN: General Discussion and Conclusion.....142

References.....146

CHAPTER ONE

Introduction

1.1 Hematopoietic stem cells

1.1.1 Properties

Hematopoietic stem cells (HSC) have the ability to self-renew and differentiate into all types of blood cells for sustaining lifelong hematopoiesis. They can undergo asymmetric cell division to produce two distinct daughter cells, one remains as a HSC with long-term self-renewal capacity and the other becomes a hematopoietic progenitor cell (HPC) which eventually gives rise to terminally differentiated blood cells of different lineages (Martinez-Agosto *et al.*, 2007).

Using long-term culture initiating cell (LTC-IC) assay, human HSC was originally identified by expression of CD34 and CD90 (Baum *et al.*, 1992; Craig *et al.*, 1993). By evaluating the long-term hematopoietic potential in the non-obese diabetic/severe combined immunodeficient (NOD/SCID) mice, human HSC was subsequently found to reside in the $CD34^{+}CD38^{-}$ cell population (Bhatia *et al.*, 1997), and was recently refined in the $CD34^{+}CD38^{-}CD90^{+}CD45RA^{-}$ population (Majeti *et al.*, 2007).

1.1.2 Functions and sources

HSC have been used in clinical transplantation for curative treatment of a large variety of malignant and non-malignant diseases. For malignant diseases, including leukemia, lymphoma, multiple myeloma, neuroblastoma and ovarian cancer, myeloablative effects mediated by high dose chemotherapy or irradiation can be rescued through autologous or allogeneic HSC transplantation. Non-maliganant diseases, including severe combined immunodeficiency, aplastic anemia and Wiskott-Aldrich syndrome, can also be corrected by allogeneic HSC transplantation through BM reconstitution (Laughlin *et al*., 2004).

HSC from bone marrow (BM), cytokine-mobilized peripheral blood (MPB) and umbilical cord blood (CB) are currently used in clinical transplantation. These HSC sources exhibit different reconstitution kinetics and immunogenic effects following transplantation. For example, MPB transplantation resulted in a more rapid hematopoietic reconstitution but increased the incidence of chronic graft-versus-host disease (GVHD) (Copelan, 2006).

1.2 Cord blood transplantation

The first CB transplantation was performed in a patient with Fanconi's anemia

(Gluckman *et al.*, 1989). Today, more than 20,000 CB transplantations have been performed worldwide and ~450,000 CB units are stored in CB banks (Rocha and Broxmeyer, 2010). In comparison with other sources of HSC, CB transplantation offer several advantages. Collection of CB is risk-free to the donor and there is a lower chance of latent viral transmission. CB transplantation is associated with lower incidence and severity of acute and chronic GVHD, partly due to the lower number of activated T cells (Rocha *et al.*, 2000; Rocha *et al.*, 2004). Moreover, due to the tolerance of 1-2 human leukocyte antigen (HLA) mismatch between donor and recipient, more than 95% of the patients can find at least one 4-6/6 HLA-matched CB unit for transplantation (Gluckman, 2009).

CB transplantation is associated with some adverse outcomes, including increased risk of graft failure, delayed engraftment and delayed immune resconstitution, when compared to transplantation using BM or MPB stem cells (Rocha *et al.*, 2001, Rocha *et al.*, 2004; Komanduri *et al.*, 2007). The median time to neutrophil and platelet recovery in CB recipients (25 and 59 days) is much slower than patients who receive BM (19 and 27 days) (Tse *et al.*, 2008). This results in prolonged neutropenia and thrombocytopenia, which are the primary causes of infection-related mortality during the aplastic period (Saavedra *et al.*, 2002). A number of factors, including low cell

dose, immaturity of stem cells, lack of facilitating cells and homing inefficiency, have been suggested to explain these undesirable incidences of CB transplantation (Broxmeyer, 2010). In particular, cell dose has been clearly identified as a limiting factor for successful CB transplantation. In a study on 550 patients, Gluckman and Rocha (2004) reported that the cumulative incidence of 100-day transplant-related mortality was significantly dependent on the cell dose (72% of those transplanted with $< 1 \times 10^7$ nucleated cells versus 24% with $> 4 \times 10^7$ cells). Thus, CB transplantation is mostly performed on patients with low body weight, and the current recommended cell dose is $\geq 3 \times 10^7$ nucleated cells or $\geq 2 \times 10^5$ $CD34^+$ cells per kilogram body weight of the recipient for providing engraftment and survival advantage (Gluckman *et al*., 2009).

1.3 Strategies to improve cord blood transplantation

In order to overcome the unfavorable outcomes of CB transplantation, several strategies have been proposed and investigated in both preclinical and clinical settings, in which the underlying principles are either to increase the cell dose or to enhance the homing/engrafting capacity of HSC.

1.3.1 *Ex vivo* expansion

Efforts to increase the CB cell dose have been attempted through *ex vivo* expansion using early-acting hematopoietic cytokines, e.g. thrombopoietin (TPO), stem cell factor (SCF), Flt-3 ligand (FL) and interleukin-6 (IL-6) or in combination with stromal cell support (Ohmizono *et al.*, 1997; Köhler *et al.*, 1999). Although transplantation of *ex vivo* expanded cells has been demonstrated to be feasible and safe in a number of clinical trials, the kinetics of neutrophil and platelet engraftment were not accelerated (Sphall *et al.*, 2002; Jaroscak *et al.*, 2003). Moreover, there has been evidence showing that exposure to cytokines generated an expanded population of committed HPC at the expense of self-renewable HSC (Bhatia *et al.*, 1997; McNiece *et al.*, 2002), and compromised their homing capacity (Guenechea *et al.*, 1999; Ahmed *et al.*, 2004).

To ensure applicability of the *ex vivo* expansion technology, it is critical that the quantity of expanded progenitor cells is sufficient to reduce the time to engraftment, in a condition that self-renewable HSC are maintained (if not expanded), and homing and engraftment capacity of these cells are uncompromised. As the molecular pathways controlling HSC proliferation and maintenance are increasingly understood, a number of novel factors, including the copper chelator tetraehtylenepentamine (Peled *et al.*, 2004), the Notch ligand Delta1 (Delaney *et al.*, 2005), the histone

deacetylase inhibitor trichostatin A (Araki *et al.*, 2006) and angiopoietin-like proteins (Zhang *et al.*, 2006), have been developed to expand the early, self-renewable HSC. Of which, a recent clinical phase I trial showed that infusion of CB progenitors *ex vivo* expanded by the Notch ligand Delta 1 together with a unmanipulated CB unit significantly shortened the time to neutrophil recovery in leukemia patients (median 16 days), when compared to a concurrent cohort of patients transplanted with two unmanipulated CB units (median 26 days). However, the expanded CB unit did not display long-term engraftment capacity (Delaney *et al.*, 2010).

1.3.2 Double cord blood transplantation

Infusion of two CB units represents another strategy to increase cell dose. In both myeloablative (Barker *et al.*, 2005) and reduced-intensity conditioning settings (Ballen *et al.*, 2007), double CB transplantation resulted in higher engraftment rate in adult patients with hematological malignancy, when compared to single CB transplantation. Verneris *et al.* (2009) further showed that the relapse rate was lower and the leukemia-free survival rate was higher in patients transplanted with two CB units. However, double CB transplantation was associated with higher risk of grade II-IV acute GVHD (MacMillan *et al.*, 2009). Interestingly, only one of the two CB units will contribute to hematopoiesis at day 100 post-transplantation (Barker *et al.*,

2005; Ballen *et al.*, 2007). Gutman *et al.* (2010) recently showed that single-unit dominance was coincided with a specific $CD8^+$ T cell response against the non-engrafting unit.

1.3.3 Intraosseous transplantation

It has been proposed that transplantation efficiency could be improved through direct intrabone injection of CB cells as a result of enhanced homing/engrafting capacity. In NOD/SCID mice, intrabone injection of CB mononuclear cells resulted in engraftment 10-times greater than those injected intravenously (Castello *et al.*, 2004). The same group recently conducted a phase I/II clinical trial to evaluate the safety and efficacy of intrabone CB transplantation in acute leukemia patients. Direct infusion of CB cells in the iliac crest resulted in faster platelet recovery (median 36 days) and reduced incidence of grade III-IV acute GVHD (Frassoni *et al.*, 2008).

1.3.4 Enhancing homing/engrafting capability by small molecules

Ex vivo treatment of HSC with agents that possess homing-enhancing activity represents another means to improve CB transplantation. Christopherson *et al.* (2004) showed that a 15-minute exposure of murine $Lineage^-Sca\text{-}1^+$ HSC to a small peptide inhibitor of CD26, diprotin A, enhanced BM homing, engraftment and survival in

lethally irradiated recipient mice. The same treatment was subsequently demonstrated to enhance long-term engraftment of human CB $CD34^+$ cells in NOD/SCID/$\beta 2m^{null}$ mice by more than 5-fold (Christopherson *et al.*, 2007). It was demonstrated that homing of human $CD34^+$ cells in NOD/SCID mice can also be enhanced through short exposure (0.5-24 hours) to the immunosuppressive drug FTY720 (Kimura *et al.*, 2004), the nucleotide uridine triphosphate (UTP) (Rossi *et al.*, 2007), and prostaglandin E2 (Hoggatt *et al.*, 2009). Notably, a phase I clinical trial has been initiated to evaluate the effects of prostaglandin E2 on CB transplantation in leukemia patients who are ineligible for myeloablative treatment.

1.4 Hematopoietic stem cell homing

1.4.1 Processes involved in HSC homing

Homing refers to the process in which HSC in the circulation actively migrate across the blood/BM endothelium barrier and retain at least transiently within the BM compartment (Lapidot *et al.*, 2005). This multistep process starts with rolling of transplanted HSC on the BM sinusoidal endothelium, which is mediated through interaction of P-selectin glycoprotein ligand-1 (PSGL-1) with endothelial selectins (Katayama *et al.*, 2003). At the same time, stromal cell derived factor-1 (SDF-1) released or presented by the endothelial cells activates integrins on rolling HSC.

Binding of activated integrins to endothelial intercellular vascular adhesion molecule-1 (ICAM-1) and vascular cellular adhesion molecule-1 (VCAM-1) induces firm shear resistant adhesion of HSC to the endothelium (Peled *et al.*, 2000). Because the BM extravascular microenvironment contains a higher level of SDF-1, the arrested HSC tranmigrate through the endothelium (extravasation) and extracellular matrix (ECM) along the SDF-1 gradient, and finally reside in the endosteal niche (Chute, 2006).

1.4.2 *In vitro* and *in vivo* models of HSC homing

There are several established *in vitro* surrogate assays for studying the processes involved in HSC homing. The motility responses of HSC to chemoattractants are commonly measured in a two-chamber transwell system, in which the porous filters are either uncoated, or coated with ECM proteins or endothelial cell monolayers (Aiuti *et al.*, 1997; Möhle *et al.*, 1997). Voermans *et al.* (2001b) showed a positive correlation between *in vitro* migratory response $CD34^+$ cells to SDF-1 and the rate of neutrophil and platelet recovery in patients transplanted with autologous MPB. Interactions of HSC with ECM proteins, endothelial cells or BM stromal cells are analyzed by adhesion assays under static or shear flow conditions (Teixidó *et al.*, 1992; Peled *et al.*, 2000). Two early cellular responses to chemokines, actin

polymerization (Voermans *et al*., 2001a) and calcium flux (Aiuti *et al*., 1999), are commonly evaluated using specific F-actin (phalloidin) and calcium (Fluo-3/4) dyes.

In vivo homing of human HSC is mainly studied in immunodeficient NOD/SCID or NOD/SCID/β2m^{null} mice. These mice lack functional B, T cells (NOD/SCID) and NK cells (NOD/SCID/β2m^{null}), and are able to support multilineage human hematopoiesis (both myeloid and lymphoid) after preconditioning with sublethal total body irradiation (Lapidot *et al*., 1992; Shultz *et al*., 1995, Angelopoulou *et al*., 2004). In both mice strains, homing of transplanted human CB CD34^{+} cells can be detected, albeit at low frequency, in the BM as early as 2 hours after infusion (Kollet *et al*., 2000). Notably, it was demonstrated that engraftment of human CD34^{+} cells in NOD/SCID and NOD/SCID/β2m^{null} mice correlated with the rate of platelet recovery after autologous MPB transplantation (Angelopoulou *et al*., 2004).

1.4.3 HSC homing efficiency

There has been controversy regarding the efficiency of HSC homing. Single cell transplant of Rhodamine^{lo}lineage^{-}Sca-1^{+}c-kit^{+} (Benveniste *et al*., 2003) or side population^{-}lineage^{-}Sca-1^{+}c-kit^{+} murine HSC (Matsuzaki *et al*., 2004) revealed a high engraftment efficiency (> 90%) of murine HSC in BM of lethally irradiated

recipients. However, van der Loo and Ploemacher (1995) demonstrated that only 18-20% of the intravenously transplanted murine HSC subset (cobblestone-area forming cells) homed to the recipient BM 16-18 hours after infusion. Cashman and Eaves (2000) also demonstrated that only 7% of the transplanted human CB HSC subset (competitive repopulation unit) homed to the BM of sublethally irradiated NOD/SCID mice 24 hours after transplantation. Intravenously transplanted $CD34^+$ cells can be detected in different organs, including spleen, lung and liver of NOD/SCID mice shortly (within 16 hours) after infusion (Kollet *et al.*, 2003), and this could be one of the reasons of low BM homing efficiency. Although it remains unclear whether HSC home at absolute efficiency, attempts to improve HSC homing in preclinical and clinical settings have already been under investigations (Section 1.3.3 and 1.3.4).

The homing efficiency of HSC is also affected by the presence of accessory cells. It was demonstrated that the addition of $CD8^+$ but not $CD4^+$ T cells augmented CB $CD34^+$ cell migration and homing to BM of NOD/SCID/$\beta 2m^{null}$ mice (Adams *et al.*, 2003). Byk *et al.* (2005) showed that cycling CB $CD34^+CD38^+$ progenitor cells enhanced migration, homing and engraftment of $CD34^+38^-$ HSC in the NOD/SCID mice model.

1.4.4 Molecular mediators of HSC homing

1.4.4.1 SDF-1/CXCR4 axis

The SDF-1/CXCR4 axis plays essential roles in regulation of HSC migration, homing and engraftment (Lapidot and Kollet, 2002). SDF-1, also known as CXCL12, is a chemokine produced by multiple cell types in the BM stroma including osteoblasts, endothelial cells and adipocytes (Nagasawa *et al.*, 1994; Imai *et al.*, 1999), while CXCR4, a G-protein coupled receptor of SDF-1, is highly expressed on HSC and their progenies. Mice lacking SDF-1 or CXCR4 exhibited embryonic lethality, and were severely defective in HSC migration from fetal livers to BM during development. As a result, these mice failed to establish BM myelopoiesis and B-lymphopoiesis (Nagasawa *et al.*, 1996; Ma *et al.*, 1998; Zou *et al.*, 1998). *In vitro*, SDF-1 induced chemotactic or transendothelial migration (Aiuti *et al.*, 1997), adhesion to ECM proteins under static or shear stress conditions (Peled *et al.*, 2000), actin polymerization (Voermans *et al.*, 2001a) and calcium flux (Aiuti *et al.*, 1997) in human $CD34^+$ cells. Pretreatment of $CD34^+$ cells with a high dose of SDF-1 (10 μg/mL) or neutralizing monoclonal antibodies (mAb) against CXCR4, inhibited their BM homing and engraftment in NOD/SCID mice (Peled *et al.*, 1999; Kollet *et al.*, 2001). On the contrary, disruption of the SDF-1/CXCR4 interactions by injection of

granulocyte colony-stimulating factor (G-CSF) or the pharmacological inhibitor of CXCR4, AMD3100, induced massive mobilization of murine and human HSC from BM to peripheral blood (Lévesque *et al*., 2003; Broxmeyer *et al*., 2005).

Binding of SDF-1 to CXCR4 activates several intracellular signal transducers including G-protein, extracellular signal-regulated kinase (ERK), Janus kinase 2 (JAK2), phosphatidylinositol 3-kinase (PI3K), phospholipase C (PLC) and protein kinase C (PKC) (Ganju *et al*., 1998; Majka *et al*., 2000; Wang *et al*., 2000; Zhang *et al*., 2001; Petit *et al*., 2005). Some of them are required for SDF/CXCR4-mediated migration, homing and engraftment of human $CD34^+$ cells. Blocking G-protein α subunit (Gα) function by pertussis toxin in $CD34^+$ cells inhibited *in vitro* migration to a SDF-1 gradient but not homing in NOD/SCID mice (Kollet *et al*., 2001). A broad-range PKC inhibitor, chelerythrine chloride, also impaired SDF-1-mediated migration and BM engraftment (Petit *et al*., 2005). Giebel *et al*. (2004) showed that SDF-1-induced migration of human $CD133^+$ cells was dependent on PI3K/Akt but not ERK pathway, while Zhang *et al*. (2001) reported that migration of BM $CD34^+$ cells was a JAK2-dependent process.

The transcriptional responses of HSC to SDF-1 and the functional consequences of

such alterations are largely unknown. In human MPB and BM $CD34^+$ cells, SDF-1 transcriptionally upregulated matrix metalloproteinase-2 and -9 (MMP-2 and MMP-9) and promoted trans-matrigel migration in a MMP2/9-dependent manner (Janowska-Wieczorek *et al*., 2000). Using Affymetrix U133A microarray, Rossi *et al*. (2007) recently showed that SDF-1 upregulated a large number of genes in MPB $CD34^+$ cells that are involved in regulation of cell motility, adhesion and cytoskeleton organization. However, these SDF-1-modulated genes have not been validated in functional homing assays.

1.4.4.2 Adhesion molecules

Interaction of transplanted HSC with the BM endothelium (rolling and tight adhesion) and the subsequent transendothelial migration are regulated by adhesion molecules (Lapidot *et al*., 2005). It was demonstrated that rolling of HSC on BM endothelium is mediated through interaction of P-selectin glycoprotein ligand-1 (PSGL-1) with endothelial E- and P-selectins. In lethally irradiated mice, BM homing of transplanted PSGL-$1^{-/-}$ HSC or homing of wild-type HSC to E-$selectin^{-/-}$ mice BM was greatly impaired (Katayama *et al*., 2003). Moreover, Xia *et al*. (2004) showed that human CB $CD34^+$ cells expressed a non-functional form of PSGL-1. Correction by fucosylation of PSGL-1 augmented rolling of CB $CD34^+$ cells on selectins and

enhanced engraftment in NOD/SCID mice.

Several integrins were shown to mediate tight adhesion of HSC to endothelium and transendothelial migration. Human $CD34^+$ cells expressed high levels of very late activation antigen-4 (VLA-4, CD49d/CD29, α4β1 integrin), very late activation antigen-5 (VLA-5, CD49e/CD29, α5β1 integrin) and lymphocyte function associated antigen-1 (LFA-1, CD11a/CD18, αLβ2 integrin) (Peled *et al.*, 2000). Using neutralizing mAbs to these integrins, Kollet *et al.* (2001) showed that homing of $CD34^+$ cells in NOD/SCID mice was dependent on VLA-4, VLA-5 and LFA-1. However, in vitro transendothelial migration to a SDF-1 gradient was dependent on VLA-4 and LFA-1, but not VLA-5 (Peled *et al.*, 2000). Under shear stress, the SDF-1-induced tight adhesion of $CD34^+$ cells to immobilized ICAM-1 or VCAM-1 was mediated by VLA-4, VLA-5 and LFA-1 (Peled *et al.*, 2000).

HSC homing and engraftment is also regulated by the adhesion receptor CD44. In NOD/SCID mice, homing was blocked by preincubation of $CD34^+$ cells with anti-CD44 mAbs or the CD44 ligand hyaluronic acid (Avigdor *et al.*, 2004). In addition, hyaluronic acid was found to be expressed on human BM sinusoidal endothelium and endosteum (the HSC niche), suggesting a role for CD44 and

hyaluronic acid in HSC interaction with endothelial cells and retention in the endosteal niche.

1.4.4.3 Proteolytic enzymes

HSC homing requires degradation of extracellular matrix, which is largely depended on the activity of several matrix metalloproteinase (MMP) (Lapidot *et al*, 2005). Based on the substrate specificity and cellular localization, MMP are grouped into gelatinase, collagenase and membrane type-MMP (MT-MMP) (Page-McCaw *et al*., 2007). Janowska-Wieczorek *et al*. (2000) showed that soluble MMP-2 (gelatinase A) and MMP-9 (gelatinase B) were secreted by human $CD34^+$ cells, and increased levels of both MMP were detected upon stimulation with SDF-1. Migration of $CD34^+$ cells across Matrigel (a mixture of ECM proteins including laminin, collagen, gelatin and heparin sulfate proteoglycans) to a SDF-1 gradient were significantly inhibited by MMP inhibitors or antibodies (Janowska-Wieczorek *et al*., 2000). *In vivo*, intraperitoneal injection of MMP-2/9 inhibitor significantly suppressed homing of $CD34^+$ cells to injured liver of NOD/SCID mice (Kollet *et al*., 2003). Recently, Vagima *et al*. (2009) showed that human MPB $CD34^+$ cells expressed cell surface MT1-MMP (a collagenase), and their transMatrigel migration and BM homing in NOD/SCID mice were impaired by anti-MT-1 MMP antibody or siRNA. They also

observed a significant reduction in homing and engraftment of murine MT1-MMP$^{-/-}$ c-kit^{+} HSC (Vagima *et al*., 2009).

Proteolytic enzymes also negatively regulate HSC migration and homing. Christopherson *et al*. (2002) showed that CD26, a membrane-bound peptidase that cleaves the N-terminus and inactivates SDF-1, was expressed on a subset of CB CD34^{+} cells. Pretreatment of CB CD34^{+} cells or murine lineage^{-}Sca^{+} HSC with a CD26 inhibitor, diprotin A, enhanced their migration to a SDF-1 gradient (Christopherson *et al*., 2002), BM homing (Christopherson *et al*., 2004) and engraftment in NOD/SCID mice (Christopherson *et al*., 2007).

1.5 CD9

1.5.1 Structure and expression

CD9 is a 24-kDa protein of the tetraspanin superfamily (also known as transmembrane 4 superfamily or TM4SF) with four transmembrane domains, two extracellular loops (SEL and LEL) and a short intracellular loop. The large extracellular loop (LEL) can be subdivided into a constant region a variable region. The constant region contains the α-helices A, B and E, which may be required for CD9 homodimerization. The variable region contains the conserved, signature CCG

motif and harbors docking sites for protein-protein interaction (Figure 1.1) (Hemler, 2005).

CD9 was originally identified on pre-B acute lymphoblastic leukemia cells (Kersey *et al*., 1981), and was subsequently found to have a wide tissue distribution (Maecker, 1997). In the hematological system, CD9 is expressed on pre-B cells, platelets, monocytes, eosinophils, basophils and activated T cells, but not on neutrophils and erythrocytes (Horejsí and Vlcek, 1991).

1.5.2 Roles in homing-related functions

CD9 regulates various physiological processes including cell motility, adhesion, sperm-egg fusion and neurite formation (Hemler, 2003; Hemler, 2005). Table 1.1 summarizes the reported evidence of CD9 in regulation of homing-related functions (cell motility and adhesion) in normal and cancer cells.

The regulatory role of CD9 in cell motility is complex. In several types of tumors, including melanoma (Si and Hersey, 1993), bladder (Mhawech *et al*., 2003), breast (Miyake *et al*., 1995), colon (Mori *et al*., 1998), lung (Adachi *et al*., 1998), prostate (Wang *et al*., 2007) and cervical cancer (Sauer *et al*., 2003), CD9 downregulation

correlates with tumor progression and metastasis. Moreover, overexpression of CD9 in lung adenocacinoma, Burkitt's lymphoma and myeloma cell lines resulted in suppression of cell motility (Ikeyama *et al*., 1993). Likewise, treatment of dendritic cells with CD9 monoclonal antibody increased their chemotactic migration (Mantegazza *et al*., 2004). These data suggest that CD9 might regulate cell motility in a negative manner. However, the converse phenomenon was also evident in recent studies. Interfering CD9 functions by monoclonal antibodies, siRNA or LEL peptides suppressed migration of mast cells (Qi *et al*., 2006), peripheral blood lymphocytes (Barreiro *et al*., 2005), melanoma (Longo *et al*., 2001) and myeloma cell lines (De Bruyne *et al*., 2006). Moreover, although the overall expression level of CD9 is downregulated in some metastatic tumors, strong CD9 expression was found in contact sites between tumor cells and endothelium, where it promoted transendothelial invasion (Longo *et al*., 2001; Sauer *et al*., Clin Cancer Res, 2003; De Bruyne *et al*., 2006). Thus, CD9 cannot be strictly classified as a motility enhancer or suppressor.

The regulation of cell adhesion by CD9 appears to be more straightforward. Pretreatment of colon carcinoma (Ovalle *et al*., 2007), melanoma (Longo *et al*., 2001) or pre-B ALL cell lines (Masellis-Smith and Shaw, 1994) with CD9 monoclonal

antibodies enhanced their adhesion to fibronectin, endothelial or BM stromal cells, suggesting that CD9 is a negative regulator of cellular adhesion.

1.5.3 Mechanisms of action

Like other tetraspanins, CD9 has the ability to interact with a variety of transmembrane and cytosolic proteins, forming membrane structures known as tetraspanin-enriched microdomains (TEM) (Hemler, 2005). The major CD9-associating partners, as identified by immunoprecipitation or proteomic approaches, are integrins and members of the immunoglobulin superfamily (Table 1.2). Some of the CD9-associating molecules, including β1 integrin, MT1-MMP and CD26, are known to play crucial roles in HSC motility and homing (Table 1.2). Within the TEM, CD9 is capable of modulating the functions of its associating molecules. For example, it has been demonstrated that the association of CD9 with β1 integrins in CHO cells potentiated integrin activation, thereby enhancing cell migration to fibronectin (Kotha *et al.*, 2008). Moreover, CD9 protected MT1-MMP from lysosomal degradation and supported its delivery to cell surface, thus increasing the invasiveness of MCF-7 cells (Lafleur *et al.*, 2009).

In general, tetraspanins do not serve as cell surface receptors (Hemler, 2008).

However, it has been recently shown that interleukin-16 (IL-16) bound to CD9 and elicited chemotactic response in human mast cells (Qi *et al.*, 2006). Moreover, IL-16 can synergize with early acting cytokines to expand CB $CD34^+$ cells and enhanced their chemotactic migration to SDF-1 (Rofani *et al.*, 2009). These data suggest that CD9-dependent biological processes can be mediated through classical ligand-receptor interaction.

1.5.4 Known functions in hematopoietic stem/progenitor cells

Clay *et al.* (2001) reported that CD9 was expressed on nearly all human BM-derived $CD34^+$ cells, and the addition of CD9 monoclonal antibody suppressed megakaryocytic differentiation in liquid culture. The presence of CD9 monoclonal antibody in long-term culture of murine BM cells also inhibited myeloid cell production (Oritani *et al.*, 1996). However, there has been no evidence on the role of CD9 in regulating homing-related functions of primary $CD34^+$ cells.

1.6 R4 RGS proteins

1.6.1 Structure and expression

Regulator of G-protein signaling (RGS) family proteins are molecular switch of the G-protein coupled receptor-mediated signal transduction. At present, 38 mammalian

RGS proteins have been identified and they can be classified into 9 subfamilies based on amino acid sequence homology (Figure 1.2) (Bansal *et al.*, 2007). All RGS proteins contain the signature RGS domain, which mediates direct interaction with G-proteins. Members of the R4 subfamily (RGS1-5, 8, 13, 16, 18 and 21) are the smallest RGS proteins (~20 to 24 kDa), containing only the RGS domain flanked by a short α-helix (Ross *et al.*, 2000).

Most R4 RGS members have a broad tissue distribution. However, expression of RGS1 and RGS13 are restricted in blood cells. RGS1 is expressed on B cells, T cells, natural killer cells, dentritic cells and monocytes, while RGS13 is expressed on B cells and mast cells (Bansal *et al.*, 2007).

1.6.2 Roles in homing-related functions

Several R4 RGS subfamily members have been shown to regulate chemokine-induced lymphocyte migration and SDF-1/CXCR4 signaling (Table 1.3).

Moratz *et al.* (2004) showed that B cells from *Rgs1* knockout mice migrated more efficiently to the chemokines SDF-1 and CXCL13, when compared to wild-type B cells. Subsequently, enhanced homing of B cells into lymphoid tissues was also

evident in *Rgs1*$^{-/-}$ mice (Han *et al.*, 2005). Likewise, shRNA knockdown of RGS1 in a human B lymphoma cell line enhanced *in vitro* migration to SDF-1 and CXCL13 (Han *et al.*, 2006). Bowman *et al.* (1998) showed that overexpression of RGS3 or RGS4 in a pre-B cell line suppressed its migration to interleukin-8 (IL-8) and monocyte chemoattractant protein-1 (MCP-1), and inhibited the formyl-methionyl-leucyl-phenylalanine (FMLP)-induced adhesion to VCAM-1 (Bowman *et al.*, 1999). Knockdown of RGS13 enhanced migration of a B lymphoma cell line (Han *et al.*, 2006) and a mast cell line (Bansal *et al.*, 2008b) to SDF-1. Although there has been no evidence for a role of RGS16 in cell migration, overexpression of RGS16 in a megakaryocytic cell line suppressed SDF-1-induced Akt and ERK activation (Berthebaud *et al.*, 2005). These studies collectively suggest that RGS proteins act as negative regulators of chemokine-mediated responses.

1.6.3 Mechanisms of action

G-protein-coupled receptors elicit signal transduction through heterotrimeric G-proteins and downstream effectors. Ligand binding induces conformational change and enhances the guanine-nucleotide exchange activity of the receptor. The activated receptor catalyzes the exchange of guanosine triphosphate (GTP) for guanosine diphosphate (GDP) on the Gα subunit, which leads to the dissociation of Gα subunit

from the Gβγ dimer and the engagement of specific effectors (adenylyl cyclase and phospholipase C) for transmitting signal (Gilman, 1987). RGS proteins bind and accelerate the intrinsic guanosine triphosphatase (GTPase) activity of the Gα subunit, and return the GTP-bound Gα subunit to GDP-bound state. This leads to the reassembly of the G-protein subunits and termination of signaling (De Vries *et al*., 2000).

1.6.4 Known functions in hematopoietic stem/progenitor cells

Yowe *et al*. (2001) reported that human $CD34^+$ cells derived from BM, CB and MPB expressed RGS1, 2, 16 and 18. However, the functions of RGS proteins in primary hematopoietic stem/progenitor cells have not been explored.

Table 1.1 CD9-regulated homing-related functions

Functions	Cell types	Evidence	Phenotypes after manipulations	References
Cell motility	Human CB-derived mast cells, murine BM-derived mast cells	CD9 mAb (ML-13), CD9 siRNA	↓ migration to IL-16	Qi *et al*., 2006
	Human monocyte-derived dentritic cells	CD9 mAb (ML-13)	↑ migration to MIP-1α and MIP-5	Mantegazza *et al*., 2004
	Human umbilical vein endothelial cells	CD9 siRNA, CD9 LEL peptides	↓ transendothelial migration of human peripheral blood lymphocytes to SDF-1	Barreiro *et al*., 2005
	Human lung adenocarcinoma cell line (MAC10), human Burkitt's lymphoma cell line (Raji), human myeloma cell line (ARH77)	CD9 overexpression	↓ spontaneous migration	Ikeyama *et al*., 1993
	Human melanoma cell line (A375)	CD9 mAb (VJ1/10, VJ1/20	↓ spontaneous transendothelial migration	Longo *et al*., 2001
	Human myeloma cell line (MM5.1), murine myeloma cell line (5T33MMvv)	CD9 mAb (ALB6, KMC8)	↓ transendothelial invasion through Matrigel	De Bruyne *et al*., 2006
	Human pre-B ALL cell lines (NALM-6, LAZ221)	CD9 mAb	↓ migration to enkephalins	Heagy *et al*., 1995

Table 1.1 CD9-regulated homing-related functions - *Continued*

Functions	Cell types	Evidence	Phenotypes after manipulations	References
Cell motility	Hamster ovary cell line (CHO-K1)	CD9 overexpression	↑ migration to fibronectin	Kotha *et al*., 2008
	Murine macrophage cell line (RAW264.7)	CD9 mAb (KMC8)	↓ migration to 10% FCS	Takeda *et al*., 2008
Cell adhesion	Human colon carcinoma cell line (BCS-TC2.2, Colo320, HT29)	CD9 mAb (VJ1/20, PAINS-13)	↑ adhesion to fibronectin and laminin	Ovalle *et al*., 2007
	Human melanoma cell line (A375)	CD9 mAb (VJ1/10, VJ1/20	↑ adhesion to human umbilical vein endothelial cells	Longo *et al*., 2001
	Human pre-B ALL cell lines (NALM-6, HOON)	CD9 mAb (50H.19, ALB6)	↑ adhesion to BM stromal fibroblasts	Masellis-Smith and Shaw, 1994
	Hamster ovary cell line (CHO)	CD9 overexpression	↓ adhesion to fibronectin	Cook *et al*., 2002

Table 1.2 A list of CD9-associated molecules

CD9-associating molecules	References	Role of CD9-associating molecules in homing-related functions of hematopoietic stem/progenitor cells	References
α1 integrin	Berditchevski, 2001; Boucheix and Rubinstein, 2001		
α2 integrin	Berditchevski, 2001; Boucheix and Rubinstein, 2001		
α3 integrin	Berditchevski, 2001; Boucheix and Rubinstein, 2001		
α4 integrin	Berditchevski, 2001; Boucheix and Rubinstein, 2001	Yes	Peled *et al*., 2000
α5 integrin	Berditchevski, 2001; Boucheix and Rubinstein, 2001	Yes	Peled *et al*., 2000
α6 integrin	Berditchevski, 2001; Boucheix and Rubinstein, 2001		
α7 integrin	Berditchevski, 2001; Boucheix and Rubinstein, 2001		
β1 integrin	Berditchevski, 2001; Boucheix and Rubinstein, 2001	Yes	Peled *et al*., 2000
ADAM10	Le Naour *et al*., 2006		

Table 1.2 A list of CD9-asscociated molecules - *Continued*

CD9-associating molecules	References	Role of CD9-associating molecules in homing-related functions of hematopoietic stem/progenitor cells	References
CD2	Tarrant *et al*., 2003		
CD3	Tarrant *et al*., 2003		
CD5	Tarrant *et al*., 2003		
CD26	Le Naour *et al*., 2006	Yes	Christopherson *et al*., 2002; Chrisropherson *et al*., 2004
CD36	Miao *et al*., 2001		
CD38	Zilber *et al*., 2005		
CD41	Boucheix and Rubinstein, 2001		
CD42	Boucheix and Rubinstein, 2001		
CD44	Le Naour *et al*., 2006	Yes	Avigdor *et al*., 2004
CD46	Le Naour *et al*., 2006		
CD47	Boucheix and Rubinstein, 2001		
CD92	Le Naour *et al*., 2006		
CD239	Le Naour *et al*., 2006		
CD318	Le Naour *et al*., 2006		
c-Kit	Anzai *et al*., 2002		
Claudin-1	Kovalenko *et al*., 2007		

Table 1.2 A list of CD9-asscociated molecules - *Continued*

CD9-associating molecules	References	Role of CD9-associating molecules in homing-related functions of hematopoietic stem/progenitor cells	References
EWI-2	Tarrant *et al*., 2003		
EWI-F	Boucheix and Rubinstein, 2001		
GPCR56	Little *et al*., 2004		
ICAM-1	Barreiro *et al*., 2008		
IgM	Le Naour *et al*., 2004		
MT1-MMP	Yañez-Mó *et al*., 2008	Yes	Vagima *et al*., 2009
Syndecan	Boucheix and Rubinstein, 2001		
TGFα	Shi *et al*., 2000		

Table 1.3 R4 RGS proteins-regulated homing-related functions

R4 RGS members	Cell types	Evidence	Phenotypes after manipulations	References
RGS1	Murine B cells	RGS1 knockout mice	↑ migration to SDF-1 and CXCL13	Moratz *et al*., 2004
	Murine B cells	RGS1 knockout mice	↑ homing to lymph node	Han *et al*., 2005
	Human B lymphoma cell line (HS-SultanT13)	RGS1 shRNA	↑ migration to SDF-1 and CXCL13	Han *et al*., 2006
RGS3	Human pre-B cell line (L1-2)	RGS3 overexpression	↓ migration to IL-8 and MCP-1, ↓ FMLP-induced adhesion to VCAM-1	Bowman *et al*., 1998
RGS4	Human pre-B cell line (L1-2)	RGS4 overexpression	↓ migration to IL-8, ↓ FMLP-induced adhesion to VCAM-1	Bowman *et al*., 1998
RGS13	Human germinal center B Lymphocytes	RGS13 overexpression	↓ migration to SDF-1	Shi *et al*., 2002
	Human B lymphoma cell line (HS-SultanT13)	RGS13 shRNA	↑ migration to SDF-1 and CXCL13	Han *et al*, 2006
	Human mast cell line (HMC-1)	RGS13 shRNA	↑ migration to SDF-1, ↑Ca^{2+} response to adenosine, sphingosine-1-phosphate, C5a and SDF-1	Bansal *et al*., 2008b
RGS16	Human megakaryocytic cell line (MO7e)	RGS16 overexpression	↓ SDF-1-induced Akt and ERK phosphorylation	Berthebaud *et al*., 2005

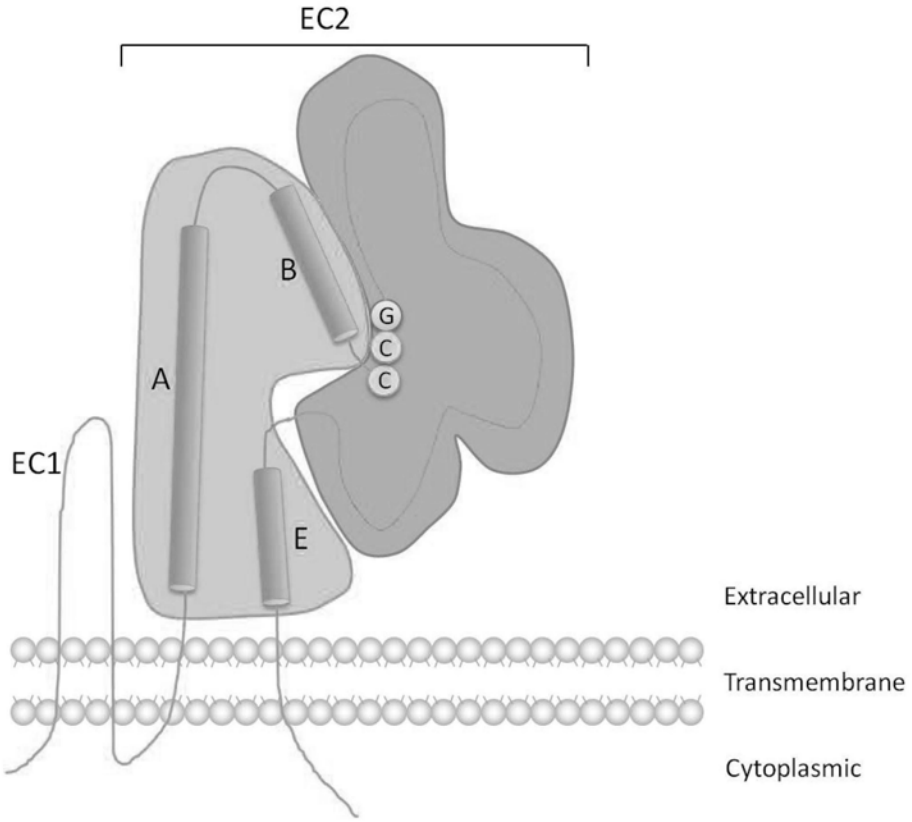

Figure 1.1 Structural features of CD9

CD9 contains 4 transmembrane domains, two extracellular loops (EC1 and EC2) and a short intracellular loop. EC2 is subdivided into a constant region (yellow, containing α-helices A, B and E,) and a variable region (blue, containing the tetraspanin signature CCG motif).

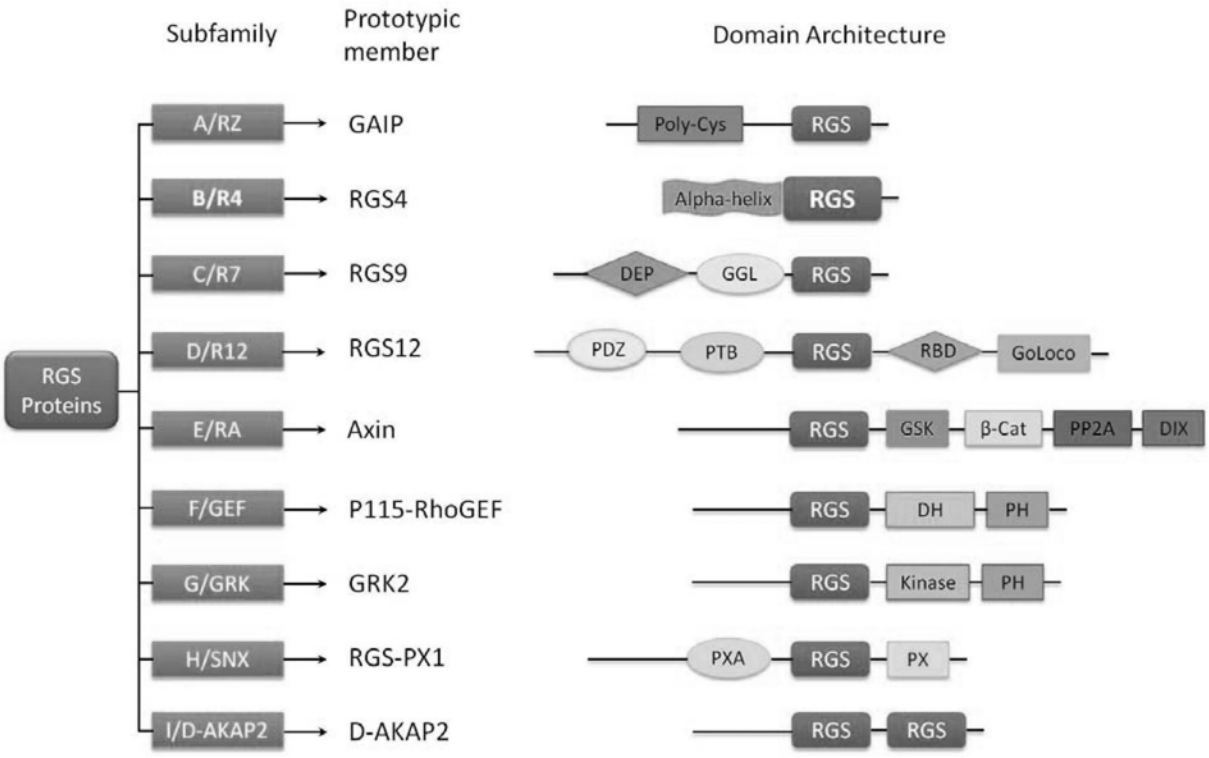

Figure 1.2 Classification of mammalian RGS proteins

Based on the amino acid sequence homology in the RGS domain (red), mammalian RGS proteins can be classified into 9 subfamilies. Members of the R4 subfamily, except for RGS3, are the smallest RGS proteins, containing a single RGS domain flanked by a short α-helix.

CHAPTER TWO

Objectives

The overall objective was to investigate the mechanisms of human CB HSC homing at the SDF-1/CXCR4 axis. The specific aims were as follows:

1. To study the effects and mechanisms of SDF-1 and its analog, CTCE-0214 on homing-related responses of human CB $CD34^+$ cells and expressions of RGS13, a regulator of G protein signal (Chapter 4).

2. By whole genome microarray techniques, to investigate the transcriptional changes of CB $CD34^+$ cells in response to SDF-1, and to identify/validate novel SDF-1-regulated genes with putative homing functions (Chapter 5).

3. To perform functional validation of a selected SDF-1-regulated gene (i.e. CD9) in homing of CB $CD34^+$ cells and its signal pathway downstream of SDF-1/CXCR4 (Chapter 6).

CHAPTER THREE

Materials and Methods

3.1 Homing-related responses of cord blood CD34$^+$ cells to SDF-1 and CTCE-0214

3.1.1 Cord blood collection

Human CB samples were collected from umbilical vein during full-term deliveries with informed written consent, and used in accordance with the procedures approved by the Ethics Committee for Clinical Research of the Chinese University of Hong Kong. The samples were stored in preservative-free heparin (10 IU/mL; Hospira, Victoria, Australia) at room temperature and processed within 24 hours.

3.1.2 Enrichment of cord blood CD34$^+$ cells

CB samples were diluted with equal volume of Iscove's Modified Dulbecco's medium (IMDM), and 30 mL of the diluted samples were layered onto 15 mL of Ficoll-Paque Plus (1.077 g/mL; Amersham Biosicences, Uppsala, Sweden). Low-density mononuclear cells (MNC) were isolated by density gradient centrifugation at 400 *g* for 45 minutes at room temperature without brake. CD34$^+$ cells were enriched using the indirect microbead kit (MiniMACS, Miltenyi Biotech,

Bergisch Gladbach, Germany) according to the manufacturer's instruction. Briefly, CB MNC were incubated in FcR blocking reagent (100 µL/1 × 10^8 cells) and hapten-conjugated CD34 antibody for 15 minutes at 4°C (clone QBEND/10; 100 µL/1 × 10^8 cells), followed by a 15-minute incubation in anti-hapten microbeads (100 µL/1 × 10^8 cells). Cells were washed twice with phosphate buffered saline (PBS; pH 7.2) (Gibco/Invitrogen, Carlsbad, CA) supplemented with 0.5 % human serum albumin (HSA) (Baxter Healthcare, Glendale, CA) and 0.6% acid citrate dextrose (ACD) (Sigma-Aldrich, St Louis, MO), and were allowed to pass through 1-2 MS columns. $CD34^+$ cells were collected by flushing the columns twice with PBS/HSA/ACD. The purity of enriched $CD34^+$ cells, evaluated by flow cytometry (Section 3.1.4), was 93.7% ± 0.5% (range, 84.4%-98.4%; n = 45; Figure 3.1).

3.1.3 *Ex vivo* expansion

Enriched $CD34^+$ cells at 2 × 10^4/mL were cultured in IMDM supplemented with 10% fetal calf serum (FCS) (Stem Cell Technologies, Vancouver, BC, Canada), TPO (50 ng/mL), SCF (50 ng/mL) and FL (80 ng/mL) for 4 days at 37°C in a fully humidified atmosphere containing 5% CO_2. TPO, SCF and FL were purchased from Peprotech (Rocky Hill, NJ). Total nucleated cells (TNC) were enumerated using a hematocytometer, and cell viability was determined by trypan blue (Stem Cell

Technologies) exclusion assay. The fold expansion was calculated by dividing the number of TNC after expansion by the number of cells seeded.

3.1.4 Flow cytometry

To detect the expression of cell surface markers, 1×10^5 enriched $CD34^+$ cells or expanded cells were stained with CD26-fluorescein isothiocyanate (FITC; clone M-A261), CD34-FITC (clone 8G12), CD38-allophycocyanin (APC; clone HB7), CD44-phycoerythrin (PE; clone 515), CD49d-PE (clone 9F10), CD49e-PE (clone IIA1), CD164-FITC (clone N6B6), CXCR4-PE (clone 12G5), and respective isotypic controls monoclonal antibodies (mAb) for 30 minutes at 4°C. All antibodies were purchased from BD Biosciences, San Jose, CA. The cells were then washed and resuspended in PBS (pH 7.4) supplemented with 0.5% bovine serum albumin (BSA) (Sigma-Aldrich), and were acquired using a FACSCalibur flow cytometer (BD Biosciences). At least 10,000 events were acquired for each sample. Data were analyzed by CellQuest (BD Biosciences) or FlowJo software (Tree Star, Ashland, OR).

To detect total RGS13 protein expression, 1×10^5 enriched $CD34^+$ cells were fixed and permeabilized using the Fixation/Permeabilization solution (BD Biosciences),

and incubated with a polyclonal goat anti-human RGS13 primary antibody (4 μg/mL; Santa Cruz Biotechnology, Santa Cruz, CA) in Perm/Wash buffer (BD Biosciences) for 30 minutes at 4°C, followed by staining with a donkey anti-goat IgG-Texas Red secondary antibody (4 μg/mL; Santa Cruz Biotechnology). Cells were then stained with CD34-FITC for 30 minutes at 4°C, washed twice, and analyzed using the FACSCalibur.

3.1.5 Immunofluorescence microscopy

$CD34^+$ cells (1×10^5) were first incubated with 10% goat serum (Zymed/Invitrogen, Carlsbad, CA) for 30 minutes at 4 °C to reduce non-specific antibody binding, and incubated with a monoclonal mouse anti-human CXCR4 primary antibody (4 μg/mL; clone 12G5; BD Biosciences) for 30 minutes at 4°C, followed by staining with a goat anti-mouse IgG2a-Alexa Fluor 555 secondary antibody (5 μg/mL; Molecular Probes, Eugene, OR). Cells were then stained with CD34-FITC for 30 minutes at 4°C, and mounted onto glass slides using the ProLong Gold antifade reagent with 4',6-diamidino-2-phenylindole (DAPI) (Molecular Probes). Images were taken using the Olympus IX71 fluorescence microscope (Melville, NY).

Immunofluorescence staining of total RGS13 was performed as described in Section

3.4, except that cells were incubated with 10% donkey serum for 30 minutes at 4°C (Santa Cruz Biotechnology) prior to addition of primary antibody. Stained cells were mounted onto glass slides using the ProLong Gold antifade reagent with DAPI, and observed using a fluorescence microscope.

3.1.6 Migration assay

Chemotactic migration experiments were performed using transwells (6.5 mm diameter; 5 μm pore; Costar, Corning, NY). Enriched $CD34^+$ cells (1×10^5 in 0.1 mL IMDM with 1% FCS) were seeded in the upper chamber, and 0.6 mL medium containing 1-500 ng/mL of SDF-1 (R&D Systems, Minneapolis, MN) or CTCE-0214 (Chemokine Therapeutics Coporation, Vancouver, BC, Canada) was added to the lower chamber. After 4 hours incubation at 37°C, migrated cells at the lower chamber were enumerated by a hematocytometer. The percentage migration was calculated as follows: (number of migrated cells / input cell number) × 100. In some experiments, CTCE-0214 (1-500 ng/mL) was added to the upper chamber or in combination with SDF-1 to the lower chamber. In pretreatment experiments, freshly isolated $CD34^+$ cells or expanded cells at 2.5×10^5/mL were incubated with SDF-1 (100 ng/mL) or CTCE-0214 (100 ng/mL) for 1, 4 or 24 hours in IMDM supplemented with 20% FCS. Cells were washed twice, and allowed to migrate towards a gradient of SDF-1 (100

ng/mL).

3.1.7 Clonogenic colony-forming unit assay

Migrated $CD34^+$ cells in the lower chamber of the transwell were plated at 1000 cells/mL in 1% methylcellulose (Sigma-Aldrich) cultures supplemented with 30% FCS, 1% BSA, 0.1 mM β-mercaptoethanol (Gibco/Invitrogen), 3 IU/mL erythropoietin (Cilag, Zug, Switzerland), 10 ng/mL granulocyte macrophage-colony stimulating factor, 10 ng/mL interleukin-3 and 50 ng/mL SCF. The cultures were incubated at 37°C for 14 days. Colonies were scored using an inverted microscope with the following criteria. Colonies derived from burst-forming unit/colony-forming unit-erythroid (BFU/CFU-E) contained hemoglobinized erythroblasts (Figure 3.2 A). Colonies derived from colony-forming unit-granulocyte macrophage (CFU-GM) contained translucent granulocytes and macrophages, with no hemoglobinized erythroblast (Figure 3.2 B). Colonies derived from colony-forming unit-granulocyte, erythroid, macrophage, megakaryocyte (CFU-GEMM) contains cells of multiple lineages (Figure 3.2 C).

3.1.8 Actin polymerization assay

$CD34^+$ cells at 1×10^6/mL were either left untreated, or treated with SDF-1 (100

ng/mL) or CTCE-0214 (100 ng/mL) in IMDM with 0.2% BSA at 37°C for 15-120 seconds. Reactions were stopped by adding 3 volumes of Fixation/Permeabilization solution, and washed twice with Perm/Wash buffer. Cells were stained with phalloidin-FITC (0.4 μM; Sigma-Aldrich) for 30 minutes at 37°C, washed, and analyzed by flow cytometry.

3.1.9 Adhesion assay

Non tissue culture-treated 24-well plates (BD Biosciences) were coated overnight with 40 μg/mL fibronectin (Sigma-Aldrich) at 4°C. Non-specific binding sites were blocked by 2.5% BSA for 1 hour at room temperature. $CD34^+$ cells (1×10^5 cells in 200 μL IMDM with 0.1% BSA) were allowed to adhere to fibronectin-coated wells in the absence or presence of SDF-1 (100 ng/mL) or CTCE-0214 (100 ng/mL) for 45 minutes at 37°C. Nonadherent cells were removed by 3 washes with prewarmed PBS. Adherent cells were collected after a 15-minute incubation with Accutase solution (Chemicon, Temecula, CA) at 37°C, and enumerated by a hematocytometer. The percentage adhesion was calculated as follows: (number of adhered cells / input cell number) × 100.

3.1.10 Quantitative polymerase chain reaction (qPCR)

Expression of R4 RGS members at the mRNA level was determined by qPCR. Total RNA was isolated using TRIzol reagent (Invitrogen) and was further purified with the RNeasy Micro Kit (Qiagen, Valencia, CA) according to the manufacturer's instruction. Briefly, 200 µL chloroform was added to 1 mL of sample in TRIzol, followed by centrifugation at 20,800 *g* for 20 minutes at 4°C. The aqueous layer was diluted with 3.5 volumes of absolute ethanol, and loaded to the RNeasy MinElute spin columns (Qiagen). Following centrifugation at 9560 *g* for 15 seconds, the columns were washed twice with buffer RPE (Qiagen) and once with 80% ethanol. RNA was eluted with 15 µL nuclease-free water, and the concentration was measured by a NanoDrop ND-1000 Spectrophotometer (Nanodrop Technologies, Wilmington, DE).

RNA (100-500 ng) was reverse transcribed by using the High Capacity cDNA Reverse Transcription Kit (Applied Biosystems, Foster City, CA) according to the manufacturer's instructions. PCR reactions (45 cycles of denaturation at 95°C for 15 seconds and annealing/extension at 60°C for 1 minute) were performed with Taqman universal PCR master mix and Taqman gene expression assays (Table 3.1) on the ABI Prism 7300 Real Time PCR System (Applied Biosystems), using 1 µL cDNA as the template. The relative expression level of each target gene was calculated by the

comparative C_T method and was normalized to glyceraldehyde 3-phosphate dehydrogenase (GAPDH) expression. No template controls were also included to avoid false positive results.

3.1.11 Statistics

The paired *t* test was used for determination of statistical significance between groups, in which *P* values ≤ .05 were considered significant. All data were expressed as mean ± SEM.

3.2 Transcriptional responses of cord blood $CD34^+$ cells to SDF-1

3.2.1 RNA quality assessment

Highly purified $CD34^+$ cells (> 95% purity, n = 4) were cultured for 4 hours in the absence or presence of 100 ng/mL SDF-1. Total RNA was isolated as described in Section 3.1.9. RNA integrity was evaluated using the Agilent 2100 Bioanalyzer and reagents in the RNA 6000 Pico LabChip kit (Agilent Technologies) according to the manusfacturer's instructions. Briefly, RNA samples (5 ng) were loaded to wells of the RNA Pico Chips (Agilent Technologies) containing filtered gels and RNA dyes. Electrophoresis of the RNA samples was performed using the Agilent 2100

Bioanalyzer, and results were analyzed with the 2100 expert software (Agilent Technologies). The given RNA integrity number (RIN) indicated the levels of degradation products in the RNA samples. All samples selected for microarray experiments had a RIN > 9.

The purity ($A_{260/280}$ ratio) of RNA samples was measured by the NanoDrop ND-1000 Spectrophometer. The quality control data of RNA samples used in microarray experiments are summarized in Table 3.2.

3.2.2 Expression profiling

Amplification and labeling of RNA, hybridization, staining and scanning were performed according to manufacturer's protocols (Affymetrix, Santa Clara, CA). Briefly, total RNA (100 ng) was subjected to two rounds of amplification using the Two-cycle cDNA Synthesis Kit. The double-stranded cDNA was labeled (biotinylation) using the IVT labeling Kit, and the resulting labeled cRNA was cleaned up, fragmented and hybridized to Human Genome U133 Plus 2.0 GeneChip, which covers more than 47,000 transcripts representing ~39,000 well-characterized genes. The chips were then washed and stained by the Fluidics Station 400 using the fluidics scripts EukGE-WS2v4. Scanning of the chips was performed using the

GeneChip Scanner 3000. All reagents and instruments used in microarray experiments were purchased from Affymetrix.

3.2.3. Microarray data analysis

The GeneChip Operating Software (GCOS) absolute analysis algorithm was applied to determine the amount of transcripts (signal) using the GCOS global scaling option. GCOS-generated data were subjected to per-chip and per-gene normalization using GeneSpring version 10.0 (Agilent Technologies) normalization algorithms. Probe sets showing an absent call in all conditions were excluded. Additional filtering procedures were performed to remove poorly and inconsistently changed genes (fold change cutoff = 1.5 between untreated and SDF-1-treated samples; paired *t* test, *P* value cutoff = .05).

DAVID 2.0 (National Institute of Allergy and Infectious Diseases, http://david.abcc.ncifcrf.gov/) was used for functional annotation of differentially expressed genes (Huang et al., 2009), and TIGR MeV (MultiExperiment Viewer version 2.2, http://www.jcvi.org/) was used for hierarchical clustering analysis (Saeed et al., 2003).

3.2.4 Validation of target genes

Expression of 18 differentially genes were validated by qPCR in $CD34^+$ cells derived from the same CB samples used in microarray experiments (n = 4) plus $CD34^+$ cells from an independent cohort of CB (n = 4-6), according to the procedures described in Section 3.1.9. The Taqman gene expression assays used were listed in Table 3.3.

3.3 Homing functions of CD9 in cord blood $CD34^+$ cells

3.3.1 Characterization of CD9 and CXCR4 membrane expression

Enriched $CD34^+$ cells were stimulated with SDF-1 (100 ng/mL) for 1, 4, or 24 hours, or with protein kinase C (PKC) activators phorbol 12-myristate 13-acetate (PMA), mezerein (MEZ) or ingenol 3,20-dibenzoate (IDB) for 4 hours in IMDM with 20% FCS at 37°C. All PKC activators were purchased from Enzo Life Sciences (Plymouth Meeting, PA) and used at 200 ng/mL. In some experiments, cells were preincubated with pharmacological inhibitors AMD3100 (CXCR4 inhibitor; Sigma-Aldrich; 10 μg/mL), pertussis toxin (Gα inhibitor; Sigma-Aldrich; 1 μg/mL), PD 98059 (MEK inhibitor; 40 μM), wortmannin (PI3K inhibitor; 50 nM), GF 109203X (PKC inhibitor; 2 μM), chelerythrine chloride (PKC inhibitor; 5 μM), AG490 (JAK2 inhibitor; 50 μM), U-73122 (PLC inhibitor; 2.5 μM) or D609 (PLC inhibitor; 10 μM) for 1 hour at 37°C prior to SDF-1 stimulation. All inhibitors were purchased from Calbiochem

(La Jolla, CA) unless otherwise specified. The cell surface expression of CD9 and CXCR4 was assessed by staining with CD9-FITC (clone M-L13) and CXCR4-PE together with anti-CD34-peridin chlorophyll protein-cyanin 5.5 (PerCP-Cy5.5) and anti-CD38-APC for 30 minutes at 4°C. All antibodies were purchased from BD Biosciences. Cells were washed and acquired using the FACSCalibur.

3.3.2 Quantitative polymerase chain reaction (qPCR)

Expressions of *CD9* and *CXCR4* mRNA were determined by qPCR according to the procedures described in Section 3.1.9. The Taqman gene expression assays used were CD9 (Assay ID: Hs00233521_m1) and CXCR4 (Assay ID: Hs00237052_m1) (Applied Biosystems).

3.3.3 Detection of phosphorylated ERK and Akt

$CD34^+$ cells were stimulated with SDF-1 (200 ng/mL) in IMDM with 20% FCS at 37°C for 1 minute, and were fixed and permeabilized using the Phosflow fixation/permeabilization kit (BD Biosciences), according to the manufacturer's protocols. Cells were stained with anti-ERK1/2-PE (pT202/pY204; BD Biosciences) or anti-Akt-Alexa Fluor 488 (pS473; BD Biosciences) for 30 minutes at room temperature, washed, and analyzed by flow cytometry.

3.3.4 Migration assay

Chemotaxis and transendothelial migration experiments were performed using transwells. Enriched $CD34^+$ cells were cultured for 4 hours in the presence of 10 μg/mL anti-CD9 mAb (clone ALB6; Beckman Coulter, Brea, CA) or an isotypic control antibody (mouse IgG1, R&D Systems), washed, and resuspended in IMDM with 1% FCS. These cells (6×10^4 to 1×10^5 in 0.1 mL assay medium) were seeded in the upper chamber, and 0.6 mL of medium containing 100 ng/mL of SDF-1 was added to the bottom chamber. After 4 hours at 37°C, migrated cells were enumerated by a hematocytometer.

For transendothelial migration, human umbilical vein endothelial cells (HUVECs; 2×10^4 cells) (Cascade Biologics, Portland, OR) were grown in Medium 200 supplemented with low serum growth supplement (Cascade Biologics) to confluence in the upper chamber of transwell precoated overnight with 10 μg/mL of fibronectin. HUVECs were pre-activated by 20 ng/mL tumor necrosis factor-α (TNF-α) (Peprotech) for 6 hours, and washed before subjected to migration assay.

3.3.5 Adhesion assay

Adhesion of $CD34^+$ cells to fibronectin was performed in high-binding 96-well plates

(Costar) as previously described (Basu and Broxmeyer, 2005) with minor modifications. Briefly, plates were coated overnight with 20 μg/mL fibronectin at 4°C, followed by incubation for 2 hours at 37°C. Non-specific binding was blocked by 2.5% BSA for 1 hour. $CD34^+$ cells were labeled with 5 μM 5-(6)-carboxyfluorescein diacetate succinimidyl ester (CFSE; Molecular Probes, Eugene, OR) for 15 minutes at 37°C, and allowed to adhere to fibronectin for 45 minutes at 37°C (1×10^5 cells/well) in the absence or presence of SDF-1 (100 ng/mL). Nonadherent cells were removed by 3 washes with prewarmed PBS. Adherent cells from 5 random fields were counted by fluorescence microscopy (Olympus IX71).

Cellular adhesion assays were performed on monolayers of HUVECs. Briefly, HUVECs ($1\text{-}2 \times 10^5$) were seeded on 96-well plates, and allowed to grow to confluence. Adhesion assays of $CD34^+$ cells were performed as described above. HUVECs were activated by 20 ng/mL TNF-α for 6 hours, and washed before addition of $CD34^+$ cells.

3.3.6 Calcium flux assay

Intracellular free Ca^{2+} was measured by flow cytometry as previously described

(Aiuti *et al.*, 1997) with minor modifications. Briefly, $CD34^+$ cells were resuspended in calcium assay buffer (Hanks' balanced salt solution [HBSS; Gibco/Invitrogen] containing 20 mM *N*-2-hydroxyethylpiperazine-*N'*-2-ethanesulfonic acid [HEPES; Gibco/Invitrogen], 0.2% BSA, pH 7.4) and loaded with 4 µM Fluo-3AM (Molecular Probes) in the presence of 0.04% pluronic acid (Molecular Probes) for 30 minutes at 37°C. After a 1:5 dilution with assay buffer followed by incubation for 40 minutes, cells were washed twice, and further incubated for 15 minutes at 37°C. Basal fluorescence in each sample was measured by flow cytometry. After stimulation with SDF-1 (100 ng/mL), change in Fluo-3 fluorescence levels was monitored for 3 minutes.

3.3.7 Actin polymerization assay

Enriched $CD34^+$ cells were cultured for 4 hours in the presence of 10 µg/mL anti-CD9 mAb (clone ALB6) or an isotypic control antibody (mouse IgG1), washed, and resuspended in IMDM with 0.2% BSA. Actin polymerization assay was performed according to the procedures described in Section 3.1.6.

3.3.8 *In vivo* homing assay

NOD.CB17-*Prkdc*^{scid}/J (NOD/SCID) mice were purchased from Jackson Laboratory

(Bar Harbor, ME), bred, and maintained in the Laboratory Animal Services Centre at The Chinese University of Hong Kong. All experiments were approved by the Animal Research Ethics Committee of The Chinese University of Hong Kong. Eight- to 11-week-old mice were sublethally irradiated (^{137}Cs; 375 cGy; Gammacell 1000 Elite Irradiator, MDS Nordion, Kanata, ON, Canada), and intravenously injected with $CD34^+$ cells (1.9×10^5 to 5×10^5 cells/mouse) 24 hours after irradiation. Prior to transplantation, cells were incubated with anti-CD9 mAb (clone ALB6) or mouse IgG1 for 4 hours at 37°C. Single-cell suspensions were prepared from BM (2 femurs) and spleen 20 hours after injection (Broxmeyer *et al.*, 2005), and red blood cells were lysed in buffer EL (Qiagen). Human cells were detected by flow cytometry using human-specific antibodies (anti-CD34-FITC, anti-CD9-PE [clone M-L13; BD Biosciences] and anti-CD45-APC [clone J.33; Beckman Coulter]). Fc receptors were blocked by anti-mouse CD16/CD32 mAb (clone 2.4G2, BD Biosciences) and human serum (Sigma-Aldrich). Dead cells were identified by 7-amino-actinomycin D (7-AAD; BD Biosciences) staining and were excluded from analysis.

Table 3.1 Taqman assays used for detection of R4 RGS subfamily members

Assay ID	Gene Symbol	Gene Title
Hs00175260_m1	RGS1	Regulator of G-protein signaling 1
Hs00180054_m1	RGS2	Regulator of G-protein signaling 2
Hs00367777_m1	RGS3	Regulator of G-protein signaling 3
Hs00194501_m1	RGS4	Regulator of G-protein signaling 4
Hs00186212_m1	RGS5	Regulator of G-protein signaling 5
Hs00364277_m1	RGS8	Regulator of G-protein signaling 8
Hs00243182_m1	RGS13	Regulator of G-protein signaling 13
Hs00892674_m1	RGS16	Regulator of G-protein signaling 16
Hs00329468_m1	RGS18	Regulator of G-protein signaling 18
Hs00982207_m1	RGS21	Regulator of G-protein signaling 21
4333764T	GAPDH	Glyceraldehyde 3-phosphate dehydrogenase

Table 3.2 RNA quality of the 4 CB cases used in microarray experiments

Sample name	$A_{260/280}$	RIN
CB1 CTRL	2	9.7
CB1 SDF	1.85	10
CB2 CTRL	1.93	10
CB2 SDF	1.95	9.9
CB3 CTRL	1.78	9.8
CB3 SDF	1.79	9.9
CB4 CTRL	1.98	9.8
CB4 SDF	1.93	9.9

Abbreviations: RIN, RNA integrity number; CTRL, control; SDF, stromal cell-derived factor-1

Table 3.3 Taqman Gene Expression Assays used in validation experiments

Assay ID	Gene Symbol	Gene Title
Hs00971411_m1	ANXA3	Annexin A3
Hs00233521_m1	CD9	CD9 molecule
Hs00738895_m1	CKLF	Chemokine-like factor
Hs00376243_m1	CMTM2	CKLF-like MARVEL transmembrane domain containing 2
Hs00736707_m1	DIXDC1	DIX containing domain 1
Hs00169257_m1	DUSP6	Dual specificity phosphatase 6
Hs00608055_m1	EMP1	Epithelial membrane protein 1
Hs00177874_m1	EPHA4	EPH receptor A4
Hs01015064_m1	ITGAX	Integrin alpha X
Hs00236976_m1	ITGB1	Integrin beta 1
Hs00609896_m1	ITGB5	Integin beta 5
Hs01573555_m1	ITPR3	Inositol 1,4,5-triphosphate receptor, type 3
Hs00153462_m1	LMNA	Lamin A/C
Hs01554892_m1	ME1	Malic enzyme 1, NADP (+) - dependent, cytosolic
Hs00957562_m1	MMP9	Matrix metallopeptidase 9
Hs00202485_m1	MYO10	Myosin X
Hs00243182_m1	RGS13	Regulator of G-protein signaling 13
Hs00541761_m1	ST6GALNAC3	ST6 (alpha-N-acetyl-neuraminyl-2,3-beta-galactosyl-1,3)-N-acetylgalactosaminide alpha-2,6-sialytransferase 3
Hs00975687_m1	SYNJ2	Synaptojanin 2
4333764T	GAPDH	Glyceraldehyde 3-phosphate dehydrogenase

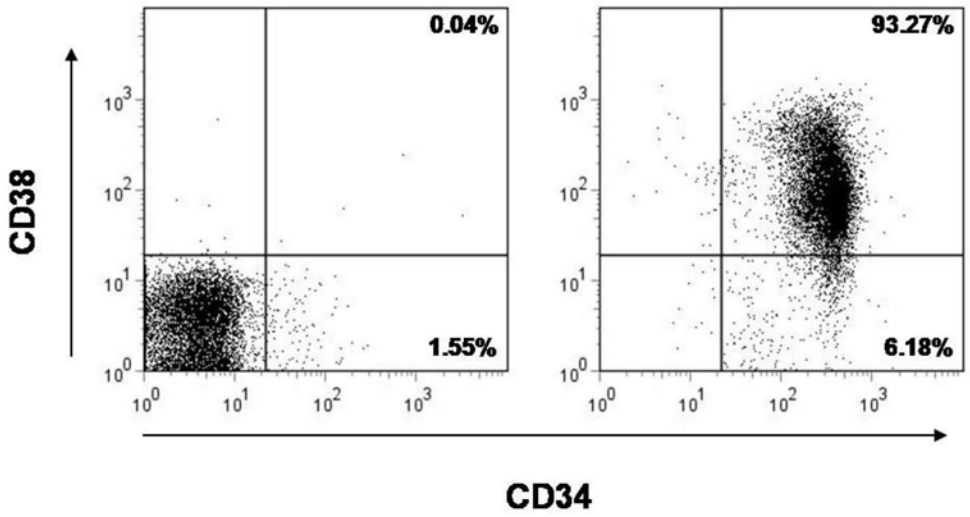

Figure 3.1 Purity of enriched CB CD34$^+$ cells

Enriched CD34$^+$ cells were stained with CD34-FITC and CD38-APC (right panel), or their respective isotypic control antibodies (left panel). The percentage of CD34$^+$ cells were evaluated using the FACSCalibur flow cytometer. A representative purity analysis of 45 independent CB samples is shown. The quadrants were set on the basis of staining with isotypic control antibodies, and the percentage of cells in each quadrant is depicted.

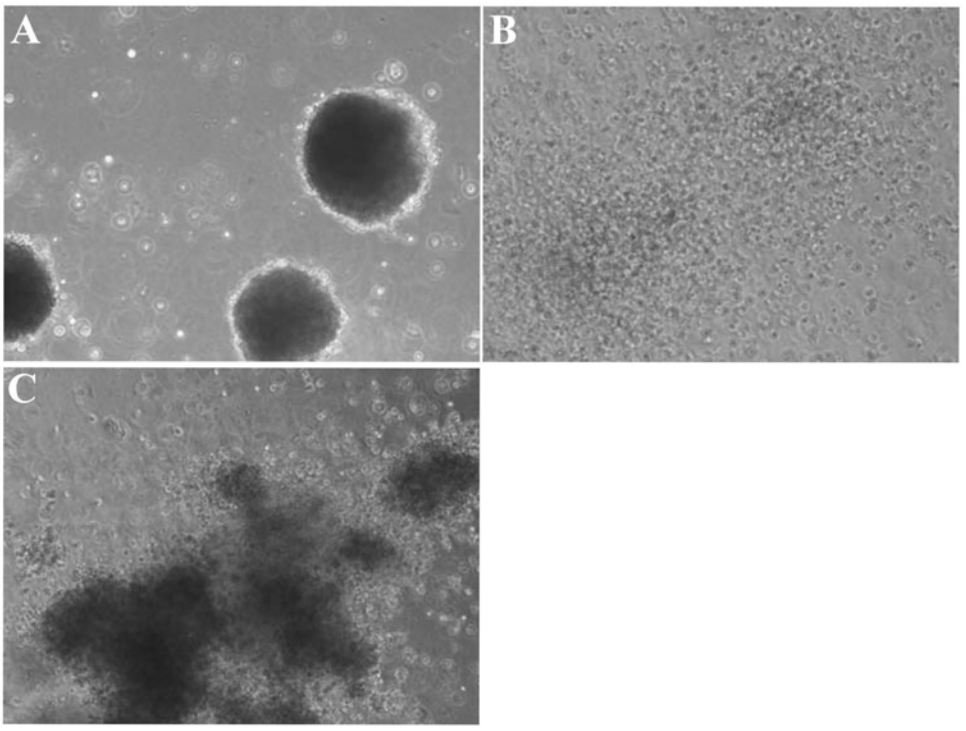

Figure 3.2 Colonies derived from CB CD34$^+$ cells

Images showing (A) BFU/CFU-E, (B) CFU-GM and (C) CFU-GEMM derived from migrated CD34$^+$ cells in the lower chamber of transwell in response to a SDF-1 gradient (100 ng/mL) (original magnification ×100).

CHAPTER FOUR

Effects of Stromal Cell-derived Factor-1 (SDF-1) and its Peptide Analog on Homing-related Responses of Human Cord Blood $CD34^+$ Hematopoietic Stem/progenitor Cells

4.1 Background and objectives

CB transplantation, especially in adult patients, is associated with increased risk of graft failure and delay in engraftment. To address this issue, strategies attempting to promote the homing capacity of CB HSC by *ex vivo* treatment with homing-enhancing agents have been recently proposed and investigated. It has been demonstrated in *in vivo* transplantation models that short exposure to FTY720 (Kimura *et al.*, 2004), UTP (Rossi *et al.*, 2007) or prostaglandin E2 (Hoggatt *et al.*, 2009) significantly improved human HSC homing. Our group previously demonstrated that a small cyclized peptide analog of SDF-1, CTCE-0214, enhanced *ex vivo* expansion of CB $CD34^+$ cells in synergy with early-acting cytokines (Li *et al.*, 2006). Interestingly, a short exposure of *ex vivo* expanded cells to CTCE-0214 enhanced their multilineage engraftment in NOD/SCID mice without changing the quantity of progenitor cells (Li *et al.*, 2006). This observation implicated a direct role of the SDF-1 analog in promoting the engraftment capacity of expanding

stem/progenitor cells, and prompted us to hypothesize that the motility and homing-related properties of these cells were enhanced. In the current study, as an extension of previous work, our specific objectives were:

(1) to investigate whether CTCE-0214 enhanced *in vitro* homing-related functions of both freshly isolated $CD34^+$ and *ex vivo* expanded cells derived from CB.

(2) to compare the effects of CTCE-0214 with its parent molecule, SDF-1, on homing-related functions of $CD34^+$ cells.

(3) to investigate the molecular mechanism of altered motility responses in SDF-1- and CTCE-0214-treated cells in relation to the expression of regulator of G-protein signaling 13 (RGS13).

4.2 Results

4.2.1 CTCE-0214 enhances the migratory response of *ex vivo* expanded cells

CTCE-0214 is a C-terminal amide peptide analog in which the N-terminal region of SDF-1 is connected to the C-terminal region by a short linker sequence (Figure 4.1). In this study, we first used the transwell chemotaxis assay to test whether the enhanced engraftment of the CTCE-treated cells is associated with altered migratory responses. Culturing enriched CB $CD34^+$ cells for 4 days in the presence of thrombopoietin (TPO), stem cell factor (SCF) and Flt-3 ligand (FL) yielded 12.9 ± 5.5-fold increase in total nucleated cells (n = 5), while 33.3 ± 5.0% of the expanded cells retained CD34 expression (Figure 4.2 A). Exposure of the expanded cells to CTCE-0214 for 4 hours enhanced their migration to a SDF-1 gradient by 28.2%, when compared to control untreated cells (P = .019; Figure 4.2 B). In contrast, treatment of the expanded cells with SDF-1 significantly inhibited migration by 74.1% (P = .003; Figure 4.2 B). Taken together, our first set of experiments provides two important implications. Firstly, exposure of *ex vivo* expanded cells to CTCE-0214 improved their migratory responses, thus posing one of the possible reasons to explain our observation that the CTCE-treated cells had higher engraftment potential in NOD/SCID mice (Li *et al.*, 2006). Secondly, we surprisingly found that SDF-1 and CTCE-0214 had differential effects on migration of *ex vivo*

expanded cells, despite that CTCE-0214 was originally designed as a more stable derivative of SDF-1.

4.2.2 Differential effects of SDF-1 and CTCE-0214 on migration of freshly isolated cord blood $CD34^+$ cells

We next characterized, in a more precise manner, the effects of SDF-1 and CTCE-0214 on migratory responses of freshly isolated $CD34^+$ cells. SDF-1 is the only known chemoattractant of murine and human hematopoietic stem/progenitor cells (Aiuti *et al*., 1997). Consistently, we found that SDF-1, when added to the lower chamber of the transwell, induced a dose-dependent migration of CB $CD34^+$ cells, in which the response was plateaued when the SDF-1 concentration was higher than 200 ng/mL (Figure 4.3 A). In contrast, CTCE-0214 was not chemotactic for $CD34^+$ cells ($P < .05$ when compared to SDF-1 at matched concentrations; Figure 4.3 A). Furthermore, the addition of CTCE-0214 together with SDF-1 to the lower chambers did not enhance SDF-1-mediated migration (Figure 4.3 B). However, CTCE-0214, when added to the upper chambers, significantly enhanced migration of $CD34^+$ cells to a SDF-1 gradient, with optimal concentration at 100 ng/mL ($P = .003$; Figure 4.3 C). Addition of CTCE-0214 to the upper chamber did not induce spontaneous cell migration in the absence of a SDF-1 gradient. These data collectively suggest that

prior exposure to CTCE-0214 is necessary for its migration-enhancing activity. To this end, we pretreated $CD34^+$ cells with CTCE-0214 or SDF-1 for 1-24 hours before transwell migration assay. As shown in Figure 4.3 D, pre-exposure of $CD34^+$ cells to CTCE-0214 for 1 hour or 4 hours enhanced their migration to a SDF-1 gradient by 22.9% and 32.4%, respectively (P = .029 for 1 hour, P = .019 for 4 hours), while extension of the exposure time to 24 hours did not further enhance their migratory responses (Figure 4.3 D). Consistent with the migration data of *ex vivo* expanded cells, pretreatment with SDF-1 time-dependently inhibited the migratory responses of freshly isolated $CD34^+$ cells ($P < .05$; Figure 4.3 D).

To investigate whether CTCE enhanced the motility of specific cell lineages within the bulk $CD34^+$ population, migrated cells were subjected to clonogenic colony-forming unit assay. Our results revealed that the presence of CTCE-0214 in upper chamber, although not reaching statistical significance, enhanced SDF-1-mediated migration of all types of colony-forming cells including colony-forming unit-mixed (CFU-GEMMs), erythroid (BFU/CFU-Es) and myeloid (CFU-GMs) progenitors (Figure 4.4 A). However, the frequency of multi-lineage colony-forming cells was similar in the migrated populations regardless of the presence of CTCE-0214 in the upper chamber (Figure 4.4 B). Similarly, phenotypic

analysis of the migrated cells revealed that CTCE-0214 did not preferentially enhance migration of the more primitive $CD34^{+}CD38^{-}$ cells (Figure 4.4 C). Taken together, these data suggest that the promoting effect of CTCE-0214 on cell migration is not limited to specific subsets within the $CD34^{+}$ population.

4.2.3 Effects of SDF-1 and CTCE-0214 on actin polymerization and adhesion of $CD34^{+}$ cells

We performed two additional assays to investigate the effects of SDF-1 and CTCE-0214 on other homing-related functions of $CD34^{+}$ cells. In response to chemokines, actin monomers polymerize into filamentous structures (F-actin) and reorganize to generate forces necessary for directional cell migration (Hall, 1999). To study the effect of SDF-1 and CTCE-0214 on this process, F-actin level in $CD34^{+}$ cells after stimulation was assessed by phalloidin-FITC staining. As shown in Figure 4.5 A, either SDF-1 or CTCE-0214 had a trend to induce a rapid and transient increase in intracellular polymerized actin levels.

Homing and retention of hematopoietic progenitors in the BM microenviroment depends on their interaction with the extracellular matrix (ECM) components (Hirsch *et al.*, 1996; Verfaillie *et al.*, 1998; Vermeulen *et al.*, 1998). We used

fibronectin-coated surfaces to study the effects of SDF-1 and CTCE-0214 on the adhesive properties of CB $CD34^+$ cells. We found that either SDF-1 or CTCE-0214 had a trend to enhance adhesion of $CD34^+$ cells to the ECM protein fibronectin, when compared with control untreated cells (Figure 4.5 B).

4.2.4 SDF-1 and CTCE-0214 differentially regulates CXCR4 expression

Given that SDF-1 and CTCE-0214 displayed an opposite effect on migration of $CD34^+$ cells, we next attempted to characterize the underlying mechanisms. CXCR4, the primary receptor of SDF-1, plays essential roles in migration, homing and engraftment of hematopoietic stem/progenitor cells (Peled *et al.*, 1999; Kollet *et al.*, 2001). To investigate whether CXCR4 expression was differentially regulated, enriched $CD34^+$ cells were pretreated with SDF-1 or CTCE-0214 for 1-24 h, and the cell surface CXCR4 level was determined by flow cytometry. Consistent with others (Signoret *et al.*, 1997; Peled *et al.*, 1999), exposure of freshly isolated $CD34^+$ cells to SDF-1 resulted in a time-dependent decrease in cell surface CXCR4 expression ($P < .05$; Figure 4.6 A), when compared with control untreated cells. In contrast, CTCE-0214 did not affect CXCR4 expression (Figure 4.6 A). These observations were further confirmed by immunofluorescence microscopy. As shown in Figure 4.6 B, the cell surface CXCR4 expression was almost completely lost after SDF-1

stimulation, while it was maintained in CTCE-0214-treated cells.

Using 4-day *ex vivo* expanded cells, we demonstrated that the differential regulation of CXCR4 level by SDF-1 and CTCE-0214 was not limited to freshly isolated $CD34^+$ cells. Exposure of *ex vivo* expanded cells to SDF-1 for 4 hours in the presence of TPO, SCF and FL resulted in 76.3% reduction in CXCR4 expression ($P = .001$, Figure 4.7), while the CXCR4 level in CTCE-0214-treated cells was maintained.

We then analyzed the CXCR4 expression on cells collected from transwell migration assay. In the presence of SDF-1 in the lower chamber, the CXCR4 expression in terms of mean fluorescence intensity (MFI) on either migrated cells or non-migrated cells was markedly reduced (-/- vs -/SDF; Figure 4.8). However, addition of CTCE-0214 to the upper chamber inhibited the SDF-1-induced CXCR4 downregulation in both migrated and non-migrated cell population (-/SDF vs CTCE/SDF; $P < .01$; Figure 4.8). These data indicate that CTCE-0214 alone does not affect CXCR4 expression, but it prevents CXCR4 downregulation in the presence of SDF-1.

We also tested the effects of SDF-1 and CTCE-0214 on the expression of several emerging regulators of hematopoietic stem/progenitor cell migration. However, the expression of CD26 (Christopherson *et al.*, 2004), CD44 (Avigdor *et al.*, 2004), CD49d/e (VLA-4/5; Imai *et al.*, 1999; Peled *et al.*, 2000) and CD164 (Forde *et al.*, 2007) was not significantly changed by either compound (Figure 4.9).

4.2.5 Differential effects of SDF-1 and CTCE-0214 on the expression of regulator of G-protein signaling 13

The regulator of G-protein signaling (RGS) proteins negatively regulates G-protein coupled receptor signaling by accelerating the intrinsic GTPase activity of the Gα subunit (Ross *et al.*, 2000; De Vries *et al.*, 2000). Specifically, several members of the R4 subfamily, including RGS1, RGS13 and RGS16, are known to regulate the SDF-1/CXCR4 signaling (Bansal *et al.*, 2007). To further decipher the mechanism leading to the observed difference in migratory responses between SDF-1- and CTCE-0214-treated cells, we investigated whether the two compounds differentially regulated the expression of R4 RGS proteins. The basal mRNA expression of the all the known members in the R4 subfamily was first characterized by qRT-PCR. As shown in Figure 4.10, enriched CB-derived $CD34^+$ cells expressed high level of *RGS1*, *RGS2* and *RGS3*, and moderate level of *RGS5*, *RGS13*, *RGS16* and *RGS18*.

Expression of *RGS8* was barely detectable in $CD34^+$ cells from two out of three CB samples, while *RGS4* and *RGS21* expression was not detectable (Figure 4.10).

We next studied the effect of SDF-1 and CTCE-0214 on the mRNA expression of the RGS proteins. Exposure of $CD34^+$ cells to either SDF-1 or CTCE-0214 for certain time points slightly upregulated *RGS1*, *RGS2* and *RGS3* expression ($P < .05$; Figure 4.11), while the expression of *RGS5*, *RGS16* and *RGS18* was not affected by either compound. Notably, SDF-1 and CTCE-0214 had an opposite effect on *RGS13* expression level. Treatment of $CD34^+$ with SDF-1 for 4 hours resulted in a significant increase in *RGS13* expression ($P = .043$), whereas CTCE-0214 induced a time-dependent decrease in *RGS13* expression ($P = .005$; Figure 4.11).

Using a specific antibody, flow cytometry analysis revealed that 96.4 ± 2.2% of $CD34^+$ cells expressed RGS13 at the protein level (Figure 4.12 A). The protein expression of RGS13 was further confirmed by immunofluorescence microscopy. As shown in Figure 3B, almost all of the $CD34^+$ cells expressed RGS13 (Figure 4.12 B). Taken together, our results indicate that SDF-1 and CTCE-0214 differentially regulate the expression of RGS13, and this could be one of the possible mechanisms to explain their differential activity on migratory responses of $CD34^+$ cells.

4.3 Discussion

In this study, we attempted to define whether CTCE-0214 has a direct effect on homing-related functions of hematopoietic progenitor cells. We demonstrated that a short exposure of *ex vivo* expanded cells to CTCE-0214 significantly enhanced their migration to a SDF-1 gradient. Voermans *et al*. (2001b) showed that higher migratory capacity of $CD34^+$ cells towards a SDF-1 gradient *in vitro* is correlated with faster neutrophil and platelet recovery after autologous stem cell transplantation. Thus, the ability of CTCE-0214 to improve the engraftability of *ex vivo* expanded cells, as suggested in our earlier study (Li *et al*., 2006), is possibly mediated by its ability to enhance stem cell migration. The use of CB for transplantation, particularly in adults, is limited by the small number of hematopoietic stem/progenitor cells in each graft (Gluckman, 2009). A logical option is to increase the number of stem/progenitor cells through controlled *ex vivo* expansion (Hofmeister *et al*., 2007). However, there has been evidence showing that exposure of HSC to cytokines in the expansion medium greatly impaired their homing and engraftment capacity (Guenechea *et al*., 1999; Ahmed *et al*., 2004). Our data suggest that the use of CTCE-0214 in *ex vivo* expansion may retrieve stem cell homing capacity, which has been adversely affected by culture conditions, through its motility-enhancing activity. Furthermore, we showed that CTCE-0214 can also be applied to improve the migratory response of

freshly isolated $CD34^+$ cells.

CTCE-0214 was originally manufactured as a peptide agonist of SDF-1 for the use in stem cell mobilization (Zhong *et al.*, 2004). When compared with SDF-1, this analog has higher plasma stability, making it less susceptible to clearance and degradation when used *in vivo* (Tudan *et al.*, 2002). Since the N-terminal residues of SDF-1 known to be important for CXCR4 binding and G-protein activation are retained in CTCE-0214 (Crump *et al.*, 1997; Heveker *et al.*, 1998; Loetscher *et al.*, 1998), its biological activities are expected to be similar to SDF-1. Using a series of *in vitro* functional assays, we demonstrated that either SDF-1 or CTCE-0214 enhanced progenitor cell adhesion and actin polymerization. However, we unexpectedly found that they have differential effects on cell migration. Firstly, pre-exposure of $CD34^+$ cells with SDF-1 markedly inhibited their motility, while pretreatment with CTCE-0214 or addition of CTCE-0214 to the upper transwell chamber significantly enhanced cell migration towards a SDF-1 gradient. Secondly, $CD34^+$ cells responded in chemotaxis assays to SDF-1 at a concentration as low as 10 ng/mL. In contrast, a 50-fold increase in CTCE-0214 concentration was still not chemotactic for $CD34^+$ cells. Zhong *et al.* (2004) reported CTCE-0214 at the concentration of 100 μg/mL can moderately attract $CD34^+$ cells from MPB. Thus, in comparison with SDF-1

which works at nanomolar concentrations, CTCE-0214 is not a potent chemoattractant. The middle region of SDF-1, which contains heparan sulfate binding sites, is missing in CTCE-0214 (Sadir *et al.*, 2004). Moreover, replacing the internal region of SDF-1 with a linker and cyclization of the resulting peptide may lead to difference in 3-dimensional structures between CTCE-0214 and SDF-1. It would be interesting to address why SDF-1 and CTCE-0214 have different biological activity on the structural basis.

CXCR4 has been shown as the principal regulator of migration, homing and retention of HSC (Lapidot *et al.*, 2005; Chute, 2006). Consistent with other reports (Signoret *et al.*, 1997; Peled *et al.*, 1999; Basu and Broxmeyer, 2005), we demonstrated that exposure of freshly isolated or expanded $CD34^+$ cells to SDF-1 significantly reduced cell surface CXCR4 level, coincident with the decrease in cell motility. On the other hand, we surprisingly found that CTCE-0214 can prevent SDF-1-induced CXCR4 downregulation, while CTCE-0214 alone did not affect CXCR4 expression. Based on these observations, we reason that the motility-enhancing activity of CTCE-0214 may attribute to its ability to inhibit CXCR4 internalization, thus keeping CXCR4 at high level to sense the SDF-1 gradient. Several mechanisms have been described for regulation of CXCR4

internalization. In HEK-293 cells, ligand-induced phosphorylation of the CXCR4 C-terminal domain by G-protein coupled receptor kinases (GRKs) promoted binding of arrestins and receptor internalization (Orsini *et al.*, 1999). In T cells, silencing the motor protein nonmuscle myosin heavy chain IIA (MIIA) inhibited SDF-1-induced CXCR4 endocytosis and enhanced cell migration (Rey *et al.*, 2007). Defining how CTCE-0214 regulates CXCR4 expression may provide further insights into the precise mechanism of its motility- and engraftment-enhancing activities.

In this study, we also showed that SDF-1 and CTCE-0214 differentially regulate gene transcription in $CD34^+$ hematopoietic progenitor cells. Characterization of the basal expression of R4 RGS subfamily proteins revealed that CB $CD34^+$ cells expressed RGS1-3, 5, 13, 16 and 18 at various levels. We also showed for the first time that the expression of RGS1-3 and 13 was subjected to regulation by either SDF-1 or CTCE-0214 in primary hematopoietic progenitors. Most importantly, we found that the expression of RGS13 was upregulated by SDF-1 and downregulated by CTCE-0214. RGS proteins bind heterotrimeric G-protein α subunit, accelerate the inactivation rate of Gα-GTP (Watson *et al.*, 1996) and they therefore function as negative regulator of G-protein-mediated signaling. In particular, RGS13 have been shown to inhibit SDF-1/CXCR4-mediated migration of human germinal center B

lymphocytes (Shi *et al.*, 2002), human mast cells (Bansal *et al.*, 2008b) and murine B cells (Hsu *et al.*, 2008). Thus, differential regulation of RGS13 expression by SDF-1 and CTCE-0214 might contribute to their opposite effects on migration of $CD34^+$ hematopoietic progenitors.

Our study provides the first evidence that SDF-1 and CTCE-0214 differentially regulate migration of hematopoietic progenitor cells. We propose that the difference in their effect on cell migration is attributed by the following mechanism (Figure 4.13). Exposure of $CD34^+$ cells to SDF-1 induces CXCR4 internalization and RGS13 expression. The binding of RGS13 to Gα subunit accelerates the rate the GTP hydrolysis and return the Gα subunit to an inactive GDP-bound form. The combined effects of CXCR4 and RGS13 inhibit signaling in response to a second SDF-1 exposure and thus leading to reduced migration. In CTCE-0214-treated cells, both CXCR4 internalization and RGS13 expression are reduced. The Gα subunit will maintain in an active GTP-bound conformation. In response to SDF-1, signaling in these cells will be enhanced and thus leading to improved cell migration.

In conclusion, the current data, together with our previous findings (Li *et al.*, 2006) demonstrated that CTCE-0214 possessed dual properties: ability to enhance (1)

expansion and (2) homing-related responses of hematopoietic stem/progenitor cells. Moreover, data from the current study also demonstrated that CTCE-0214 and SDF-1 exhibited different effects on migratory properties of CB $CD34^+$ cells, which might be resulted from their differential regulation on CXCR4 and RGS13 expression. We shall focus our future study on resolving the role of RGS13 in the hematopoietic progenitor compartment. If proven to be a signal for specific homing functions, RGS13 might be a new component for further development of strategies to improve HSC engraftment.

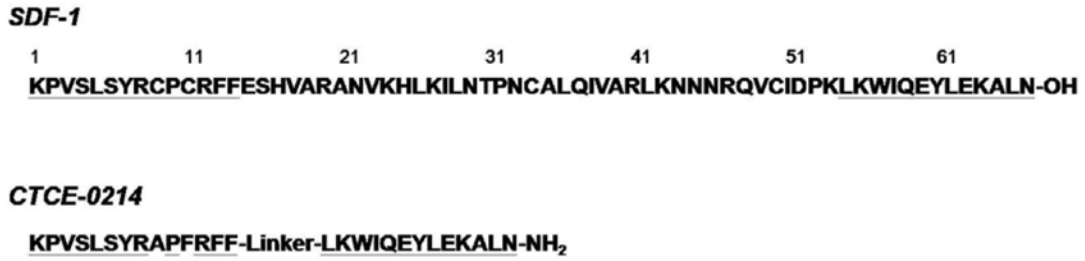

Figure 4.1 Amino acid sequences of SDF-1 and CTCE-0214

The amino acid positions are shown and common sequences are underlined. (Sequences adapted from Merzouk *et al*., 2004)

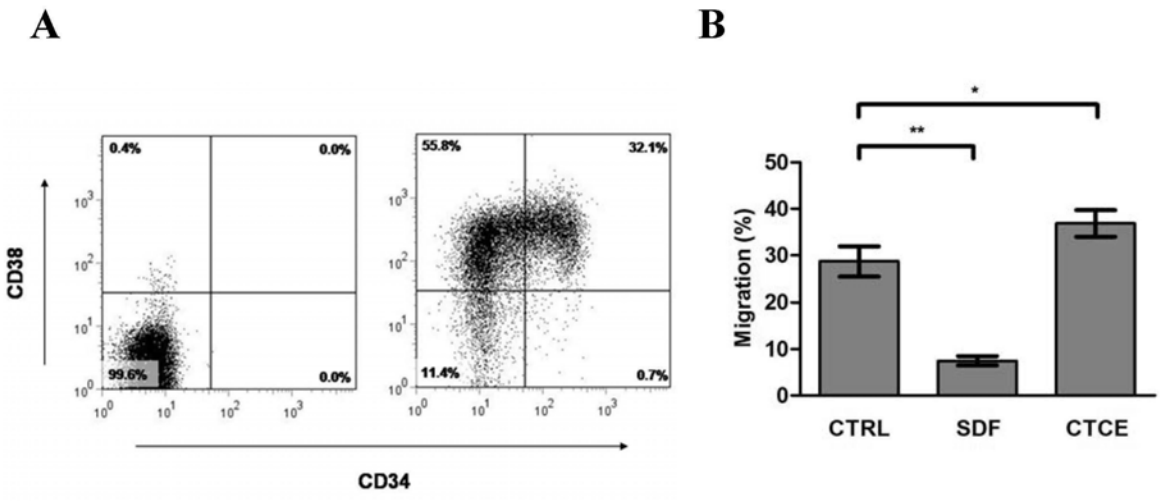

Figure 4.2 Effects of SDF-1 and CTCE-0214 on migration of *ex vivo* expanded cells

(A) Enriched CB $CD34^+$ cells were cultured for 4 days in the presence of TPO (50 ng/mL), SCF (50 ng/mL) and FL (80 ng/mL). Cell surface expression of CD34 and CD38 was determined by staining with CD34-FITC and CD38-PE mAbs, and was analyzed by flow cytometry (n = 5). Isotypic control mAbs staining is shown on the left. The percentage of cells in each quadrant is depicted. (B) *Ex vivo* expanded cells were pretreated with medium (CTRL), SDF-1 (100 ng/mL) or CTCE-0214 (100 ng/mL) for 4 hours. Cell migration to a gradient of SDF-1 (100 ng/mL) was determined using transwell (n = 5). Data are mean ± SEM. *, $P < .05$; **, $P < .01$.

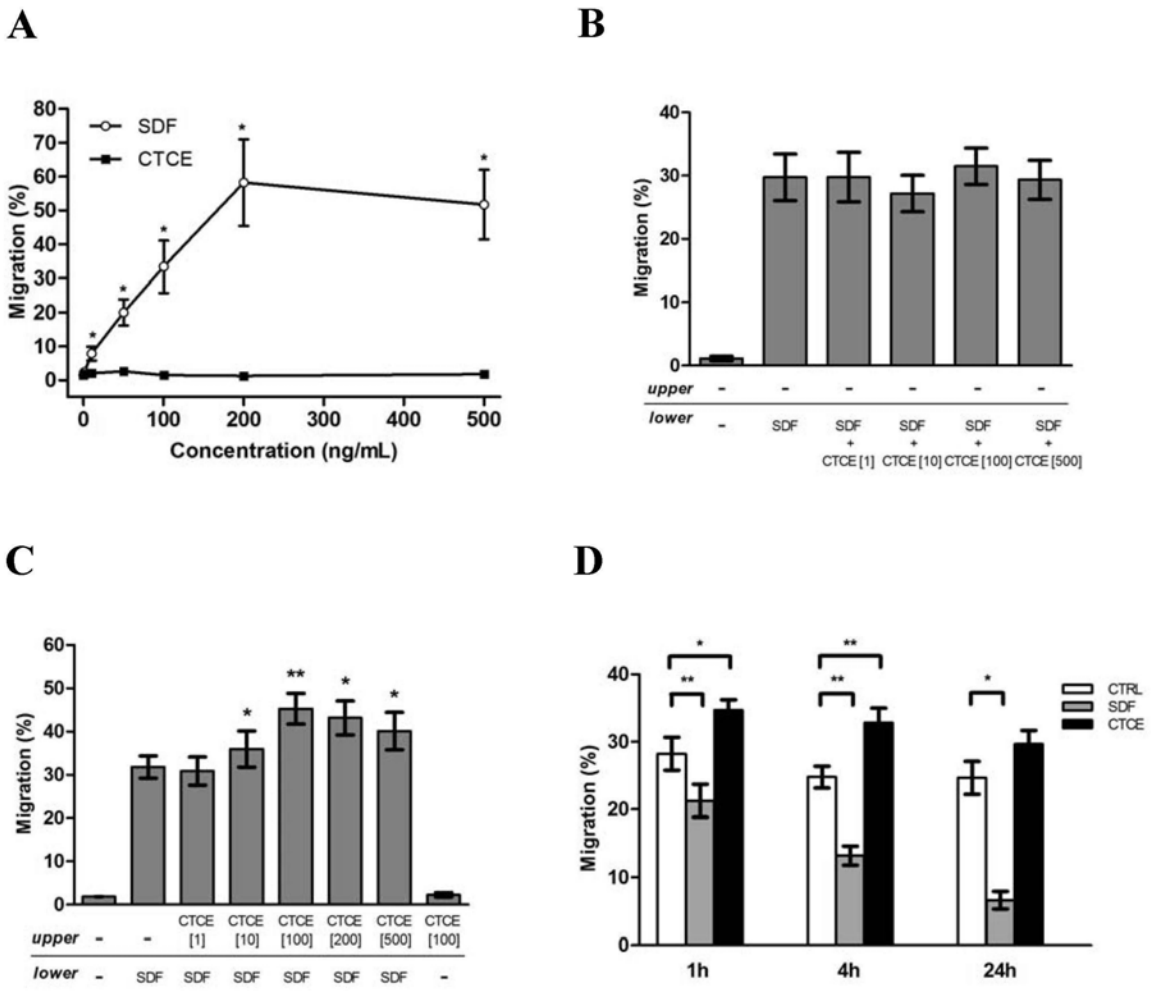

Figure 4.3 Effects of SDF-1 and CTCE-0214 on transwell migration of freshly isolated CB CD34$^+$ cells

(A) Migration of freshly isolated CB CD34$^+$ cells to gradients of increasing doses of SDF-1 or CTCE-0214 in the lower chamber of the transwell (n = 3). (B) Migration of CD34$^+$ cells to SDF-1 (100 ng/mL) or in combination with various concentrations of CTCE-0214 in the lower chamber (n = 3). (C) Migration of CD34$^+$ cells to SDF-1 (100 ng/mL) in the absence or presence of various concentrations of CTCE-0214 in

the upper chamber (n = 4-6). (D) $CD34^+$ cells were pretreated with medium (CTRL), SDF-1 (100 ng/mL) or CTCE-0214 (100 ng/mL) for 1, 4 or 24 hours. Cell migration to a gradient of SDF-1 (100 ng/mL) in the lower chamber of the transwell was determined (n = 4-6). Data are mean ± SEM. *, $P < .05$; **, $P < .01$.

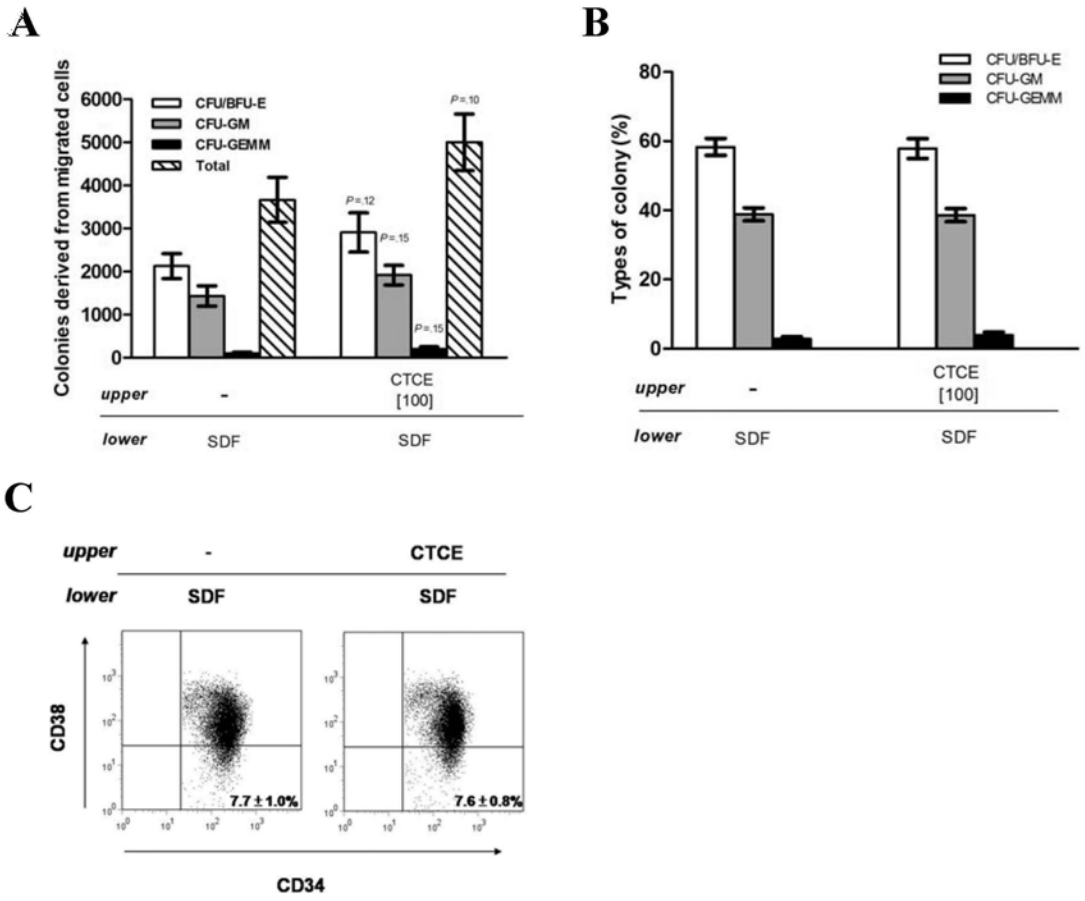

Figure 4.4 Lineage analysis of the migrated CD34$^+$ cells

Enriched CB CD34$^+$ cells were allowed to migrate towards SDF-1 (100 ng/mL) in the absence or presence of CTCE-0214 (100 ng/mL) in the upper chamber. Migrated cells in the lower chamber (1000 cells) were grown in methylcellulose culture supplemented with growth cytokines to determine the (A) number (total number of migrated cells to the lower chamber × number of colonies derived from 1000 migrated cells / 1000) and (B) percentage of different types of colony-forming cells (n =3). (C) Migrated cells were stained with anti-CD34 and anti-CD38 mAbs and analyzed by flow cytometry (n = 4). The percentage of the more primitive CD34$^+$CD38$^-$ cells is shown in the lower right quadrants. Data are mean ± SEM.

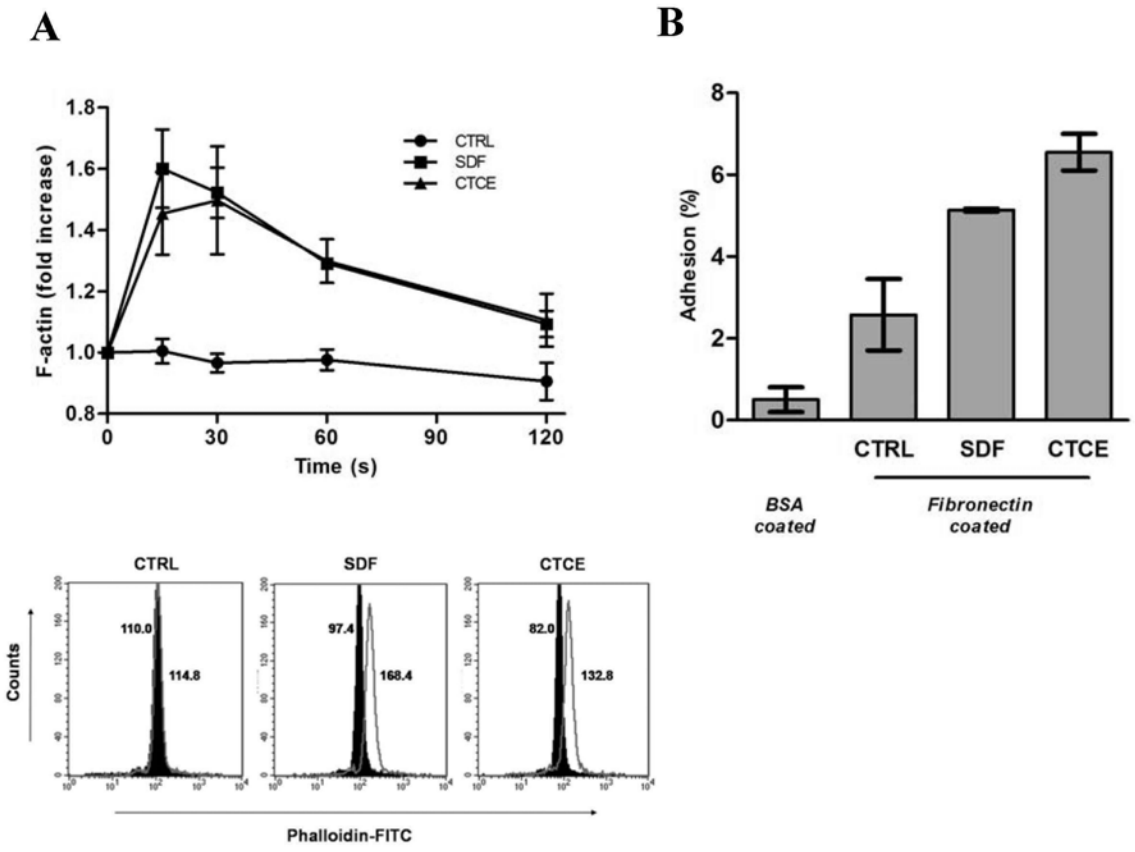

Figure 4.5 Effects of SDF-1 and CTCE-0214 on actin polymerization and adhesion of CB CD34$^+$ cells

(A) Actin polymerization assay. CD34$^+$ cells were stimulated with medium (CTRL), SDF-1 (100 ng/mL) or CTCE-0214 for the indicated times. F-actin levels were determined by phalloidin-FITC staining and analyzed by flow cytometry (n = 2). (Bottom panel) Representative histograms showing the phalloidin-FITC fluorescence intensities in CD34$^+$ cells before (filled histograms) and after a 15-second stimulation (open histograms) with medium (CTRL), SDF-1 or CTCE-0214. Mean fluorescence intensity (MFI) is shown. (B) Adhesion assay. Cells were plated on bovine serum albumin (BSA)- or fibronectin-coated wells, and either left unstimulated (CTRL) or

stimulated with SDF-1 (100 ng/mL) or CTCE-0214 for 45 minutes. Adherent cells were collected after Accutase treatment, and enumerated using a hematocytometer (n = 2). Data represent mean ± SEM.

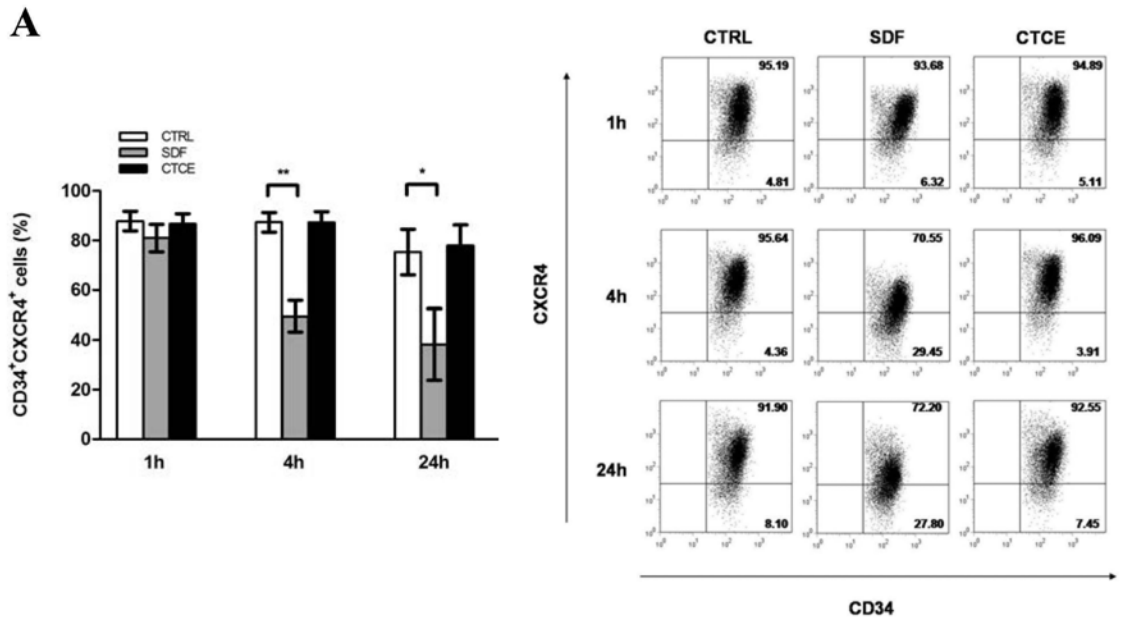

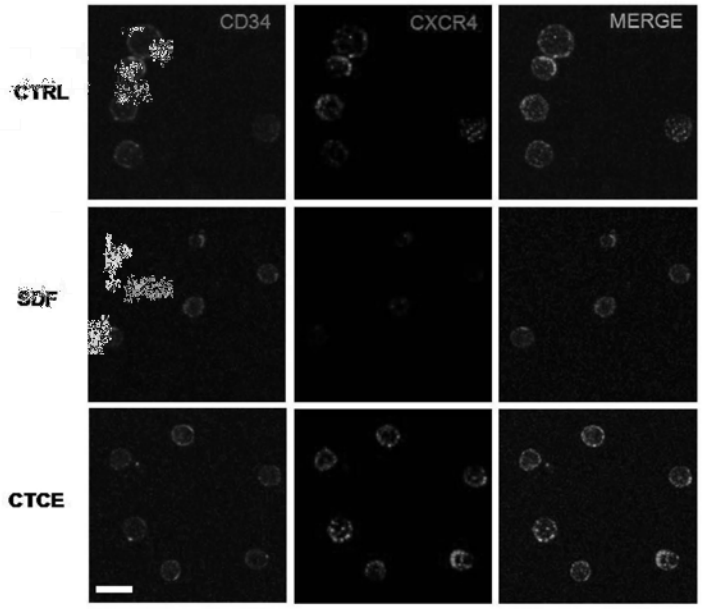

Figure 4.6 Effects of SDF-1 and CTCE-0214 on CXCR4 expression of freshly isolated CD34$^+$ cells

(A) Surface expression of CXCR4 on CD34$^+$ cells after 1, 4 or 24 hours culture in medium alone (CTRL), SDF-1 (100 ng/mL) or CTCE-0214 (100 ng/mL) were

determined by CD34-FITC and CXCR4-PE staining and analyzed by flow cytometry (n = 3). Data are mean ± SEM. *, $P < .05$; **, $P < .01$. (Right panel) Dot plots of CXCR4 expression of a representative experiment. Quadrants were set on the basis of staining with isotypic control antibodies, and the percentage of cells in each quadrant is depicted. (B) Immunofluorescence microscopy analysis of CD34 (green) and CXCR4 (red) membrane expression on $CD34^+$ cells exposed for 4 hours to medium (CTRL), or in the presence of SDF-1 (100 ng/mL) or CTCE-0214 (100 ng/mL) Bar = 10 μm.

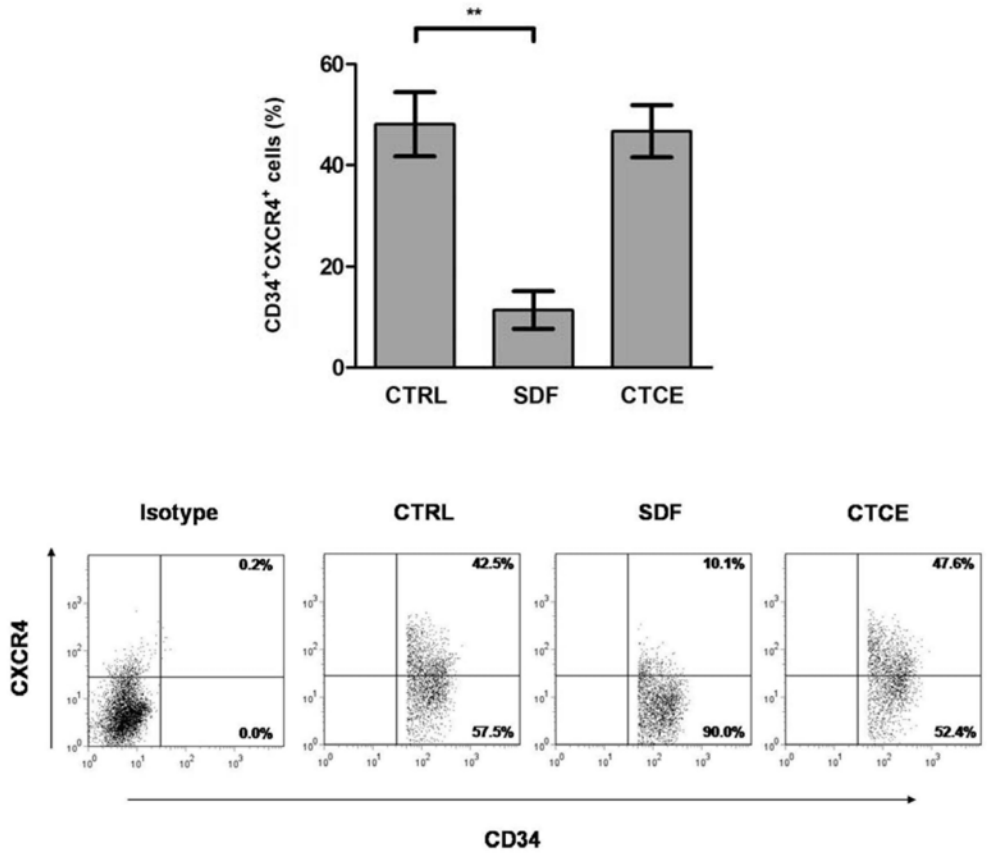

Figure 4.7 Effects of SDF-1 and CTCE-0214 on CXCR4 expression of *ex vivo* expanded cells

(A) Enriched CB $CD34^+$ cells were cultured for 4 days in the presence of TPO (50 ng/mL), SCF (50 ng/mL) and FL (80 ng/mL).Surface expression of CXCR4 on *ex vivo* expanded cells after 4 hours culture in medium alone (CTRL), or in the presence of SDF-1 (100 ng/mL) or CTCE-0214 (100 ng/mL) were determined by CD34-FITC and CXCR4-PE staining and analyzed by flow cytometry (n = 4). Data are mean ± SEM. **, $P < .01$. Bottom panel, dot plots of CXCR4 expression in gated $CD34^+$ cells of a representative experiment. The percentage of cells in each quadrant is depicted.

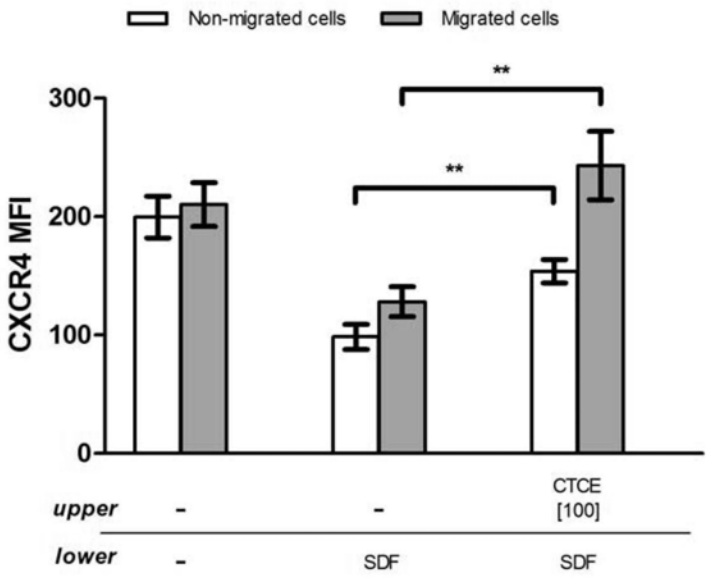

Figure 4.8 CXCR4 expression in non-migrated and migrated CD34$^+$ cells

Freshly isolated CD34$^+$ cells were allowed to migrate towards the assay medium (-/-) or SDF-1 (100 ng/mL) in the lower chamber, in the absence (-/SDF) or presence of CTCE-0214 (100 ng/mL) in the upper chamber (CTCE/SDF). Non-migrated and migrated cells were stained with anti-CXCR4 mAb and the CXCR4 mean fluorescence intensity (MFI) was measured by flow cytometry (n = 4). Data are mean ± SEM. **, $P < .01$.

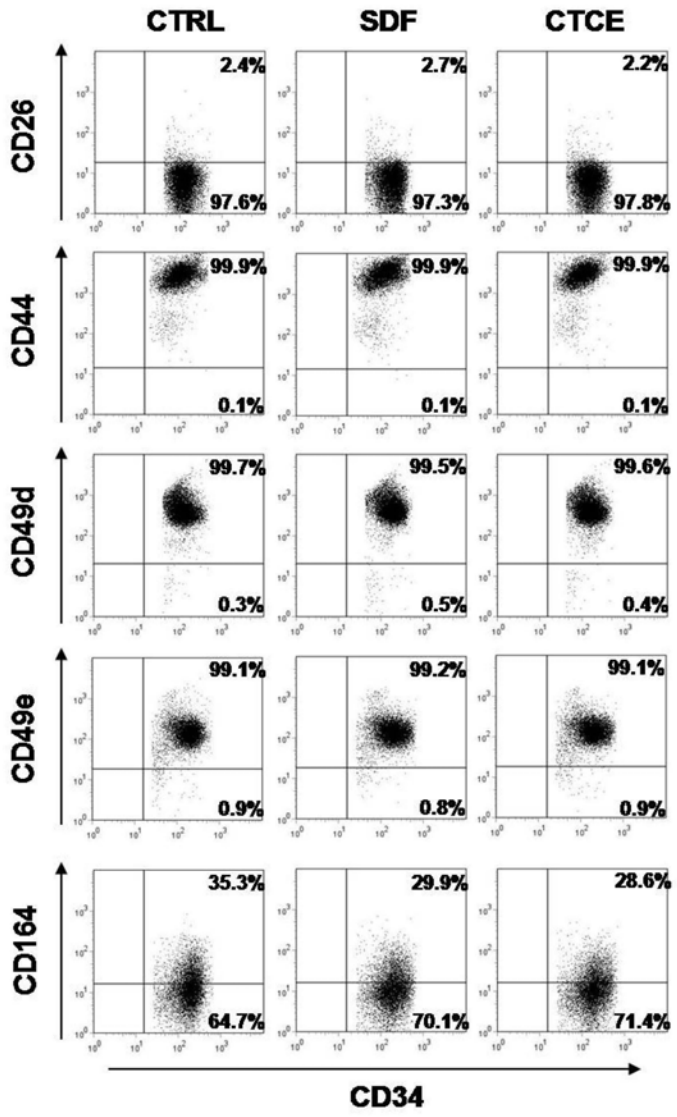

Figure 4.9 Effects of SDF-1 and CTCE-0214 on expression of several known regulators of HSC homing

Surface expression of CD26, CD44, CD49d, CD49e and CD164 on freshly isolated $CD34^+$ cells after 4 hours culture in medium alone (CTRL), SDF-1 (100 ng/mL) or CTCE-0214 (100 ng/mL) were determined by flow cytometry. A representative of 2 independent experiments is shown.

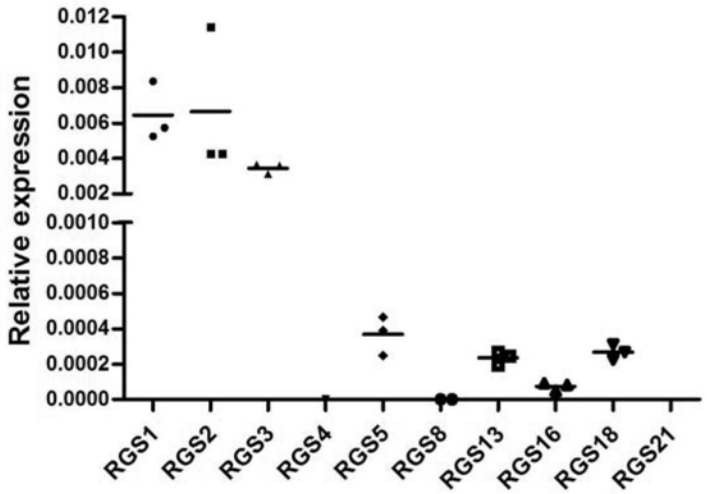

Figure 4.10 Basal mRNA expression of R4 RGS subfamily members

Total RNA (500 ng) from freshly isolated CB $CD34^+$ cells (n = 3) were reversed transcribed and RGS expression was determined by qPCR using gene-specific Taqman assays. Results are expressed as gene expression level relative to *GAPDH* expression.

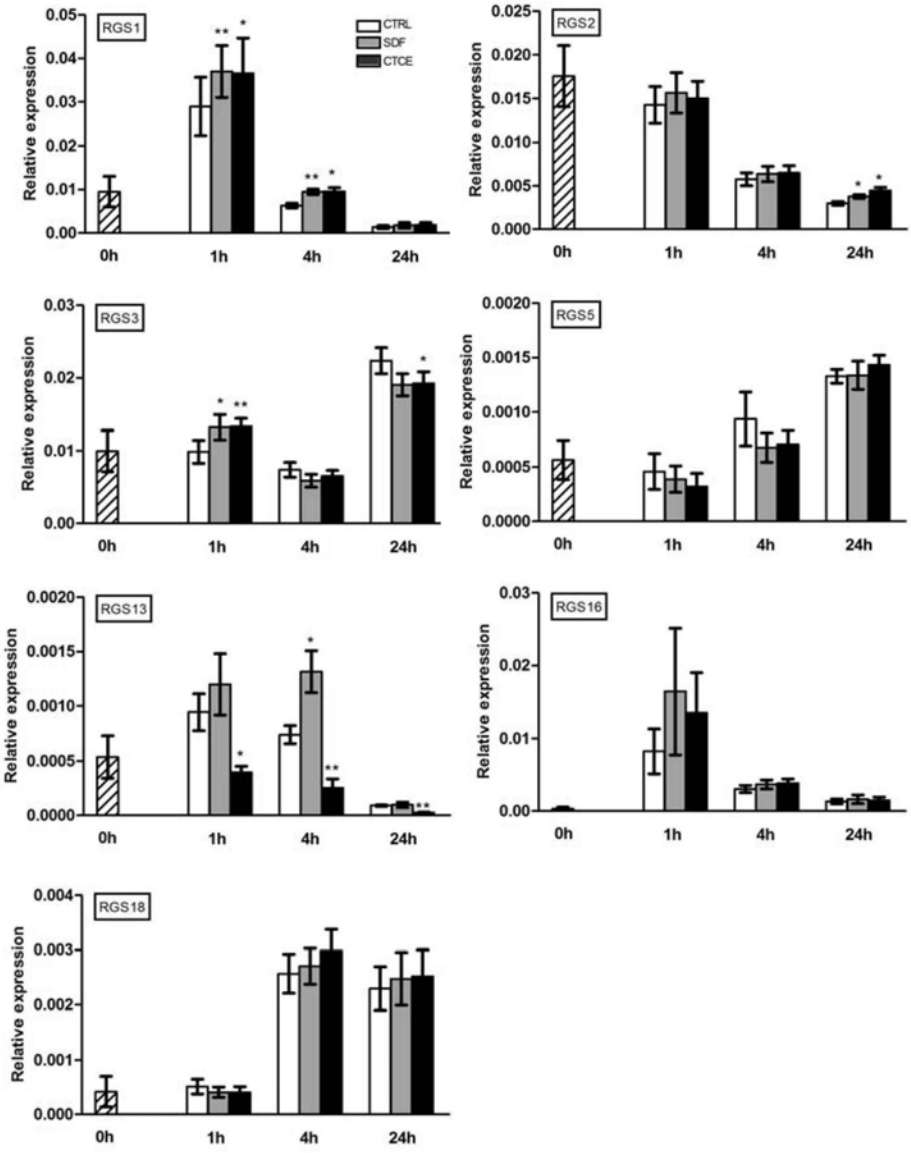

Figure 4.11 Effects of SDF-1 and CTCE-0214 on mRNA expression of R4 RGS subfamily members

Freshly isolated CB $CD34^+$ cells (0h) were cultured in medium alone (CTRL), or in the presence of SDF-1 (100 ng/mL) or CTCE-0214 (100 ng/mL) for 1, 4, or 24 hours (n = 3-4). RGS mRNA expression was determined by qPCR using gene-specific Taqman assays. Results are mean ± SEM and expressed as gene expression level relative to *GAPDH* expression. *, $P < .05$; **, $P < .01$.

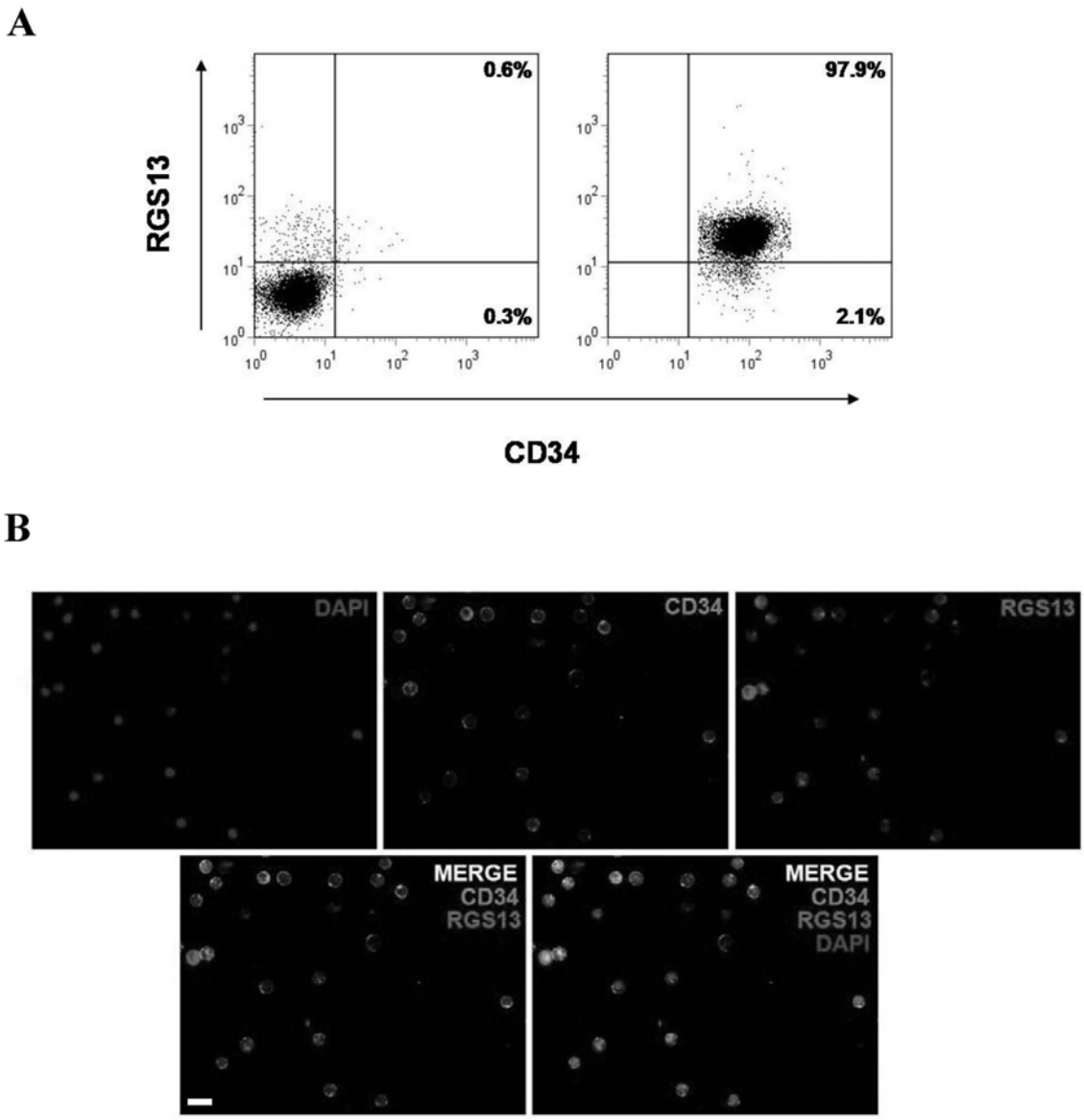

Figure 4.12 Protein expression of RGS13 on CB CD34$^+$ cells

(A) Expression of RGS13 on permeabilized CD34$^+$ cells was determined by flow cytometry using RGS13 and CD34 mAbs (right). Isotypic control mAbs staining is shown on the left. (B) Immunofluorescence microscopy analysis of CD34-FITC (green), RGS13-Texas Red (red) and nucleus (DAPI; blue) in CD34$^+$ cells. Bar = 10 μm.

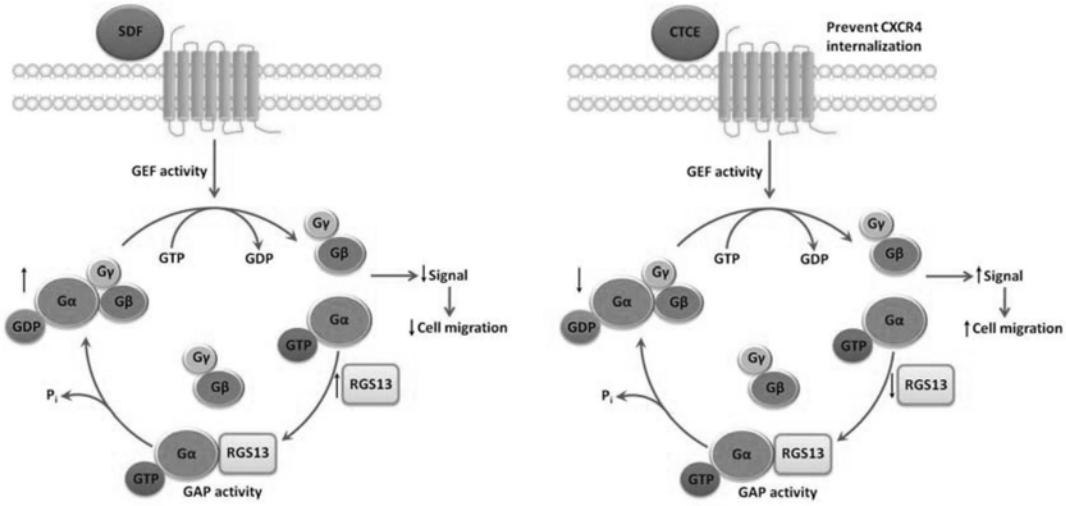

Figure 4.13 Proposed mechanisms of the differential effect of SDF-1 and CTCE-0214 on migration of CD34$^+$ cells

Exposure of CD34$^+$ cells to SDF-1 induces CXCR4 internalization and increases RGS13 expression. RGS13 binds to and increases the GTPase activity of the Gα subunit, resulting in conversion of active GTP-bound to inactive GDP-bound form. In response to a second challenge of SDF-1, because of the reduced CXCR4 level and inactivated Gα subunit, signaling in these cells will be impaired and thus leading to reduced migration. In CTCE-0214-treated cells, CXCR4 expression is maintained and RGS13 expression is decreased. The Gα subunit is constantly maintained in an active GTP-bound conformation. In response to SDF-1, signaling in these cells will thus be enhanced. Since CTCE-0214 also inhibits SDF-1-induced CXCR4 internalization, the combined effects on CXCR4 and RGS13 lead to improved cell migration. Abbreviations: GEF, guanine nucleotide exchange; GAP, GTPase-accelerating protein.

CHAPTER FIVE

Expression Profiling of Human Cord Blood $CD34^+$ Hematopoietic Stem/progenitor Cells in Response to SDF-1

5.1 Background and objectives

Homing of HSC to their BM niches is crucial to successful transplantation. However, the precise molecular mechanism controlling this important process is still not fully understood. Recent evidence suggests that homing efficiency can be improved through modulating the functions of intrinsic regulators of HSC motility. For example, CD26 was originally identified as a motility-suppressor of human CB hematopoietic progenitors (Christopherson *et al*., 2002). Subsequently, inhibition of CD26 activity by diprotin A was shown to be a promising approach to enhance homing of murine $Lineage^-Sca\text{-}1^+$ (Christopherson *et al*., 2004) and CB $CD34^+$ hematopoietic stem/progenitor cells (Christopherson *et al*., 2007). Thus, discovery of additional mediators governing stem cell homing may lead to new strategies for improving the efficacy of clinical stem cell transplantation. The approach is particularly applicable for CB transplantation in which the donor cell dose is a critical limiting factor for timely engraftment.

As HSC motility, homing and engraftment are primarily regulated by the SDF-1/CXCR4 axis (Lapidot and Kollet, 2002), we hypothesized that the SDF-1-induced transcriptional changes might play a role in regulating HSC homing. Using a genome-wide expression profiling approach, our specific objectives were:

(1) to conduct a comprehensive investigation on the transcriptional changes of CB $CD34^+$ cells in response to SDF-1.

(2) to identify/validate novel SDF-1-responsive genes that may be putatively involved in HSC homing.

5.2 Results

5.2.1 Effects of SDF-1 on the transcriptome of CB $CD34^+$ cells

By using the Affymetrix expression array, we first analyzed the SDF-1-induced transcriptional alterations in highly purified $CD34^+$ cells from 4 independent CB samples. An overview of the microarray analysis strategy is shown in Figure 5.1. The number of probe sets that had present signals in CB $CD34^+$ cells, as determined by the GCOS absolute analysis algorithm, was 26,469 ± 489 (representing 48.4% of total probe sets on the U133 Plus 2.0 GeneChips). Unsupervised hierarchical clustering analysis by the GeneSpring software revealed that the individual CB samples were clustered under the same branches despite the SDF-1 treatment, suggesting that the overall transcriptome changes induced by SDF-1 were mild. By statistical analysis, 745 transcripts ($P < .05$, paired t test), corresponding to 477 well-characterized genes, were found to be differentially expressed in SDF-1-treated $CD34^+$ cells with at least an 1.5-fold change in expression level when compared with control untreated cells. Among these transcripts, 524 were up-regulated and 221 were down-regulated by SDF-1 stimulation.

5.2.2 Functional annotation of the SDF-1-modulated genes

Using the DAVID functional annotation tool, we performed gene-gene ontogeny (GO) terms enrichment analysis of the SDF-1-modulated gene set. Of the 745 SDF-1-modulated transcripts, 683 transcripts were recognized by the DAVID tool for functional annotation. The GO terms (biological process) that were significantly modulated ($P < .05$) by SDF-1 are listed in Table 5.1.

SDF-1 regulates HSC homing by eliciting multiple cellular responses including cell motility (Aiuti *et al.*, 1997), adhesion (Peled *et al.*, 2000), actin cytoskeleton organization (Voermans *et al.*, 2001a) and small GTPase mediated signal transduction (Gu *et al.*, 2005). Consistently, functional annotation of the SDF-1-modulated gene set identified a significant enrichment of genes regulating these processes ($P < .05$; Table 5.1). Heat maps showing the expression levels of the SDF-1-modulated genes involved in the above 4 processes are shown in Figure 5.3. There were 39 genes associated with cell motility (Table 5.2), 28 genes associated with cell adhesion (Table 5.3), 19 genes associated with actin cytoskeleton organization (Table 5.4), and 19 genes associated with small GTPase mediated signal transduction (Table 5.5).

5.2.3 Quantitative PCR validation of selected SDF-1 modulated genes

To validate the microarray data, 19 genes were selected from the SDF-1-modulated gene set for assessment of their expression levels by qPCR. The selected genes can be classified into 4 main groups: (A) genes that have been shown to participate in homing of $CD34^+$ cells (MMP-9); (B) genes that have not been shown to participate in homing of $CD34^+$ cells, but were functionally annotated with homing-related functions such as cell motility and adhesion (CD9, CKLF, CMTM2, ITGAX, ITGB1, ITGB5); (C) genes that have not been functionally annotated with homing-related functions but were demonstrated to regulate cell motility or adhesion in at least one cell type (ANXA3, EPHA4, ITPR3, LMNA, MYO10, RGS13, SYNJ2); (D) genes without any known homing-related functions but with relatively high expressional changes (> 2.5-fold) in response to SDF-1 (DIXDC1, DUSP6, EMP1, ME1, ST6GALNAC3). Using a 1.5-fold cutoff as for microarray data filtering, differential expressions of 17 SDF-1-modulated genes (89.5%) were confirmed by qPCR with fold differences ranging from 1.51 to 6.23 (SDF-1 versus Control, $P < .01$; Table 5.6, Figure 5.4).

5.3 Discussion

Although the functional properties of SDF-1 have been investigated in both murine and human HSC, the impact of SDF-1 on $CD34^+$ cells at the gene transcription level and the functional relevance of such changes are largely unexplored. Matrix metalloproteinase-9 (MMP-9) is one of the very few genes known to be transcriptionally regulated by SDF-1, and its gelatinase activity was shown to be necessary for $CD34^+$ cells to migrate across the subendothelial basement membrane (Janowska-Wieczorek *et al.*, 2000). Thus, it may be possible to identify novel regulators of HSC homing through investigation of the SDF-1-mediated transcriptional changes in primary hematopoietic stem/progenitor cells.

In this study, we performed, to our knowledge, the first transcriptome profiling experiment on CB $CD34^+$ cells in response to a short-term (4 hours) SDF-1 exposure. Our results revealed that SDF-1 altered the expression of a large number of genes involved in cell motility, adhesion, cytoskeleton organization and small GTPase mediated signal transduction, which are crucial processes necessary for homing of HSC. These data are in line with a recent microarray study using $CD34^+$ cells derived from MPB (Rossi *et al.*, 2007). Intriguingly, the SDF-1-modulated genes identified in

our profiling experiments only displayed modest overlapping with those reported by Rossi *et al.* (2007). Among the 1,463 SDF-1-modulated genes identified in their microarray experiments, only 69 of them were regulated by SDF-1 in CB $CD34^+$ cells. This discrepancy could be due to the use of $CD34^+$ cells from different sources (Georgantas *et al.*, 2004). Since $CD34^+$ cells derived from MPB are pre-exposed to G-CSF before collection, it is possible that G-CSF may alter the transcriptional response of $CD34^+$ cells to SDF-1. Another possible reason could be the difference in timing of SDF-1 treatment (4 hours for CB $CD34^+$ cells versus 24 hours for MPB $CD34^+$ cells).

Notably, although some of the identified SDF-1-regulated genes have already been shown to participate in homing of human $CD34^+$ cells, e.g. MMP-9 (Janowska-Wieczorek *et al.*, 2000) and integrins (Peled *et al.*, 2000; Papayannopoulou *et al.*, 2001), we discovered many others that have not been characterized in HSC but were involved in regulating homing-related functions in other cell types, e.g. CD9 (Hemler, 2005), CKLF (Han *et al.*, 2001), CMTM2 (Han *et al.*, 2003), ANXA3 (Park *et al.*, 2005), EPHA4 (Fukai *et al.*, 2008), ITPR3 (Hardin and Vallejo, 2009), LMNA (Willis *et al.*, 2008; Emerson *et al.*, 2009), MYO10 (Pi *et al.*, 2007; Nie *et al.*, 2009), RGS13 (Shi *et al.*, 2002; Han *et al.*, 2006) and SYNJ2

(Chuang *et al*., 2004). Moreover, the homing-related functions of 5 highly changed genes (DIXDC1, DUSP6, EMP1, ME1 and ST6GALNAC3) have not been explored in any cell types. Thus, further characterization of their functional roles in human hematopoietic progenitors may potentially lead to discovery of novel regulators of stem cell homing.

Table 5.1 GO categories significantly modulated by SDF-1

GO ID	GO Terms	Count	%	*P* Value
GO:0065007	biological regulation	207	30.3%	4.35E-07
GO:0042060	wound healing	17	2.5%	1.37E-06
GO:0009605	response to external stimulus	43	6.3%	1.46E-06
GO:0009611	response to wounding	33	4.8%	1.92E-06
GO:0048731	system development	86	12.6%	3.52E-06
GO:0065008	regulation of biological quality	52	7.6%	3.62E-06
GO:0048523	negative regulation of cellular process	62	9.1%	3.86E-06
GO:0032502	developmental process	138	20.2%	4.64E-06
GO:0007596	blood coagulation	14	2.1%	7.10E-06
GO:0048519	negative regulation of biological process	63	9.2%	7.25E-06
GO:0006950	response to stress	59	8.6%	7.85E-06
GO:0050817	coagulation	14	2.1%	8.88E-06
GO:0048856	anatomical structure development	98	14.4%	1.20E-05
GO:0007599	hemostasis	14	2.1%	1.23E-05
GO:0000902	cell morphogenesis	34	5.0%	1.54E-05
GO:0032989	cellular structure morphogenesis	34	5.0%	1.54E-05
GO:0065009	regulation of a molecular function	36	5.3%	2.21E-05
GO:0051223	regulation of protein transport	8	1.2%	2.75E-05
GO:0007275	multicellular organismal development	103	15.1%	3.24E-05
GO:0046822	regulation of nucleocytoplasmic transport	8	1.2%	3.43E-05
GO:0007167	enzyme linked receptor protein signaling pathway	23	3.4%	4.39E-05
GO:0048513	organ development	64	9.4%	4.64E-05
GO:0030154	cell differentiation	84	12.3%	5.23E-05
GO:0048869	cellular developmental process	84	12.3%	5.23E-05
GO:0050790	regulation of catalytic activity	32	4.7%	5.95E-05
GO:0006928	cell motility	29	4.3%	6.21E-05
GO:0051674	localization of cell	29	4.3%	6.21E-05
GO:0007169	transmembrane receptor protein tyrosine kinase signaling pathway	18	2.6%	6.86E-05
GO:0009987	cellular process	414	60.6%	6.95E-05
GO:0050878	regulation of body fluid levels	14	2.1%	7.40E-05
GO:0009653	anatomical structure morphogenesis	57	8.4%	1.11E-04
GO:0048468	cell development	61	8.9%	1.24E-04
GO:0007154	cell communication	158	23.1%	1.75E-04
GO:0045859	regulation of protein kinase activity	19	2.8%	1.80E-04
GO:0016043	cellular component organization and biogenesis	112	16.4%	1.87E-04
GO:0050789	regulation of biological process	178	26.1%	1.87E-04
GO:0048518	positive regulation of biological process	55	8.1%	2.02E-04
GO:0008283	cell proliferation	43	6.3%	2.18E-04

Table 5.1 GO categories significantly modulated by SDF-1 - *Continued*

GO ID	GO Terms	Count	%	*P* Value
GO:0022610	biological adhesion	42	6.2%	2.38E-04
GO:0007155	cell adhesion	42	6.2%	2.38E-04
GO:0043549	regulation of kinase activity	19	2.8%	2.48E-04
GO:0008284	positive regulation of cell proliferation	19	2.8%	3.05E-04
GO:0051338	regulation of transferase activity	19	2.8%	3.20E-04
GO:0032501	multicellular organismal process	144	21.1%	4.26E-04
GO:0016265	death	43	6.3%	5.70E-04
GO:0008219	cell death	43	6.3%	5.70E-04
GO:0006915	apoptosis	41	6.0%	5.89E-04
GO:0042306	regulation of protein import into nucleus	6	0.9%	6.01E-04
GO:0033157	regulation of intracellular protein transport	6	0.9%	6.01E-04
GO:0012501	programmed cell death	41	6.0%	7.20E-04
GO:0001775	cell activation	18	2.6%	7.72E-04
GO:0050794	regulation of cellular process	163	23.9%	9.11E-04
GO:0051049	regulation of transport	12	1.8%	9.50E-04
GO:0044255	cellular lipid metabolic process	34	5.0%	9.76E-04
GO:0032386	regulation of intracellular transport	6	0.9%	1.06E-03
GO:0048522	positive regulation of cellular process	48	7.0%	1.11E-03
GO:0042221	response to chemical stimulus	33	4.8%	1.20E-03
GO:0007049	cell cycle	44	6.4%	1.22E-03
GO:0007165	signal transduction	141	20.6%	1.25E-03
GO:0016477	cell migration	19	2.8%	1.26E-03
GO:0006629	lipid metabolic process	39	5.7%	1.28E-03
GO:0007243	protein kinase cascade	24	3.5%	1.59E-03
GO:0016049	cell growth	15	2.2%	1.81E-03
GO:0000074	regulation of progression through cell cycle	29	4.3%	2.15E-03
GO:0008361	regulation of cell size	15	2.2%	2.30E-03
GO:0051726	regulation of cell cycle	29	4.3%	2.32E-03
GO:0007626	locomotory behavior	15	2.2%	2.40E-03
GO:0040007	growth	19	2.8%	2.76E-03
GO:0007242	intracellular signaling cascade	64	9.4%	2.78E-03
GO:0042981	regulation of apoptosis	29	4.3%	3.00E-03
GO:0043067	regulation of programmed cell death	29	4.3%	3.41E-03
GO:0046824	positive regulation of nucleocytoplasmic transport	4	0.6%	3.59E-03
GO:0009966	regulation of signal transduction	30	4.4%	3.74E-03
GO:0008202	steroid metabolic process	14	2.1%	3.91E-03
GO:0042127	regulation of cell proliferation	27	4.0%	4.03E-03
GO:0045321	leukocyte activation	15	2.2%	4.09E-03
GO:0042991	transcription factor import into nucleus	5	0.7%	4.34E-03

Table 5.1 GO categories significantly modulated by SDF-1 - *Continued*

GO ID	GO Terms	Count	%	*P* Value
GO:0042990	regulation of transcription factor import into nucleus	5	0.7%	4.34E-03
GO:0048858	cell projection morphogenesis	16	2.3%	4.52E-03
GO:0032990	cell part morphogenesis	16	2.3%	4.52E-03
GO:0051222	positive regulation of protein transport	4	0.6%	4.68E-03
GO:0007399	nervous system development	37	5.4%	5.86E-03
GO:0042348	NF-kappaB import into nucleus	4	0.6%	5.95E-03
GO:0042345	regulation of NF-kappaB import into nucleus	4	0.6%	5.95E-03
GO:0009410	response to xenobiotic stimulus	6	0.9%	6.31E-03
GO:0007249	I-kappaB kinase/NF-kappaB cascade	11	1.6%	7.74E-03
GO:0043066	negative regulation of apoptosis	15	2.2%	8.94E-03
GO:0046649	lymphocyte activation	13	1.9%	9.31E-03
GO:0043069	negative regulation of programmed cell death	15	2.2%	9.89E-03
GO:0031175	neurite development	12	1.8%	1.12E-02
GO:0042347	negative regulation of NF-kappaB import into nucleus	3	0.4%	1.22E-02
GO:0043085	positive regulation of catalytic activity	15	2.2%	1.22E-02
GO:0030097	hemopoiesis	13	1.9%	1.23E-02
GO:0048699	generation of neurons	17	2.5%	1.28E-02
GO:0006270	DNA replication initiation	5	0.7%	1.28E-02
GO:0007264	small GTPase mediated signal transduction	25	3.7%	1.34E-02
GO:0051051	negative regulation of transport	5	0.7%	1.43E-02
GO:0022402	cell cycle process	34	5.0%	1.54E-02
GO:0044271	nitrogen compound biosynthetic process	9	1.3%	1.59E-02
GO:0030029	actin filament-based process	14	2.1%	1.77E-02
GO:0048646	anatomical structure formation	12	1.8%	1.80E-02
GO:0006954	inflammatory response	17	2.5%	1.81E-02
GO:0045860	positive regulation of protein kinase activity	10	1.5%	1.85E-02
GO:0007610	behavior	18	2.6%	1.89E-02
GO:0048534	hemopoietic or lymphoid organ development	13	1.9%	2.03E-02
GO:0033674	positive regulation of kinase activity	10	1.5%	2.19E-02
GO:0045786	negative regulation of progression through cell cycle	13	1.9%	2.24E-02
GO:0006952	defense response	27	4.0%	2.31E-02
GO:0030036	actin cytoskeleton organization and biogenesis	13	1.9%	2.37E-02
GO:0022008	neurogenesis	17	2.5%	2.44E-02
GO:0051347	positive regulation of transferase activity	10	1.5%	2.48E-02
GO:0001568	blood vessel development	12	1.8%	2.49E-02
GO:0007010	cytoskeleton organization and biogenesis	25	3.7%	2.51E-02
GO:0030509	BMP signaling pathway	4	0.6%	2.63E-02
GO:0043405	regulation of MAP kinase activity	8	1.2%	2.66E-02

Table 5.1 GO categories significantly modulated by SDF-1 - *Continued*

GO ID	GO Terms	Count	%	*P* Value
GO:0051179	localization	112	16.4%	2.75E-02
GO:0001944	vasculature development	12	1.8%	2.75E-02
GO:0042307	positive regulation of protein import into nucleus	3	0.4%	2.76E-02
GO:0030866	cortical actin cytoskeleton organization and biogenesis	3	0.4%	2.76E-02
GO:0048666	neuron development	12	1.8%	2.94E-02
GO:0006916	anti-apoptosis	11	1.6%	2.95E-02
GO:0007595	lactation	4	0.6%	2.96E-02
GO:0002520	immune system development	13	1.9%	2.96E-02
GO:0051050	positive regulation of transport	5	0.7%	3.27E-02
GO:0030168	platelet activation	4	0.6%	3.31E-02
GO:0042330	taxis	10	1.5%	3.38E-02
GO:0006935	chemotaxis	10	1.5%	3.38E-02
GO:0030334	regulation of cell migration	6	0.9%	3.45E-02
GO:0050896	response to stimulus	108	15.8%	3.45E-02
GO:0051336	regulation of hydrolase activity	12	1.8%	3.78E-02
GO:0007267	cell-cell signaling	29	4.3%	3.79E-02
GO:0008610	lipid biosynthetic process	15	2.2%	3.84E-02
GO:0001558	regulation of cell growth	10	1.5%	4.04E-02
GO:0030865	cortical cytoskeleton organization and biogenesis	3	0.4%	4.05E-02
GO:0046209	nitric oxide metabolic process	4	0.6%	4.08E-02
GO:0006809	nitric oxide biosynthetic process	4	0.6%	4.08E-02
GO:0009887	organ morphogenesis	20	2.9%	4.15E-02
GO:0032535	regulation of cellular component size	5	0.7%	4.39E-02
GO:0000904	cellular morphogenesis during differentiation	10	1.5%	4.62E-02
GO:0050865	regulation of cell activation	7	1.0%	4.68E-02
GO:0002521	leukocyte differentiation	8	1.2%	4.73E-02

The SDF-1-modulated transcripts (paired *t* test, $P < .05$ and fold change ≥ 1.5) were analyzed for association with GO terms using the DAVID functional annotation tool. The GO terms with *P* values < .05 are listed.

Table 5.2 SDF-modulated genes associated with cell motility

Probe Set ID	Gene Symbol	Gene Title	SDF/CTRL (Fold Change)	*P* Value
216598_s_at	CCL2	chemokine (C-C motif) ligand 2	3.76 (± 0.93)	2.91E-02
201005_at	CD9	CD9 molecule	3.53 (± 0.17)	1.23E-04
1557126_a_at	PLD1	phospholipase D1, phosphatidylcholine-specific	2.45 (± 0.55)	3.96E-02
229967_at	CMTM2	CKLF-like MARVEL transmembrane domain containing 2	2.15 (± 0.23)	8.18E-03
231219_at	CMTM1	CKLF-like MARVEL transmembrane domain containing 1	2.10 (± 0.43)	4.73E-02
223451_s_at	CKLF	chemokine-like factor	2.00 (± 0.11)	9.90E-04
203085_s_at	TGFB1	transforming growth factor, beta 1	1.93 (± 0.28)	1.99E-02
87100_at	ABHD2	abhydrolase domain containing 2	1.91 (± 0.34)	3.06E-02
219257_s_at	SPHK1	sphingosine kinase 1	1.90 (± 0.15)	4.29E-03
229797_at	MCOLN3	mucolipin 3	1.89 (± 0.23)	1.23E-02
213746_s_at	FLNA	filamin A, alpha (actin binding protein 280)	1.80 (± 0.14)	6.41E-03
218368_s_at	TNFRSF12A	tumor necrosis factor receptor superfamily, member 12A	1.79 (± 0.19)	1.72E-02
203037_s_at	MTSS1	metastasis suppressor 1	1.77 (± 0.07)	6.88E-04
202910_s_at	CD97	CD97 molecule	1.73 (± 0.22)	2.13E-02
230045_at	CNTN2	contactin 2 (axonal)	1.73 (± 0.15)	8.14E-03
242517_at	KISS1R	KISS1 receptor	1.66 (± 0.07)	1.56E-03
210512_s_at	VEGFA	vascular endothelial growth factor A	1.65 (± 0.12)	7.67E-03
203510_at	MET	met proto-oncogene (hepatocyte growth factor receptor)	1.63 (± 0.21)	4.19E-02
218829_s_at	CHD7	chromodomain helicase DNA binding protein 7	1.62 (± 0.16)	1.38E-02
211924_s_at	PLAUR	plasminogen activator, urokinase receptor	1.61 (± 0.20)	2.87E-02

Table 5.2 SDF-modulated genes associated with cell motility - *Continued*

Probe Set ID	Gene Symbol	Gene Title	SDF/CTRL (Fold Change)	*P* Value
201136_at	PLP2	proteolipid protein 2 (colonic epithelium-enriched)	1.61 (± 0.05)	7.56E-04
204889_s_at	NEURL	neuralized homolog (Drosophila)	1.61 (± 0.23)	4.50E-02
208983_s_at	PECAM1	platelet/endothelial cell adhesion molecule	1.58 (± 0.12)	1.15E-02
224788_at	ARF6	ADP-ribosylation factor 6	1.57 (± 0.09)	6.04E-03
207206_s_at	ALOX12	arachidonate 12-lipoxygenase	1.55 (± 0.08)	3.85E-03
232184_at	ALS2	amyotrophic lateral sclerosis 2 (juvenile)	1.53 (± 0.15)	2.80E-02
212985_at	APBB2	amyloid beta (A4) precursor protein-binding, family B, member 2	1.52 (± 0.13)	1.79E-02
229936_at	GFRA3	GDNF family receptor alpha 3	1.52 (± 0.11)	1.20E-02
205786_s_at	ITGAM	integrin, alpha M (complement component 3 receptor 3 subunit)	1.52 (± 0.08)	5.03E-03
37117_at	ARHGAP8	Rho GTPase activating protein 8	0.67 (± 0.01)	2.39E-04
221748_s_at	TNS1	tensin 1	0.65 (± 0.06)	2.17E-02
1564241_at	ATP1A4	ATPase, Na+/K+ transporting, alpha 4 polypeptide	0.64 (± 0.08)	4.77E-02
1565484_x_at	EGFR	epidermal growth factor receptor	0.62 (± 0.07)	1.97E-02
201427_s_at	SEPP1	selenoprotein P, plasma, 1	0.58 (± 0.09)	2.40E-02
204563_at	SELL	selectin L	0.57 (± 0.09)	3.34E-02
206622_at	TRH	thyrotropin-releasing hormone	0.54 (± 0.07)	2.11E-02
206991_s_at	CCR5	chemokine (C-C motif) receptor 5	0.49 (± 0.04)	3.90E-03
206189_at	UNC5C	unc-5 homolog C (C. elegans)	0.21 (± 0.06)	1.43E-02
210683_at	NRTN	neurturin	0.19 (± 0.06)	3.96E-02

The SDF-1 modulated genes (paired *t* test, $P < .05$ and fold change ≥ 1.5) associated with cell motility are listed. Data are presented as the fold ratio of normalized signal intensities (SDF/CTRL).

Table 5.3 SDF-modulated genes associated with cell adhesion

Probe Set ID	Gene Symbol	Gene Title	SDF/CTRL (Fold Change)	*P* Value
210184_at	ITGAX	integrin, alpha X (complement component 3 receptor 4 subunit)	5.05 (± 1.92)	4.78E-02
214020_x_at	ITGB5	integrin, beta 5	4.51 (± 0.28)	1.41E-04
216598_s_at	CCL2	chemokine (C-C motif) ligand 2	3.76 (± 0.93)	2.91E-02
201005_at	CD9	CD9 molecule	3.53 (± 0.17)	1.23E-04
209875_s_at	SPP1	secreted phosphoprotein 1	3.18 (± 0.75)	2.47E-02
235944_at	HMCN1	hemicentin 1	2.76 (± 0.49)	1.73E-02
226189_at	ITGB8	integrin, beta 8	2.17 (± 0.40)	3.25E-02
201438_at	COL6A3	collagen, type VI, alpha 3	1.91 (± 0.07)	3.66E-04
203780_at	MPZL2	myelin protein zero-like 2	1.88 (± 0.10)	1.45E-03
38487_at	STAB1	stabilin 1	1.85 (± 0.18)	8.23E-03
227747_at	MPZL3	myelin protein zero-like 3	1.81 (± 0.30)	3.67E-02
209767_s_at	GP1BB	glycoprotein Ib (platelet), beta polypeptide	1.81 (± 0.19)	1.40E-02
202252_at	RAB13	RAB13, member RAS oncogene family	1.81 (± 0.33)	4.65E-02
218368_s_at	TNFRSF12A	tumor necrosis factor receptor superfamily, member 12A	1.79 (± 0.19)	1.72E-02
203037_s_at	MTSS1	metastasis suppressor 1	1.77 (± 0.07)	6.88E-04
202910_s_at	CD97	CD97 molecule	1.73 (± 0.22)	2.13E-02
230045_at	CNTN2	contactin 2 (axonal)	1.73 (± 0.15)	8.14E-03
206488_s_at	CD36	CD36 molecule (thrombospondin receptor)	1.72 (± 0.17)	1.21E-02
229335_at	CADM4	cell adhesion molecule 4	1.70 (± 0.17)	1.59E-02
202878_s_at	CD93	CD93 molecule	1.68 (± 0.05)	4.18E-04

Table 5.3 SDF-modulated genes associated with cell adhesion - *Continued*

Probe Set ID	Gene Symbol	Gene Title	SDF/CTRL (Fold Change)	*P* Value
202112_at	VWF	von Willebrand factor	1.66 (± 0.25)	3.91E-02
228094_at	AMICA1	adhesion molecule, interacts with CXADR antigen 1	1.64 (± 0.22)	4.75E-02
202896_s_at	SIRPA	signal-regulatory protein alpha	1.60 (± 0.16)	1.64E-02
216250_s_at	LPXN	leupaxin	1.60 (± 0.03)	1.35E-04
208983_s_at	PECAM1	platelet/endothelial cell adhesion molecule	1.58 (± 0.12)	1.15E-02
203612_at	BYSL	bystin-like	1.57 (± 0.12)	1.31E-02
224788_at	ARF6	ADP-ribosylation factor 6	1.57 (± 0.09)	6.04E-03
201655_s_at	HSPG2	heparan sulfate proteoglycan 2	1.55 (± 0.09)	4.60E-03
207206_s_at	ALOX12	arachidonate 12-lipoxygenase	1.55 (± 0.08)	3.85E-03
205786_s_at	ITGAM	integrin, alpha M (complement component 3 receptor 3 subunit)	1.52 (± 0.08)	5.03E-03
1565484_x_at	EGFR	epidermal growth factor receptor	0.62 (± 0.07)	1.97E-02
232523_at	MEGF10	multiple EGF-like-domains 10	0.62 (± 0.09)	4.51E-02
204563_at	SELL	selectin L	0.57 (± 0.09)	3.34E-02
238732_at	COL24A1	collagen, type XXIV, alpha 1	0.57 (± 0.06)	1.04E-02
207093_s_at	OMG	oligodendrocyte myelin glycoprotein	0.55 (± 0.05)	5.29E-03
206346_at	PRLR	prolactin receptor	0.46 (± 0.10)	4.40E-02
242064_at	SDK2	sidekick homolog 2 (chicken)	0.40 (± 0.06)	7.96E-03
242450_at	RGMB	RGM domain family, member B	0.19 (± 0.06)	3.07E-02

The SDF-1 modulated genes (paired *t* test, $P < .05$ and fold change ≥ 1.5) associated with cell adhesion are listed. Data are presented as the fold ratio of normalized signal intensities (SDF/CTRL).

Table 5.4 SDF-modulated genes associated with actin cytoskeleton organization and biogenesis

Probe Set ID	Gene Symbol	Gene Title	SDF/CTRL (Fold Change)	*P* Value
1559680_at	TTL	tubulin tyrosine ligase	2.23 (± 0.38)	2.08E-02
213746_s_at	FLNA	filamin A, alpha (actin binding protein 280)	1.80 (± 0.14)	6.41E-03
203037_s_at	MTSS1	metastasis suppressor 1	1.77 (± 0.07)	6.88E-04
200696_s_at	GSN	gelsolin (amyloidosis, Finnish type)	1.76 (± 0.13)	4.34E-03
216867_s_at	PDGFA	platelet-derived growth factor alpha polypeptide	1.71 (± 0.15)	7.50E-03
45297_at	EHD2	EH-domain containing 2	1.71 (± 0.15)	8.70E-03
205054_at	NEB	nebulin	1.69 (± 0.20)	2.60E-02
202483_s_at	RANBP1	RAN binding protein 1	1.63 (± 0.12)	8.19E-03
202192_s_at	GAS7	growth arrest-specific 7	1.63 (± 0.12)	8.81E-03
204889_s_at	NEURL	neuralized homolog (Drosophila)	1.61 (± 0.23)	4.50E-02
217849_s_at	CDC42BPB	CDC42 binding protein kinase beta (DMPK-like)	1.57 (± 0.18)	2.66E-02
224788_at	ARF6	ADP-ribosylation factor 6	1.57 (± 0.09)	6.04E-03
1554481_a_at	EPB41	erythrocyte membrane protein band 4.1	1.55 (± 0.19)	3.51E-02
202566_s_at	SVIL	supervillin	1.54 (± 0.17)	3.02E-02
228680_at	KIF3A	kinesin family member 3A	1.53 (± 0.16)	2.32E-02
212985_at	APBB2	amyloid beta (A4) precursor protein-binding, family B, member 2	1.52 (± 0.13)	1.79E-02
37117_at	ARHGAP8	Rho GTPase activating protein 8	0.67 (± 0.01)	2.39E-04
230891_at	TUBE1	Tubulin, epsilon 1, mRNA	0.61 (± 0.06)	1.29E-02
210650_s_at	PCLO	piccolo (presynaptic cytomatrix protein)	0.46 (± 0.07)	1.00E-02

The SDF-1 modulated genes (paired *t* test, $P < .05$ and fold change ≥ 1.5) associated with actin cytoskeleton organization and biogenesis are listed. Data are presented as the fold ratio of normalized signal intensities (SDF/CTRL).

Table 5.5 SDF-modulated genes associated with small GTPase mediated signal transduction

Probe Set ID	Gene Symbol	Gene Title	SDF/CTRL(Fold Change)	*P* Value
210790_s_at	SAR1A	SAR1 homolog A (S. cerevisiae)	2.63 (± 0.34)	5.82E-03
1557126_a_at	PLD1	phospholipase D1, phosphatidylcholine-specific	2.45 (± 0.55)	3.96E-02
233462_at	TBC1D28	TBC1 domain family, member 28	2.06 (± 0.30)	2.58E-02
1570035_at	TBC1D10A	CDNA clone IMAGE:4299416	1.99 (± 0.32)	2.16E-02
206636_at	RASA2	RAS p21 protein activator 2	1.87 (± 0.19)	7.62E-03
209514_s_at	RAB27A	RAB27A, member RAS oncogene family	1.86 (± 0.29)	2.76E-02
228708_at	RAB27B	Small GTP-binding protein Rab27b	1.83 (± 0.13)	3.56E-03
202252_at	RAB13	RAB13, member RAS oncogene family	1.80 (± 0.33)	4.65E-02
208840_s_at	G3BP2	GTPase activating protein (SH3 domain) binding protein 2	1.70 (± 0.19)	1.91E-02
202207_at	ARL4C	ADP-ribosylation factor-like 4C	1.68 (± 0.11)	6.12E-03
219412_at	RAB38	RAB38, member RAS oncogene family	1.66 (± 0.13)	8.17E-03
227123_at	RAB3B	Small GTP binding protein RAB3B (RAB3B)	1.61 (± 0.21)	4.15E-02
216620_s_at	ARHGEF10	Rho guanine nucleotide exchange factor (GEF) 10	1.59 (± 0.13)	1.37E-02
208983_s_at	PECAM1	platelet/endothelial cell adhesion molecule	1.58 (± 0.12)	1.15E-02
217849_s_at	CDC42BPB	CDC42 binding protein kinase beta (DMPK-like)	1.57 (± 0.18)	2.66E-02
224788_at	ARF6	ADP-ribosylation factor 6	1.57 (± 0.09)	6.04E-03
232184_at	ALS2	amyotrophic lateral sclerosis 2 (juvenile)	1.53 (± 0.15)	2.80E-02
1568713_a_at	TBC1D1	TBC1 (tre-2/USP6, BUB2, cdc16) domain family, member 1	0.66 (± 0.04)	5.34E-03
201813_s_at	TBC1D5	TBC1 domain family, member 5	0.59 (± 0.04)	3.12E-03

The SDF-1 modulated genes (paired *t* test, $P < .05$ and fold change ≥ 1.5) associated with small GTPase mediated signal transduction are listed.

Data are presented as the fold ratio of normalized signal intensities (SDF/CTRL).

Table 5.6 Expression data of 19 selected target genes in microarray and qPCR experiments

Gene Symbol	Gene Title	SDF/CTRL (Fold Change)	
		Array (n = 4)	qPCR (n = 8-10)
ANXA3	annexin A3	2.12 (± 0.29)	1.76 (± 0.12)***
CD9	CD9 molecule	3.53 (± 0.17)	2.91 (± 0.17)***
CKLF	chemokine-like factor	2.00 (± 0.11)	1.73 (± 0.06)***
CMTM2	CKLF-like MARVEL transmembrane domain containing 2	2.15 (± 0.23)	2.31 (± 0.40)**
DIXDC1	DIX domain containing 1	2.71 (± 0.57)	2.70 (± 0.11)**
DUSP6	dual specificity phosphatase 6	4.05 (± 1.21)	2.25 (± 0.12)***
EMP1	epithelial membrane protein 1	3.64 (± 0.58)	2.85 (± 0.29)***
EPHA4	EPH receptor A4	3.50 (± 0.52)	2.92 (± 0.29)***
ITGAX	integrin, alpha X (complement component 3 receptor 4 subunit)	5.05 (± 1.92)	1.42 (± 0.17)*
ITGB1	integrin, beta 1 (fibronectin receptor, beta polypeptide, antigen CD29 includes MDF2, MSK12)	1.55 (± 0.08)	1.03 (± 0.02)
ITGB5	integrin, beta 5	4.51 (± 0.28)	4.34 (± 0.58)***
ITPR3	inositol 1,4,5-triphosphate receptor, type 3	2.18 (± 0.19)	1.51 (± 0.14)**
LMNA	lamin A/C	2.75 (± 0.32)	2.44 (± 0.22)***
ME1	malic enzyme 1, NADP(+)-dependent, cytosolic	3.79 (± 0.82)	2.69 (± 0.32)***
MMP9	matrix metallopeptidase 9 (gelatinase B, 92kDa gelatinase, 92kDa type IV collagenase)	2.15 (± 0.35)	6.23 (± 3.32)**
MYO10	myosin X	5.49 (± 1.41)	2.56 (± 0.21)***

Table 5.6 Expression data of 19 selected target genes in microarray and qPCR experiments - *Continued*

Gene Symbol	Gene Title	SDF/CTRL (Fold Change)	
		Array (n = 4)	qPCR (n = 8-10)
RGS13	regulator of G-protein signaling 13	2.24 (± 0.41)	1.87 (± 0.15)***
ST6GALNAC3	ST6 (alpha-N-acetyl-neuraminyl-2,3-beta-galactosyl-1,3)-N-acetylgalactosaminide alpha-2,6-sialyltransferase 3	5.40 (± 0.58)	4.24 (± 0.58)***
SYNJ2	synaptojanin 2	3.02 (± 0.43)	1.94 (± 0.13)***

Nineteen SDF-1-modulated genes in microarray experiments (paired *t* test, $P < .05$ and fold change ≥ 1.5) were selected for qPCR validation. Microarray data are presented as the fold ratio of normalized signal intensities (SDF/CTRL). For qPCR data, gene expression levels were calculated by the comparative C_T method (normalized to GAPDH expression) and are represented as the fold ratio of relative expression levels (SDF/CTRL). *, $P < .05$; **, $P < .01$, ***, $P < .001$ Data are mean ± SEM.

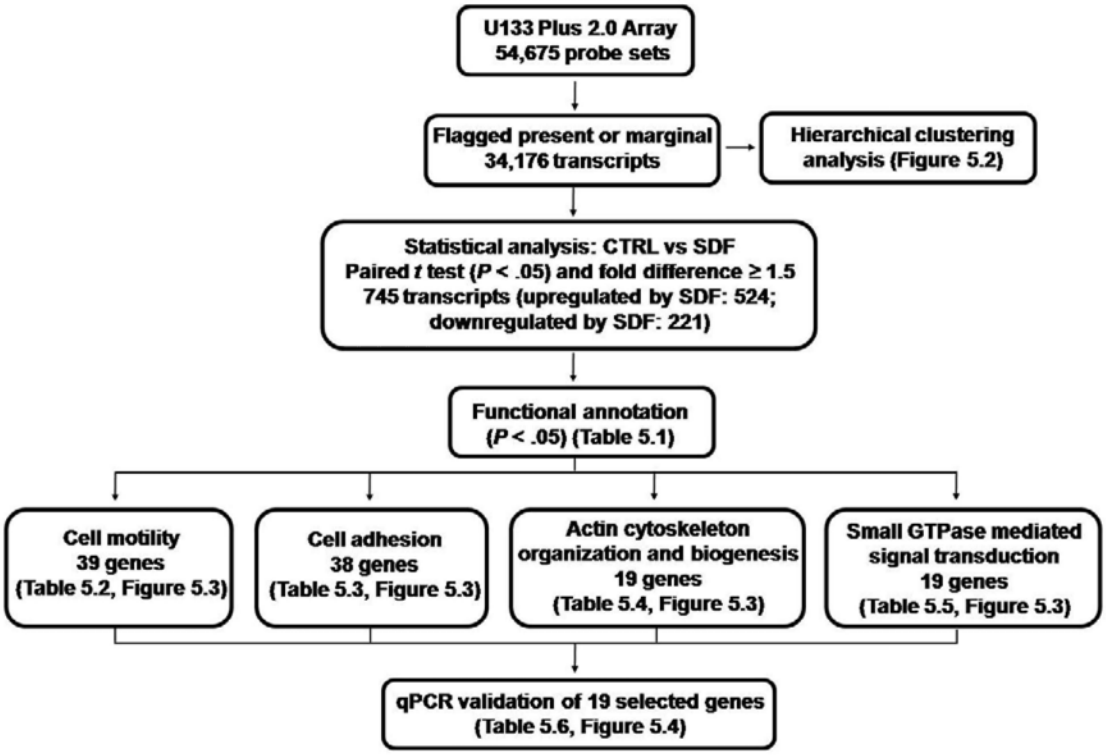

Figure 5.1 Workflow of microarray data analysis

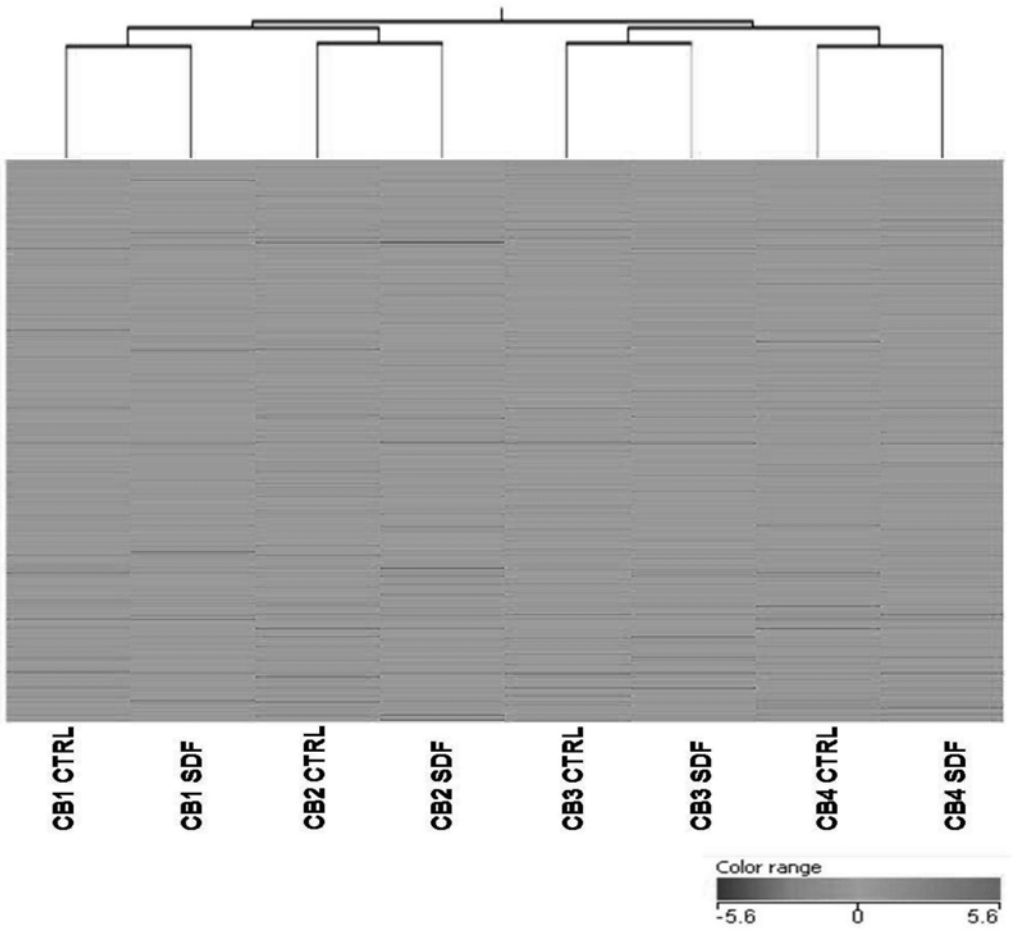

Figure 5.2 Hierarchical clustering analysis

Gene expression of SDF-1-stimulated (100 ng/mL) CB $CD34^+$ cells and the paired unstimulated control samples (CTRL) was analyzed by Affymetrix U133 Plus 2.0 GeneChip (n = 4). Hierarchical clustering analysis of the 34,176 probesets that had present or marginal signals in at least 1 of the 8 samples was performed using the GeneSpring GX10.0 software (Euclidean distance metric). Each row represents the expression data of a single probe set. The color scale represents the normalized signal intensity: red, relatively high expression; blue, relatively low expression when compared to the median expression level of each gene in all samples.

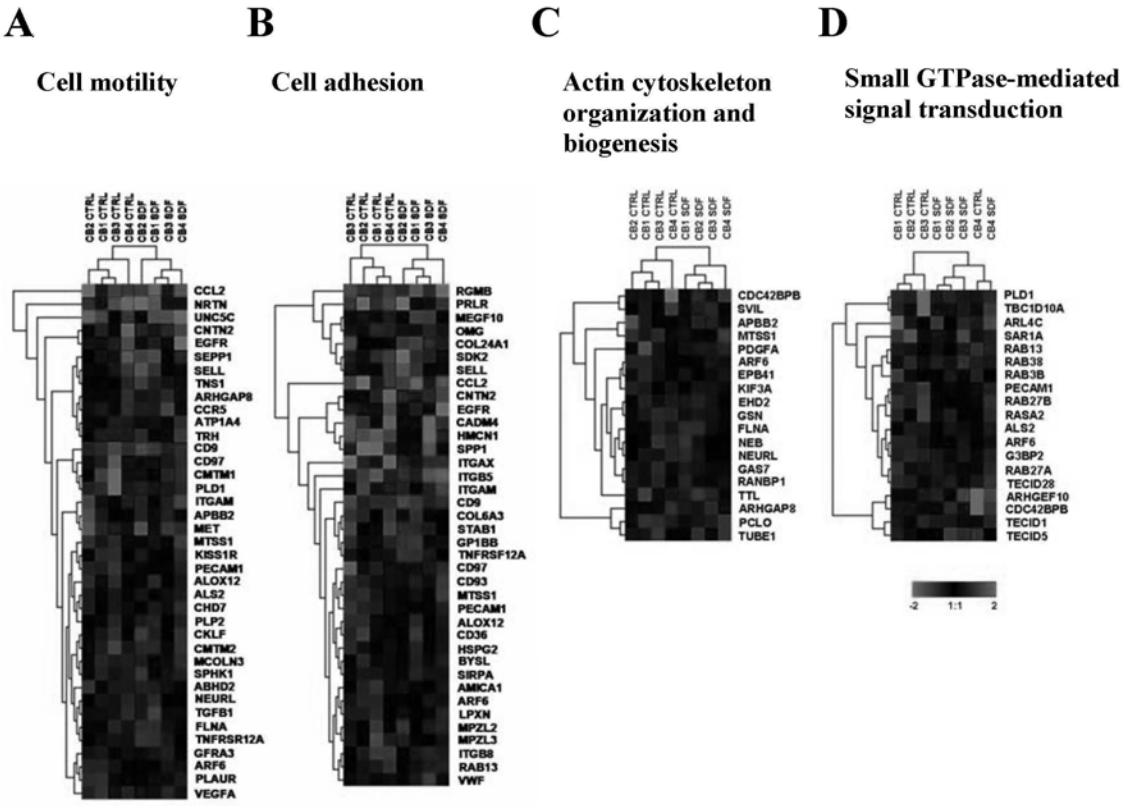

Figure 5.3 Functional classification of the SDF-1-modulated genes

Expression profiling of CB $CD34^+$ cells was performed after 4 hours incubation of SDF-1 (100 ng/mL; n = 4). Heat maps were constructed using the TIGR MeV software (Euclidean distance metric) on the SDF-1-modulated genes belonging to GO categories of (A) cell motility, (B) adhesion, (C) actin cytoskeleton organization and biogenesis and (D) small GTPase mediated signal transduction. using the TIGR MeV 2.2 software. The color scale represents $\log_2$ normalized signal intensity.

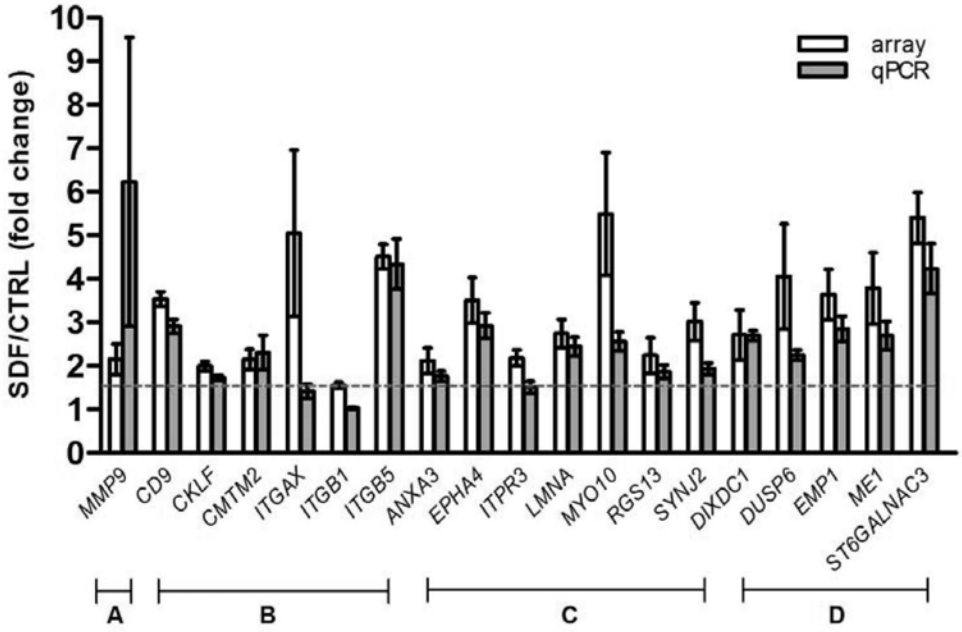

Figure 5.4 qPCR validation of the microarray data

Differential expression of 19 selected SDF-1-induced genes was validated by qPCR in $CD34^+$ cells derived from the same CB samples used in microarray experiments (n = 4) plus $CD34^+$ cells from an independent cohort of CB (n = 4-6). Gene expression levels were calculated by the comparative C_T method (normalized to GAPDH expression) and are represented as the fold ratio of relative expression levels (SDF/CTRL). The red dashed line represents the 1.5-fold cut-off. Results are depicted as mean ± SEM. Selected genes can be classified into 4 main groups: (A) genes that have been shown to participate in homing of $CD34^+$ cells; (B) genes that have not been shown to participate in homing of $CD34^+$ cells, but were functionally

annotated with homing-related functions such as cell motility and adhesion; (C) genes that have not been functionally annotated with homing-related functions but were demonstrated to regulate cell motility or adhesion in at least one cell type; (D) genes without any known homing-related functions but with relatively higher expressional changes (> 2.5-fold) in response to SDF-1 .

CHAPTER SIX

Role of the Tetraspanin CD9 in Homing of Human Cord Blood $CD34^+$ Hematopoietic Stem/progenitor Cells

6.1 Background and objectives

In chapter five, we have characterized the transcriptional changes of CB $CB34^+$ cells in response to SDF-1 using genome-wide expression microarray. In addition to genes that have been shown to participate in HSC homing (MMP-9 and integrins), we identified a panel of SDF-1-responsive genes that have not been characterized in hematopoietic progenitors but were demonstrated to be involved in homing-related functions in other cell types. Further validation of these genes functionally in primary $CD34^+$ cells may thus potentially leads to discovery of novel regulators of HSC homing. In the current study, our specific objectives were:

(1) to characterize the expression of a selected SDF-1-modulated gene, CD9, on CB $CD34^+$ cells and their subpopulations.

(2) to identify the signal transduction pathways along the SDF-1/CXCR4 axis leading to CD9 induction.

(3) to examine the role of CD9 in migration, adhesion and homing of $CD34^+$ cells using a series of *in vitro* and *in vivo* functional homing assays.

6.2 Results

6.2.1 CD9 is expressed in cord blood $CD34^+$ cells and is regulated by SDF-1 via specific signaling pathways

From the list of regulatory genes responsive to SDF-1 with putative homing functions (Figure 5.3), we focused on characterization of CD9 because it has been reported to modulate motility and adhesion in various cell types (Ikeyama *et al.*, 1993; Masellis-Smith and Shaw, 1994; Heagy *et al.*, 1995; Hemler, 2005). Moreover, its functions can be easily altered by neutralizing antibodies (Huang *et al.*, 2004; De Bruyne *et al.*, 2006). Flow cytometric analysis revealed that 14.2% ± 1.6% of CB $CD34^+$ cells expressed CD9 on their surfaces. Of importance, the more primitive $CD34^+CD38^{-/lo}$ subpopulation did express CD9, with level being slightly but significantly lower than the more lineage committed $CD34^+CD38^{hi}$ cells ($P = .002$; Figure 6.1). Simultaneous analysis demonstrated similar levels of CXCR4 expressions in the $CD34^+CD38^{-/lo}$ and $CD34^+CD38^{hi}$ subpopulations (Figure 6.1). Exposure of $CD34^+$ cells to SDF-1 (100 ng/mL) for 4 hours resulted in > 2-fold increase in CD9 expressions in total $CD34^+$ cells or their $CD38^{-/lo}$ or $CD38^{hi}$ subpopulations (Figure 6.2), confirming the microarray data at protein level (Figure 5.4). We then investigated the kinetics of SDF-1-induced CD9 expression in $CD34^+$ cells. Treatment with SDF-1 for 1 hour did not change the percentage of $CD34^+CD9^+$

cells (Figure 6.3 A). In contrast, a time-dependent increase in $CD9^+$ cells was observed at 4 hours and stayed at high levels at 24 hours ($P < .01$; Figure 6.3 A). At the mRNA level, induction of *CD9* was noted at 4 hours of SDF-1 treatment (2.6-fold increase; $P = .003$; Figure 6.3 B), but its expression declined to the basal level thereafter. Consistent with other reports (Signoret *et al.*, 1997; Basu and Broxmeyer, 2005), SDF-1 decreased cell surface CXCR4 expressions on both $CD34^+CD38^{-/lo}$ and $CD34^+CD38^{hi}$ cells (Figure 6.2), which was noted at 4 hours and 24 hours post-SDF-1 treatment (Figure 6.3 C). In line with membrane protein expression, exposure of $CD34^+$ cells to SDF-1 reduced *CXCR4* mRNA levels at 1 hour and 4 hours (Figure 6.3 D). In general, *CXCR4* mRNA expressions declined with duration in culture (Figure 6.3 D).

We then used a panel of pharmacological inhibitors of specific SDF-1 signal transducers (Ganju *et al.*, 1998; Majka *et al.*, 2000; Wang *et al.*, 2000; Zhang *et al.*, 2001; Petit *et al.*, 2005) to dissect the pathways leading to CD9 induction. As shown in Figure 6.4 A, SDF-1-induced CD9 expression was totally blocked by a CXCR4 antagonist AMD3100, while pre-exposure of $CD34^+$ cells to specific inhibitors of the G-protein alpha subunit (Gα; pertussis toxin), and Janus kinase 2 (JAK2; AG 490) partially inhibited CD9 induction (Figure 6.4 A). Interestingly, although SDF-1

activated Akt (Figure 6.5 A) and ERK (Figure 6.5 B) in $CD34^+$ cells, an inhibitor of MAP kinase kinase (MEK; PD 98059), but not the inhibitor of phosphatidylinositol 3-kinase (PI3K; wortmannin) suppressed SDF-1-induced CD9 upregulation (Figure 6.4 A). We also found that CD9 expression was partially blocked by GF 109203X, a protein kinase C (PKC) inhibitor, and completely blocked by a broader-range PKC inhibitor chelerythrine chloride (Figure 6.4 A). U-73122, a selective inhibitor of phosphatidylinositol-specific phospholipase C (PI-PLC), completely blocked SDF-1-induced CD9 expression, while the inhibitor of phosphatidylcholine-specific phospholipase C (PC-PLC; D609) had no effect (Figure 6.4 A). In parallel, we investigated the effect of these inhibitors on SDF-1-mediated CXCR4 downregulation. As shown in Figure 6.4 B, the decrease in $CD34^+CXCR4^+$ cells was significantly inhibited by pretreatment with AMD3100, pertussis toxin, PD 98059, wortmannin, chelerythrine chloride and U-73122, while AG490 slightly promoted CXCR4 downregulation.

We next studied the effect of specific inhibitors on SDF-1-induced ERK activation (an immediate downstream target of MEK). Exposure of $CD34^+$ cells to SDF-1 resulted in 2.1-fold increase in phosphorylated ERK level (Figure 6.6). Pretreatment with chelerythrine chloride or U-73122 significantly blocked ERK activation, while

wortmannin and AG490 had no effect (Figure 6.6). These data indicated that SDF-1-induced ERK activation was PKC- and PLC-dependent, but PI3K- and JAK2-independent.

We also tested whether direct activation of the identified signal transducers can enhance CD9 expression. As shown in Figure 6.7 A, exposure of $CD34^+$ cells to PKC activators phorbol 12-myristate 13-acetate (PMA), mezerein (MEZ) or ingenol 3,20-dibenzoate (IDB) significantly increased $CD34^+CD9^+$ cells by > 2.4-fold ($P < .05$). Consistent with other reports (Signoret *et al.*, 1997; Peled *et al.*, 1999), these PKC activators markedly reduced CXCR4 expression (Figure 6.7 B).

6.2.2 Anti-CD9 antibody alters migratory and adhesive functions of cord blood $CD34^+$ cells *in vitro*

To address possible involvement of CD9 in SDF-1-mediated motility, $CD34^+$ cells were cultured for 4 hours in the presence of a neutralizing anti-CD9 mAb (clone ALB6) (Huang *et al.*, 2004; De Bruyne *et al.*, 2006), or an isotype-matched control antibody (mouse IgG1). Without changing CXCR4 expression (Figure 6.8), pretreatment with anti-CD9 mAb enhanced transwell chemotactic migration of $CD34^+$ cells to a gradient of SDF-1 by 30.2% ($P = .033$; Figure 6.9 A). To investigate

whether migration can still be improved under a situation where CXCR4 expression is suppressed, we pretreated $CD34^+$ cells with SDF-1 (100 ng/mL) in the absence or presence of anti-CD9 mAb. Exposure of $CD34^+$ cells to SDF-1 decreased cell surface CXCR4 expression (Figure 6.8), which coincided with a significant inhibition of SDF-1-mediated migration (P = .004; Figure 4B). However, the presence of anti-CD9 mAb did not affect the migratory potential of SDF-1-pretreated cells (Figure 6.9 A).

The functional involvement of CD9 in migration across a human umbilical vein endothelial cell (HUVEC) monolayer was further explored. Unexpectedly, incubation of $CD34^+$ cells with anti-CD9 mAb resulted in an opposite effect on transendothelial migration when compared with migration across a bare transwell insert. As shown in Figure 6.9 B, anti-CD9 mAb inhibited transendothelial migration of $CD34^+$ cells towards a SDF-1 gradient by 12.3% (P = .024). However, transmigration of SDF-1-pretreated cells was not affected by anti-CD9 mAb (Figure 6.9 B).

Actin polymerization and mobilization of intracellular calcium are early cellular responses to SDF-1 in $CD34^+$ cells. In agreement with others (Voermans *et al.*,

2001a), SDF-1 markedly increased the polymerized actin content after a 15-second stimulation, which was inhibited by 4 hours of SDF-1 pretreatment (Figure 6.10 A). Blocking $CD34^+$ cells with anti-CD9 mAb did not significantly alter these responses (Figure 6.10 A). In contrast, CD9 neutralization significantly inhibited SDF-induced calcium flux in $CD34^+$ cells (Figure 6.10 B). We also found that anti-CD9 mAb did not affect SDF-1-induced Akt phosphorylation (Figure 6.10 C), an important signal leading to directional cell motility (Wang *et al.*, 2000).

We next examined the role of CD9 in $CD34^+$ cell adhesion to fibronectin- or HUVEC-coated surfaces. Anti-CD9 mAb significantly enhanced basal adhesion of $CD34^+$ cells to fibronectin ($P = .035$; Figure 6.11) and HUVEC monolayer ($P = .006$; Figure 6.12) by 55% and 16.6%, respectively. Consistent with reported findings (Peled *et al*, 2000), addition of SDF-1 significantly increased adhesion to either fibronectin ($P = .004$; Figure 6.11) or HUVEC ($P = .021$; Figure 6.12). In the presence of SDF-1, CD9 mAb did not affect adhesion of $CD34^+$ cells to fibronectin (Figure 6.11), but further promoted adhesion to HUVECs by 9.1% ($P = .054$; Figure 6.12).

6.2.3 CD9 neutralization impairs homing of transplanted $CD34^+$ cells in

NOD/SCID mice

To assess whether CD9 regulates the *in vivo* homing process, $CD34^+$ cells were cultured with either anti-CD9 mAb or isotypic control antibody for 4 hours, and injected into sublethally irradiated NOD/SCID mice. Preincubation of $CD34^+$ cells with anti-CD9 mAb significantly reduced homing to the recipient BM and spleen by 69.1% and 82.2%, respectively ($P < .05$; Figure 6.13).

To investigate whether $CD34^+CD9^+$ cells would home preferentially to hematopoietic organs, we compared the proportions of $CD34^+CD9^+$ cells in the initial injected $CD34^+$ population with those homed to BM and spleen 20 hours after cell infusion. In the injected population, 34.2% of $CD34^+$ cells expressed CD9, while a 1.6- and 1.7-fold increase in $CD34^+CD9^+$ cells were found in the NOD/SCID BM and spleen, respectively ($P < .05$; Figure 6.14). These data collectively indicated that CD9 expression in $CD34^+$ cells could be functionally important in the homing process.

6.3 Discussion

In this study, we identified the tetraspanin CD9 as one of the SDF-1-downstream protein that was regulated via the CXCR4, G-protein, PKC, PLC, ERK and JAK2 signals. We also provided the first evidence that CD9 was functionally involved in modulating SDF-1-mediated migration, adhesion and *in vivo* homing of $CD34^+$ cells.

Our results revealed that membrane CD9 was expressed on 14% of CB $CD34^+$ cells, and its expression could be rapidly inducible by SDF-1 stimulation in both $CD34^+CD38^{-/lo}$ and $CD34^+CD38^+$ subpopulations. Binding of SDF-1 to CXCR4 has been known to activate several signal transducers including ERK, JAK2, PI3K, PKC and PLC in several types of hematopoietic cells (Ganju *et al.*, 1998; Majka *et al.*, 2000; Wang *et al.*, 2000; Zhang *et al.*, 2001; Petit *et al.*, 2005). In human $CD34^+$ cells, Petit *et al* (2005) showed that SDF-1-induced MMP-9 transcription was dependent on ERK, PI3K, PI-PLC and PKC. Using a panel of inhibitors, we identified G-protein, JAK2, PKC, PLC and ERK, but not PI3K, as the downstream signals leading to protein expression of CD9 on CD34 cells via the SDF-1/CXCR4 axis. However, the SDF-1-induced CXCR4 downregulation was partially dependent on PI3K activity. We also observed that CD9 expression could be increased by activation of PKC. Based on the above data and reported SDF-1 signals (Chung *et al.*,

1997; Ganju *et al.*, 1998; Majka *et al.*, 2000; Wang *et al.*, 2000; Wu *et al.*, 2000; Zhang *et al.*, 2001; Petit *et al.*, 2005), we proposed a model of the SDF-1/CXCR4 signaling cascade leading to CD9 expressions in human $CD34^+$ cells (Figure 6.15). Upon binding of SDF-1 to CXCR4, uncoupling of the G-protein subunits might activate PI-PLC, which would result in activation of various PKC isoforms. PKC, in turn, would lead to MEK/ERK activation, followed by JAK2 activation. Finally, JAK2 might mediate CD9 expression via activation of the transcription factor STAT.

In the *in vitro* assays of homing-related functions, we showed that effects of anti-CD9 mAb on $CD34^+$ cells were specific and could be modulated by pre-treatment with SDF-1. While neutralizing CD9 had no effect on actin polymerization, it inhibited transendothelial motility towards a SDF-1 gradient and reduced calcium influx. On the other hand, anti-CD9 mAb increased $CD34^+$ cell motility through a bare filter and enhanced fibronectin or HUVEC adhesion. In SDF-1-pretreated cells, the situation appeared different. Despite CD9 expression in these cells was significantly enhanced, anti-CD9 mAb failed to alter their migratory responses, suggesting that the migratory function of CD9 might be masked when the CXCR4 expression is suppressed. Furthermore, the regulatory role of CD9 in cell motility appeared complex, and may vary depending on the presence of an

endothelial barrier. Such complications have also been reported in a variety of cancer cells (Zöller, 2009). While an inverse correlation between CD9 expression and metastastic development was observed in melanoma (Longo *et al.*, 2001), cervical carcinoma (Sauer *et al.*, 2003) and multiple myeloma (De Bruyne *et al.*, 2006), strong CD9 expression was found in contact sites between tumor and endothelial cells, where it promoted transendothelial migration and invasion. The regulation of cell adhesion by CD9 appears to be more straightforward. Pretreatment of cancer cells such as colon carcinoma (Ovalle *et al.*, 2007), melanoma (Longo *et al.*, 2001) or pre-B ALL (Masellis-Smith and Shaw, 1994) with CD9 mAb enhanced their adhesion to fibronectin, endothelial or BM stromal cells, suggesting that CD9 is a negative regulator of cellular adhesion. In agreement with these findings, our transwell experiments revealed that the neutralizing anti-CD9 mAb enhanced SDF-1-mediated migration without affecting CXCR4 expression, but it significantly inhibited migration of $CD34^+$ cells across an endothelial monolayer. Our observations, together with those in metastatic tumors, suggested that the presence of CD9 on $CD34^+$ cells might inhibit SDF-1-mediated cell motility to a certain extent, but such activities could be modulated by adhesion to endothelial cells. As a result, CD9 neutralization may strengthen heterotypic cell-cell interaction, and thus hamper transendothelial migration.

Importantly, we demonstrated that CD9 was involved in homing of $CD45^+CD34^+$ cells in the NOD/SCID mice transplantation model. While CD9 neutralization mildly inhibited transendothelial migration of $CD34^+$ cells *in vitro*, we found that the same treatment resulted in approximately 70% inhibition of CB $CD34^+$ cells homing to murine BM and over 80% inhibition to the spleen. By comparing the CD9 expression on injected $CD34^+$ cells with those homed to the NOD/SCID BM and spleen, we also observed a significant enrichment of $CD9^+$ cells in both hematopoietic niches. Thus, we speculated that $CD9^+$ cells might possess higher homing potential, although we cannot rule out the possibility that CD9 expression on $CD34^+$ cells was enhanced *in vivo*. A similar observation has been recently demonstrated in human B-acute lymphoblastic leukemia cells. Using the NOD/SCID/gc^{null} mice model, Nishida *et al.* (2009) found that transplantation of sorted $CD9^+$, but not $CD9^-$ leukemic cells resulted in tumorigenesis in the recipient BM and spleen. Since both $CD9^+$ and $CD9^-$ cells were capable of proliferation, defective homing of $CD9^-$ cells to hematopoietic organs may account for their inability of leukomogenesis. The homing efficiency of $CD34^+$ subpopulations has remained a controversial issue. Kollet *et al.* (2001) demonstrated that only $CD34^+CD38^{-/lo}$ cells could home to BM and spleen in NOD/SCID and NOD/SCID/$B2m^{null}$ mice, whereas Kerre *et al.* (2001) showed that both $CD34^+CD38^{-/lo}$ and $CD34^+CD38^+$ cells were capable of homing. Although CD9

expressions were demonstrated in both $CD34^+CD38^+$ and the more primitive $CD34^+CD38^{-/lo}$ cells, our *in vivo* experiments were limited by the cell dose transplantable to a NOD/SCID animal and did not reveal the relevance of CD9 on homing of these subpopulations. Such information would be particularly important for determining the role of CD9 in long-term engraftment of $CD34^+$ cells.

In summary, we provided the first evidence that the gene and membrane protein expressions of CD9 were upregulated by a short exposure to SDF-1 and mediated by specific CXCR4 downstream signals. Significantly, CD9 was shown to play a role in *in vitro* homing-related assays and *in vivo* homing of $CD34^+$ cells to the BM and spleen of NOD/SCID mice. We speculate that CD9 might be involved in the interaction of $CD34^+$ cells with endothelial cells during the homing process. It is anticipated that strategies for modulating CD9 expression and functions might improve homing of $CD34^+$ cells to their hematopoietic niches.

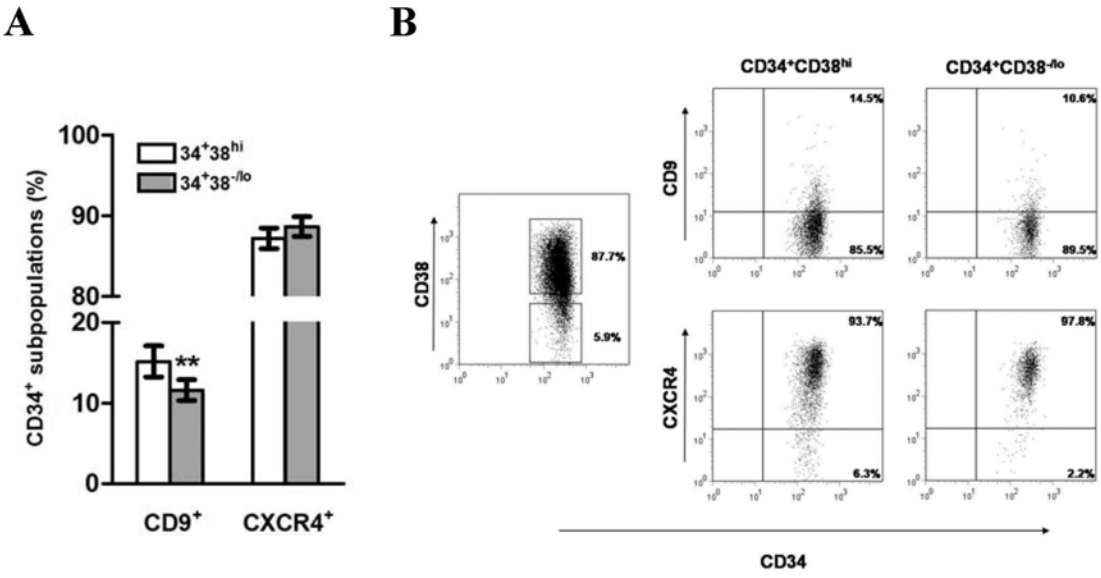

Figure 6.1 Basal CD9 and CXCR4 membrane expression on subpopulations of CB CD34$^+$ cells

(A) Cell surface expressions of CD9 and CXCR4 on CD34$^+$CD38^{hi} and the more primitive CD34$^+$CD38$^{-/lo}$ cells were determined by staining with CD9-FITC, CXCR4-PE, CD34-PerCP-Cy5.5 and CD38-APC mAbs, and were analyzed by flow cytometry (n = 41). (B) Gating strategy of CB CD34$^+$ subsets based on CD38 expression, and representative dot plots showing CD9 and CXCR4 expression on these subpopulations. Quadrants were set on the basis of staining with isotypic control antibodies, and the percentage of cells in each quadrant is depicted.

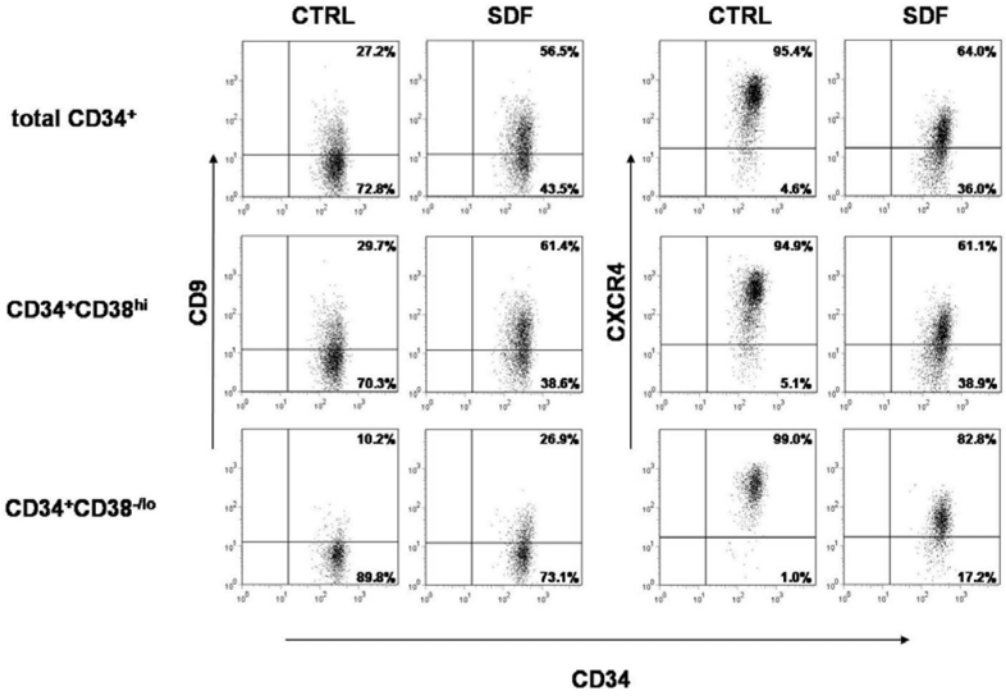

Figure 6.2 Cell surface expressions of CD9 and CXCR4 on CB CD34$^+$ cells and their subpopulations in response to SDF-1

Expressions of CD9 and CXCR4 expression on total CD34$^+$, CD34$^+$CD38^{hi} and CD34$^+$CD38$^{-/lo}$ cells after 4 hours culture in medium alone (CTRL) or in the presence of SDF-1 (100 ng/mL) were determined by flow cytometry. A representative of 4 independent experiments is shown.

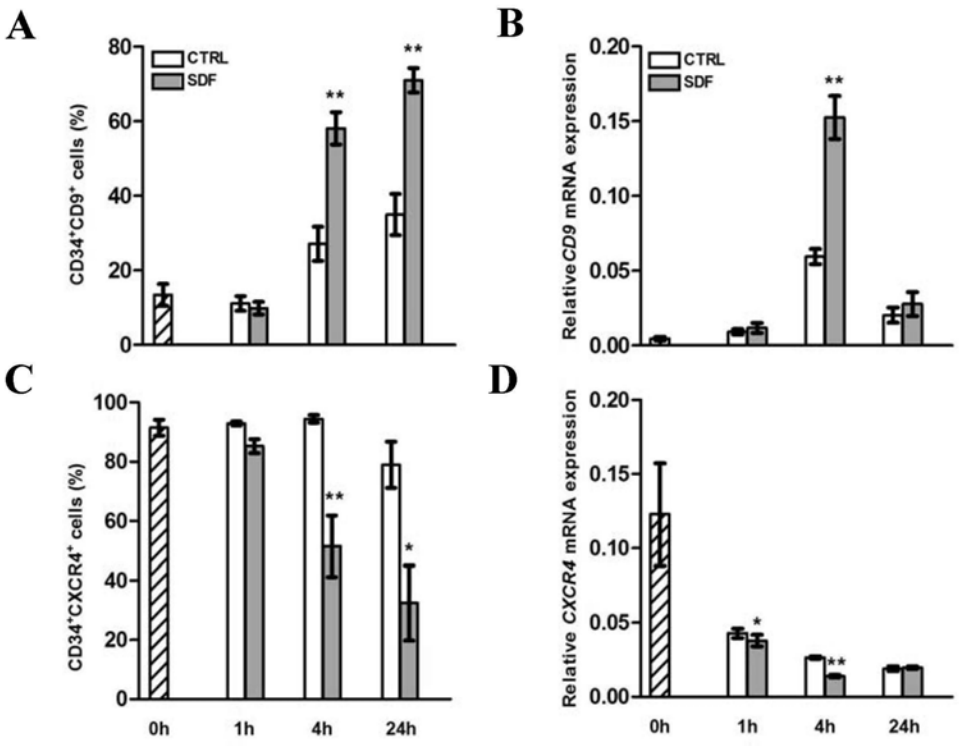

Figure 6.3 Kinetics of SDF-1-regulated CD9 and CXCR4 expressions

Freshly isolated CB $CD34^+$ cells (0h) were stimulated in the absence (CTRL) or presence of SDF-1 (100 ng/mL) for 1, 4 or 24 hours. (A and C) CD9 and CXCR4 cell surface (n = 3-5) and (B and D) mRNA expressions (n = 3-4) were determined by flow cytometry and qPCR, respectively. Results in (B) and (D) represent the gene expression levels relative to *GAPDH* expression. Data are mean ± SEM. *, $P < .05$; **, $P < .01$.

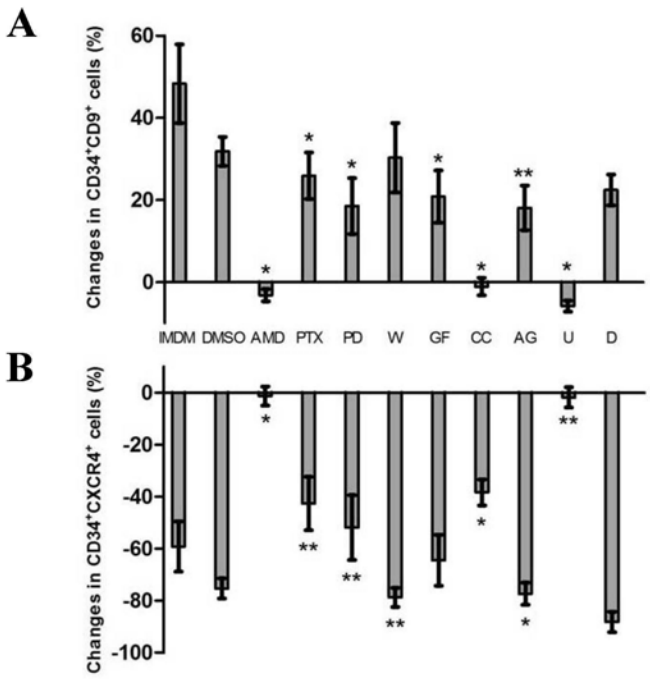

Figure 6.4 Effects of specific inhibitors of selected signal transducers on SDF-1-modulated CD9 and CXCR4 membrane expressions

Enriched CB $CD34^+$ cells, either untreated (IMDM or DMSO), or pretreated with AMD3100 (AMD; 10 μg/mL), pertussis toxin (PTX; 1 μg/mL), PD 98059 (PD; 40 μM), wortmannin (W; 50 nM), GF 109203X (GF; 2 μM), chelerythrine chloride (CC; 5 μM), AG490 (AG; 50 μM), U-73122 (U; 2.5 μM) or D609 (D; 10 μM) for 1 hour, were stimulated with or without SDF-1 (100 ng/mL) for 4 hours. (A) CD9 and (B) CXCR4 expressions were detected by flow cytometry (n = 4-8). Results are represented as the percentage changes in $CD9^+$ or $CXCR4^+$ cells after SDF-1 stimulation in the presence of each inhibitor. AMD and PTX were dissolved in IMDM, while other inhibitors were dissolved in DMSO. Data are mean ± SEM. *, $P < .05$; **, $P < .01$.

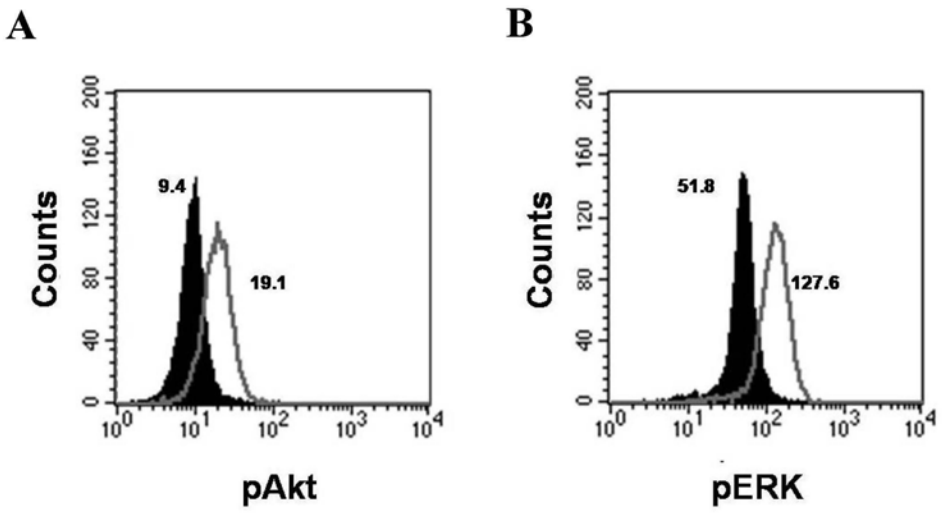

Figure 6.5 Effects of SDF-1 on Akt and ERK activation

Enriched CB $CD34^+$ cells were left untreated (filled histogram) or stimulated with SDF-1 (200 ng/mL; open histogram) for 1 minute. (A) Phosphorylated Akt (pAkt) and (B) phosphorylated ERK (pERK) levels were measured by flow cytometry. Representative histograms and the mean fluorescence intensity (MFI) are shown.

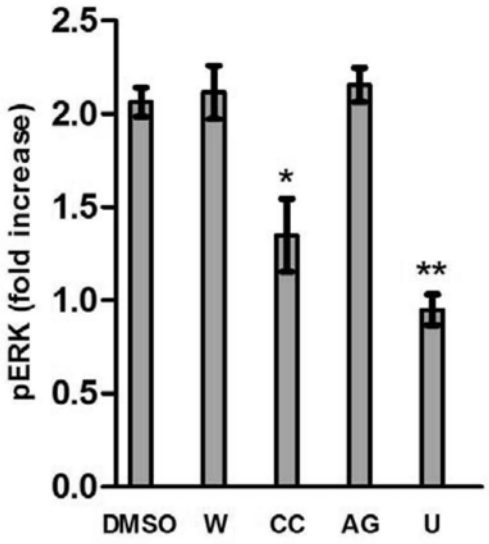

Figure 6.6 Effects of specific inhibitors of selected signal transducers on SDF-1-induced ERK activation

Enriched CB $CD34^+$ cells were stimulated with SDF-1 (200 ng/mL) for 1 minute after pretreatment with wortmannin (W; 50 nM), chelerythrine chloride (CC; 5 μM), AG490 (AG; 50 μM) or U-73122 (U; 2.5 μM) for 1 hour. Phosphorylated ERK (p-ERK) level was detected by flow cytometry (n = 3). Results are depicted as mean ± SEM. *, $P \leq .05$; **, $P < .01$.

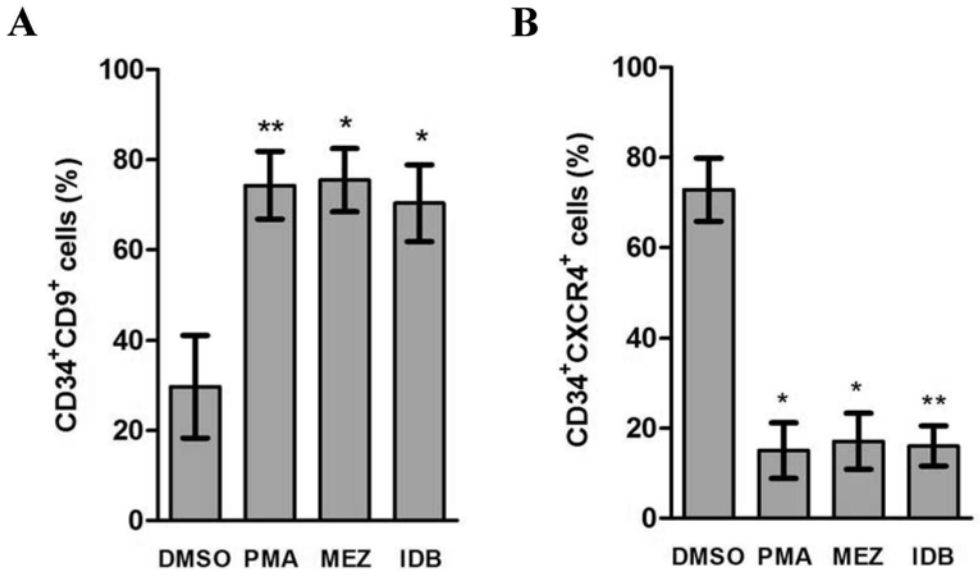

Figure 6.7 Effects of PKC activators on membrane expression of CD9 and CXCR4

Enriched CB $CD34^+$ cells were cultured for 4 hours in the absence (DMSO) or presence of PKC activators phorbol 12-myristate 13-acetate (PMA; 200 ng/mL), mezerein (MEZ; 200 ng/mL) or ingenol 3,20-dibenzoate (IDB; 200 ng/mL). Cell surface (A) CD9 and (B) CXCR4 expressions were detected by flow cytometry (n = 3). Results are depicted as mean ± SEM. *, $P \leq .05$; **, $P < .01$.

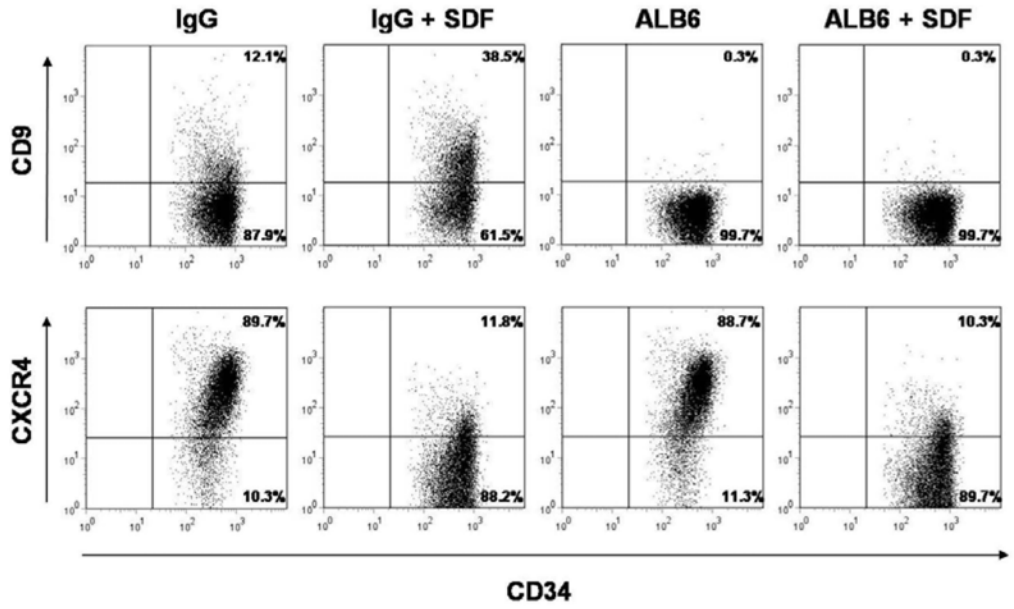

Figure 6.8 Effects of the anti-CD9 antibody, ALB6, on membrane expression of CD9 and CXCR4

Enriched CB $CD34^+$ cells were cultured in the presence of an anti-CD9 mAb (ALB6; 10 μg/mL) or an irrelevant isotypic control mAb (IgG; 10 μg/mL), or pretreated with SDF-1 (100 ng/mL) for 4 hours in the presence of the anti-CD9 mAb (ALB + SDF-1) or the isotypic control mAb (IgG + SDF-1). Cell surface expressions of CD9 and CXCR4 were detected by flow cytometry. Representative dot plots of CD9 and CXCR4 expression and the percentage of cells in each quadrant are shown.

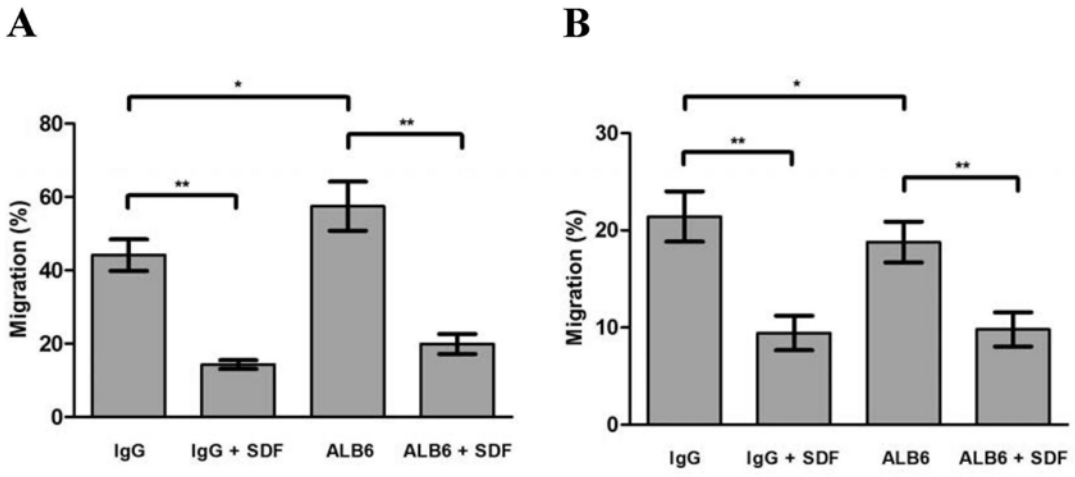

Figure 6.9 Effects of ALB6 on migration of CB CD34$^+$ cells

CD34$^+$ cells were cultured in the presence of an anti-CD9 mAb (ALB6; 10 μg/mL) or an irrelevant isotypic control mAb (IgG; 10 μg/mL), or pretreated with SDF-1 (100 ng/mL) for 4 hours in the presence of the anti-CD9 mAb (ALB + SDF-1) or the isotypic control mAb (IgG + SDF-1). Cell migration through (A) bare filters (n = 4) or across (B) HUVEC monolayers (n = 4) to a gradient of SDF-1 (100 ng/mL) was determined using transwells.

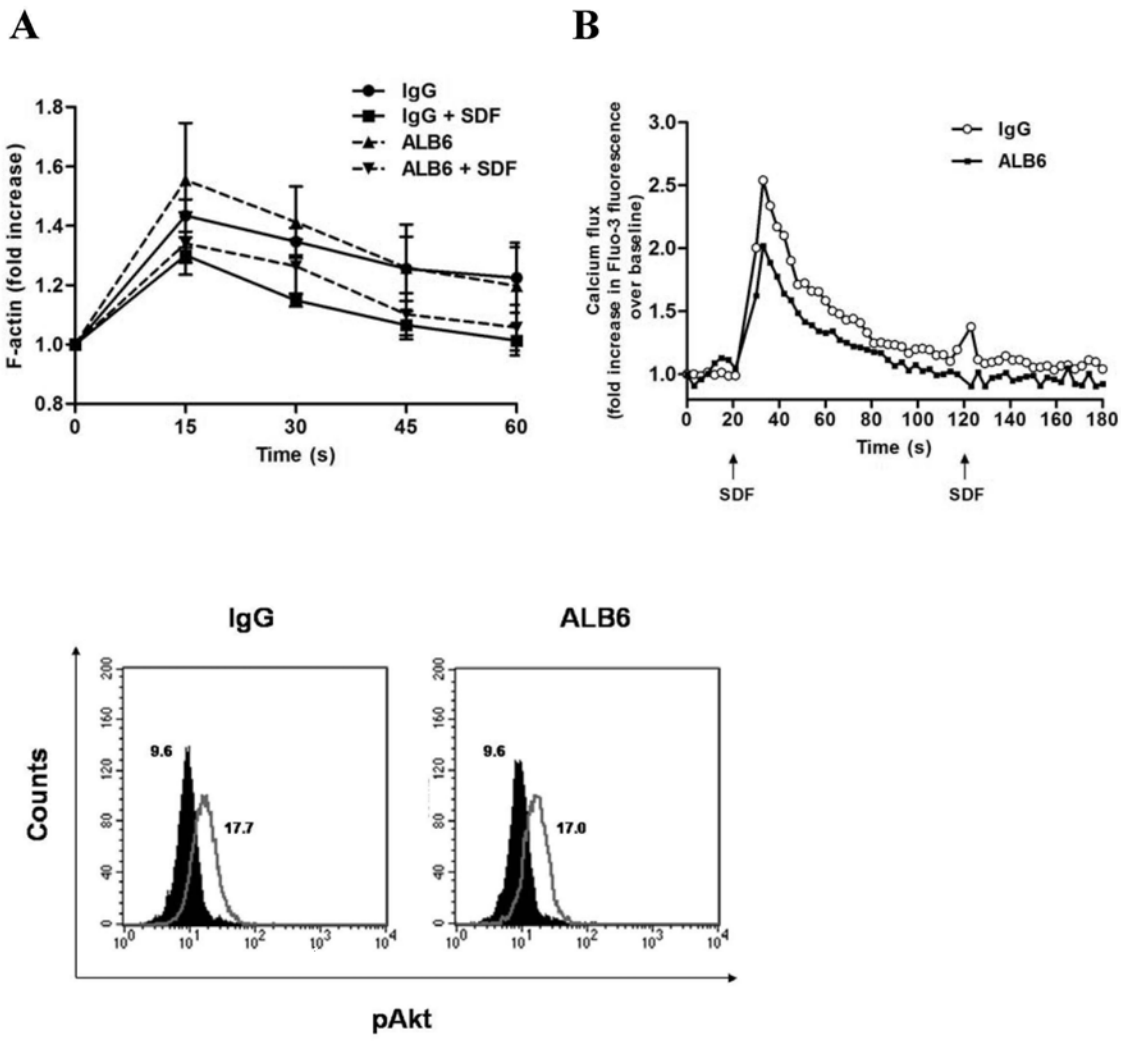

Figure 6.10 Effects of ALB6 on actin polymerization, calcium flux and Akt activation

$CD34^+$ cells were cultured in the presence of an anti-CD9 mAb (ALB6; 10 μg/mL) or an irrelevant isotypic control mAb (IgG; 10 μg/mL), or pretreated with SDF-1 (100 ng/mL) for 4 hours in the presence of the anti-CD9 mAb (ALB + SDF-1) or the isotypic control mAb (IgG + SDF-1). (A) Actin polymerization assay. Cells were

stimulated with SDF-1 (100 ng/mL) for the indicated times, and phalloidin-FITC fluorescence was measured by flow cytometry (n = 3-4). Results are depicted as mean ± SEM. (B) Cells were loaded with the Fluo-3AM and calcium flux following SDF-1 stimulation (100 ng/mL) was monitored by flow cytometry (n = 4). (C) Cells were left untreated (filled histogram) or stimulated with SDF-1 (200 ng/mL; open histogram) for 1 minute. Phosphorylated Akt (pAkt) levels were measured by flow cytometry (n = 2). Representative histograms and the mean fluorescence intensity (MFI) are shown.

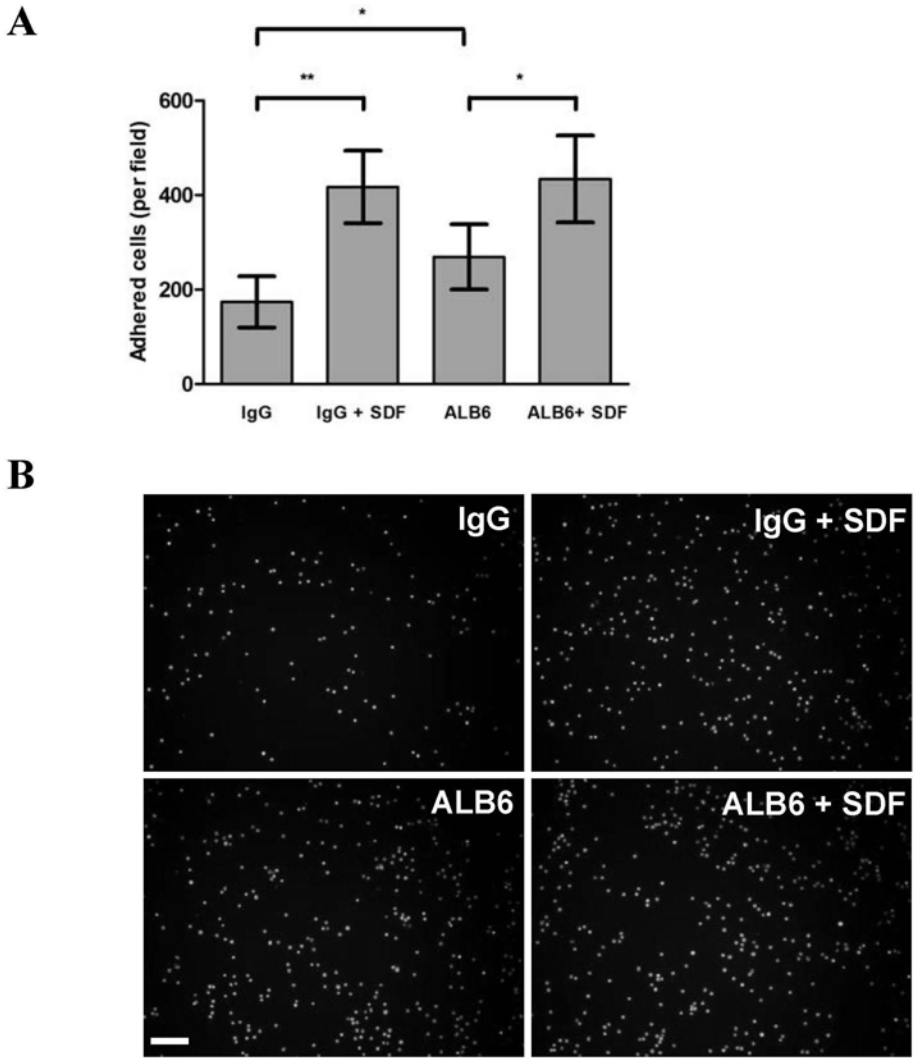

Figure 6.11 Effects of ALB6 on adhesion of CB CD34$^+$ cells to fibronectin

(A) CFSE-labeled cells were pretreated with IgG1 (10 μg/mL) or ALB6 (10 μg/mL) for 4 hours and plated on fibronectin-coated microwell plates (n = 4). Cells were either left unstimulated or stimulated with SDF-1 (100 ng/mL) for 45 minutes. Adherent cells from 5 random 20× fields were counted under the Olympus IX71 fluorescence microscope. Data represent mean ± SEM. *, $P \leq .05$; **, $P < .01$. (B) Representative fluorescence images showing adhered CD34$^+$ cells (green) under different conditions. Bar = 50 μm.

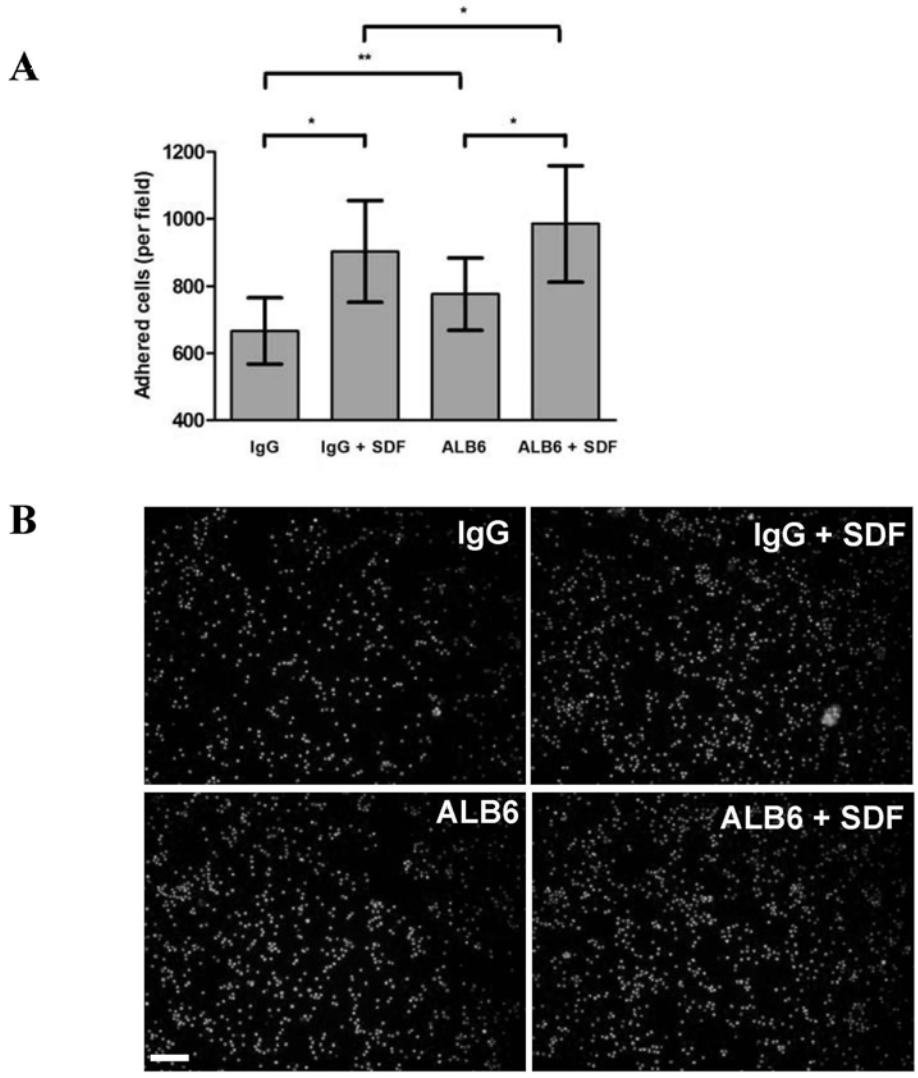

Figure 6.12 Effects of ALB6 on adhesion of CB CD34$^+$ cells to HUVEC

(A) CFSE-labeled cells were pretreated with IgG1 (10 μg/mL) or ALB6 (10 μg/mL) for 4 hours and plated on HUVEC-coated microwell plates (n = 4). Cells were either left unstimulated or stimulated with SDF-1 (100 ng/mL) for 45 minutes. Adherent cells from 5 random 20× fields were counted under the Olympus IX71 fluorescence microscope. Data represent mean ± SEM. *, $P \leq .05$; **, $P < .01$. (B) Representative fluorescence images showing adhered CD34$^+$ cells (green) under different conditions. Bar = 50 μm.

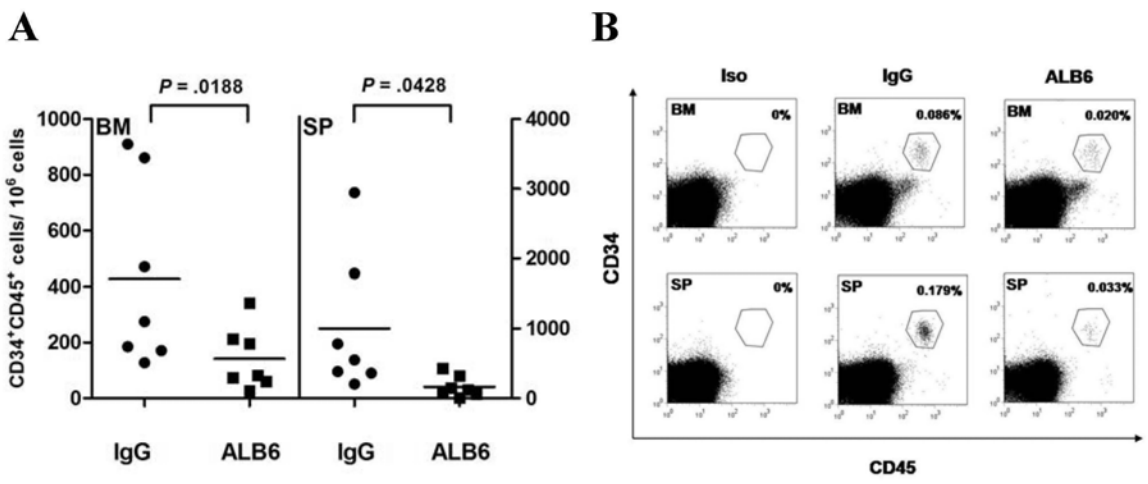

Figure 6.13 Effects of ALB6 on homing of CB CD34$^+$ cells in NOD/SCID mice

(A) CB CD34$^+$ cells were cultured in the presence of an anti-CD9 mAb (ALB6; 10 μg/mL) or an isotypic control mAb (IgG; 10 μg/mL) for 4 hours, and injected intravenously into NOD/SCID mice (1.9×10^5 to 5×10^5 cells per mouse). Bone marrow (BM) and spleen (SP) of recipient mice were analyzed for the presence of human CD45$^+$CD34$^+$ cells by flow cytometry 20 hours after transplantation. *P* values are indicated. (B) Representative flow cytometry analysis plots of human cell detection in BM and SP samples of transplanted mice. BM and SP samples from a mouse stained with isotypic control antibodies (Iso) are also presented. The gates used for identification of human CD45$^+$CD34$^+$ cells and the frequency of human cells in each gate are indicated.

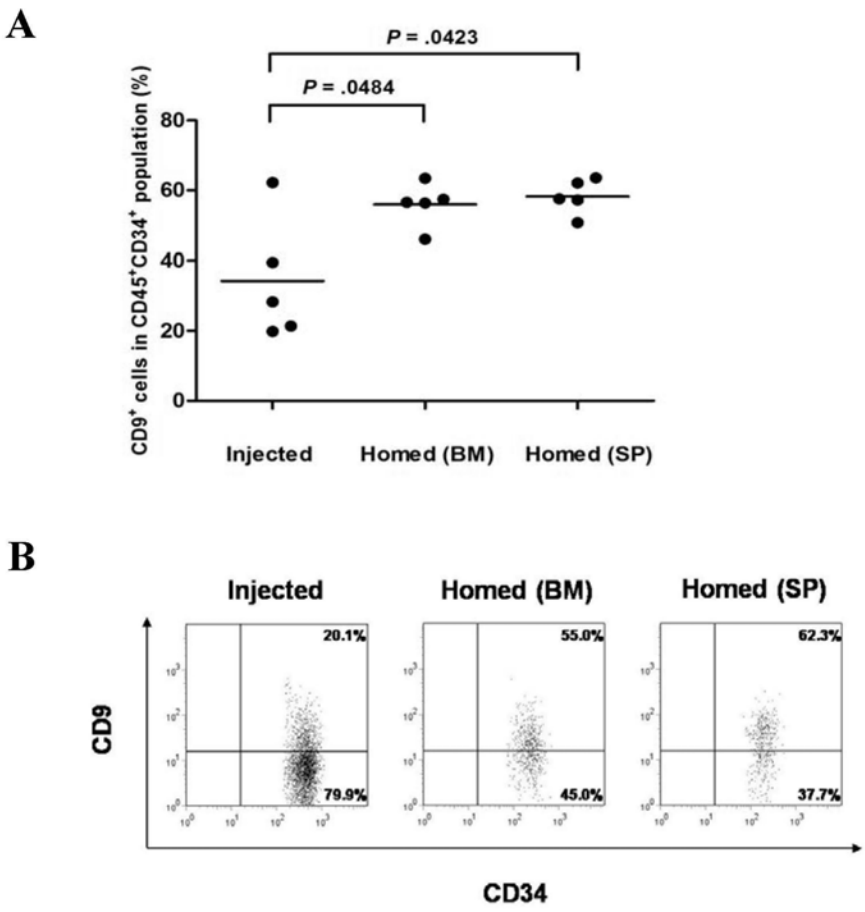

Figure 6.14 Comparison of CD9 expression on injected with homed CD34$^+$ cells

(A) CD9 membrane expressions on injected CB CD34$^+$ cells and those homed to BM and SP in NOD/SCID mice were analyzed by flow cytometry. Data summarize the results of 5 independent experiments. (B) Representative dot plots showing the CD9 expressions on injected and homed CD34$^+$ cells. The percentage of cells in each quadrant is depicted.

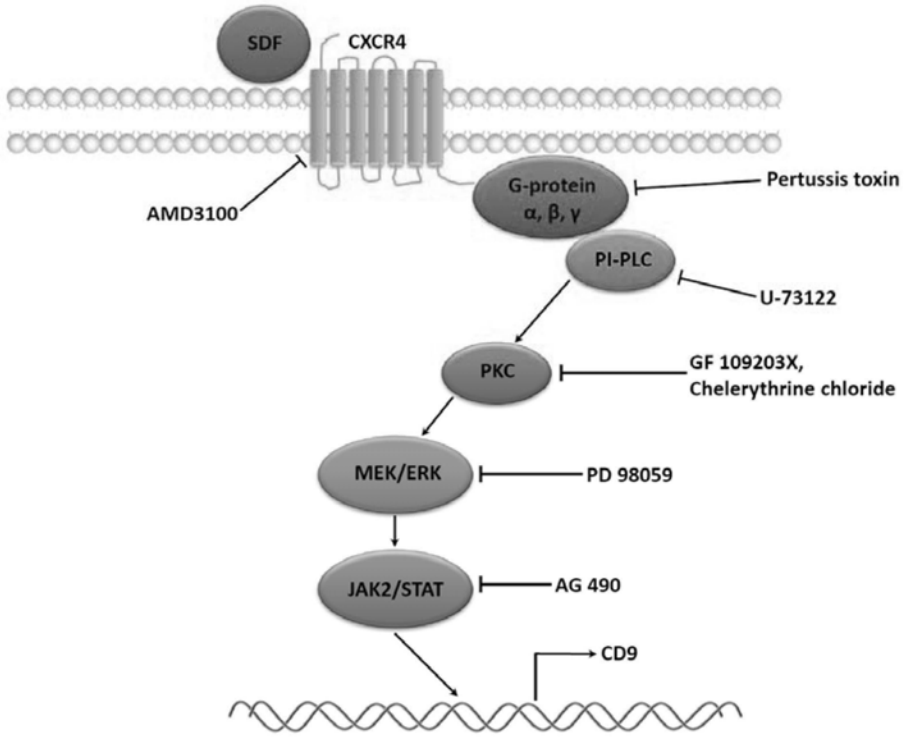

Figure 6.15 Proposed signaling pathways of SDF-1-induced CD9 expression in CB CD34$^+$ cells

Binding of SDF-1 to CXCR4 might lead to dissociation of G-proteins subunits and activation of PI-PLC and various PKC isoforms. Activated PKC, in turn, might activate MEK/ERK, followed by JAK2 activation. Activated JAK2 might finally mediate CD9 expression via activation of the transcription factor STAT.

CHAPTER SEVEN

General Discussion and Conclusion

In this study, we attempted to characterize novel regulators of HSC homing by investigating the effector molecules downstream of the SDF-1/CXCR4 axis. In the first part of our study, we investigated the homing-related responses of CB $CD34^+$ cells to SDF-1 and its peptide analog, CTCE-0214. We provided the first evidence that they differentially regulated cell motility and the expression of a negative regulator of G-protein signaling, RGS13. As RGS13 has been shown to inhibit the SDF-1/CXCR4-mediated cell migration or homing of several mature cell types of the hematological system (Shi *et al.*, 2002; Bansal *et al.*, 2008b, Hsu *et al.*, 2008), our results may thus potentially lead to the discovery of a new regulator of HSC homing.

In the second part of our study, we performed the first genome-wide expression profiling of $CB34^+$ cells in response to a short exposure of SDF-1. By functional categorization of the SDF-1-modulated gene set, we identified a panel of genes with putative homing functions. Using a series of *in vitro* and *in vivo* functional homing assays, we demonstrated for the first time that CD9 was involved in regulation of migration, adhesion and BM homing of CB $CD34^+$ cells. We also identified the

SDF-1/CXCR4 downstream signaling pathways leading to CD9 induction. To our knowledge, this is the first experimental evidence for the role of a tetraspanin in HSC homing.

One of the future directions for the RGS13 study is to conduct proof-of-function experiments in HSC. This can be achieved through investigating the effects of transfected RGS13-specific siRNA or expression vector on migration, homing and engraftment efficiency of $CD34^+$ cells. Furthermore, the role of RGS13 in HSC homing and engraftment can also be studied by comparing the homing and engraftment capacity of transplanted $Lineage^-Sca\text{-}1^+c\text{-}kit^+$ HSC from wild-type mice with the same population derived from *Rgs13*$^{-/-}$ mice (Bansal *et al.*, 2008a). Our data provided evidence that RGS13 expression on $CD34^+$ cells was subjected to regulation by SDF-1 *in vitro*. It will be interesting to determine whether the same regulation exists in the SDF-1-rich BM microenviroment *in vivo*. To address this question, the RGS13 expression on HSC that resides in the BM can be compared with those in circulation under normal physiological conditions, or after disruption of the SDF-1/CXCR4 axis by G-CSF or AMD3100 treatment. Such information would provide preliminary insights into the role of RGS13 in regulation of HSC retention/mobilization.

For CD9, further studies could be directed to investigate its role in long-term engraftment of HSC and the mode of action. We have already started to study the engraftment capacity of transplanted CB $CD34^+$ cells pretreated with the CD9 neutralizing antibody in the NOD/SCID mice model. Preliminary data of a small number of animals appear confirmative of the short term homing results. It is anticipated that results of long term engraftment (6 to 10 weeks post-transplantation) will be available within 6 months. These results will be important to confirm our current short-term homing data and to determine whether CD9 expressed on $CD34^+CD38^-$ cells is functional. Similar to other tetraspanins, CD9 has the ability to associate with a variety of cellular proteins and modulate their functions (Hemler, 2005). It will be interesting to identify the CD9-associating proteins that cause the altered migration, adhesion and homing responses in CB $CD34^+$ cells. This could be investigated by proteomic analysis of the CD9-immunoprecipitates or confocal microscopic analysis of the known CD9 partners such as integrins.

Homing and engraftment efficiency of HSC to their BM niches is a critical determinant of successful transplantation. With the mechanism being insufficiently understood, limited clinical studies have been performed to interfere the homing

process. It is anticipated that our findings would contribute to the development of new strategies for improving homing and engraftment of HSC. Moreover, our results might also be relevant to the understanding of mobilization of HSC and metastasis of leukemic stem cells from the BM microenvironment.

References

Adachi M., Taki T., Konishi T., Huang C. I., Higashiyama M. and Miyake M. Novel staging protocol for non-small-cell lung cancers according to MRP-1/CD9 and KAI1/CD82 gene expression. *J Clin Oncol.* 1998; 16(4): 1397-1406.

Adams G. B., Chabner K. T., Foxall R. B., Weibrecht K. W., Rodrigues N. P., Dombkowski D., Fallon R., Poznansky M. C. and Scadden D. T. Heterologous cells cooperate to augment stem cell migration, homing, and engraftment. *Blood.* 2003; 101(1): 45-51.

Ahmed F., Ings S. J., Pizzey A. R., Blundell M. P., Thrasher A. J., Ye H. T., Fahey A., Linch D. C. and Yong K. L. Impaired bone marrow homing of cytokine-activated CD34+ cells in the NOD/SCID model. *Blood.* 2004; 103(6): 2079-2087.

Aiuti A., Webb I. J., Bleul C., Springer T. and Gutierrez-Ramos J. C. The chemokine SDF-1 is a chemoattractant for human CD34+ hematopoietic progenitor cells and provides a new mechanism to explain the mobilization of CD34+ progenitors to peripheral blood. *J Exp Med.* 1997; 185(1) :111-120.

Angelopoulou M. K., Rinder H., Wang C., Burtness B., Cooper D. L. and Krause D. S. A preclinical xenotransplantation animal model to assess human hematopoietic stem cell engraftment. *Transfusion.* 2004; 44(4): 555-566.

Anzai N., Lee Y., Youn B. S., Fukuda S., Kim Y. J., Mantel C., Akashi M. and Broxmeyer H. E. C-kit associated with the transmembrane 4 superfamily proteins constitutes a functionally distinct subunit in human hematopoietic progenitors. *Blood.* 2002; 99(12): 4413-4421.

Araki H., Mahmud N., Milhem M., Nunez R., Xu M., Beam C. A. and Hoffman R. Expansion of human umbilical cord blood SCID-repopulating cells using chromatin-modifying agents. *Exp Hematol.* 2006; 34(2): 140-149.

Avigdor A., Goichberg P., Shivtiel S., Dar A., Peled A., Samira S., Kollet O., Hershkoviz R., Alon R., Hardan I., Ben-Hur H., Naor D., Nagler A. and Lapidot T. CD44 and hyaluronic acid cooperate with SDF-1 in the trafficking of human CD34+ stem/progenitor cells to bone marrow. *Blood.* 2004; 103(8): 2981-2989.

Ballen K. K., Shpall E. J., Avigan D., Yeap B. Y., Fisher D. C., McDermott K., Dey B. R., Attar E., McAfee S., Konopleva M., Antin J. H. and Spitzer TR. Phase I trial of parathyroid hormone to facilitate stem cell mobilization. *Biol Blood Marrow Transplant.* 2007; 13(7): 838-843.

Bansal G., DiVietro J. A., Kuehn H. S., Rao S., Nocka K. H., Gilfillan A. M. and Druey K. M. RGS13 controls g protein-coupled receptor-evoked responses of human mast cells. *J Immunol.* 2008b; 181(11): 7882-7890.

Bansal G., Druey K. M. and Xie Z. R4 RGS proteins: regulation of G-protein signaling and beyond. *Pharmacol Ther.* 2007; 116(3): 473-495.

Bansal G., Xie Z., Rao S., Nocka K. H. and Druey K. M. Suppression of immunoglobulin E-mediated allergic responses by regulator of G protein signaling 13. *Nat Immunol.* 2008a; 9(1): 73-80.

Barker J. N., Weisdorf D. J., DeFor T. E., Blazar B. R., McGlave P. B., Miller J. S., Verfaillie C. M. and Wagner J. E. Transplantation of 2 partially HLA-matched umbilical cord blood units to enhance engraftment in adults with hematologic malignancy. *Blood.* 2005; 105(3): 1343-1347.

Barreiro O., Yáñez-Mó M., Sala-Valdés M., Gutiérrez-López M. D., Ovalle S., Higginbottom A., Monk P. N., Cabañas C. and Sánchez-Madrid F. Endothelial tetraspanin microdomains regulate leukocyte firm adhesion during extravasation. *Blood.* 2005; 105(7): 2852-2861.

Barreiro O., Zamai M., Yáñez-Mó M., Tejera E., López-Romero P., Monk P. N., Gratton E., Caiolfa V. R. and Sánchez-Madrid F. Endothelial adhesion receptors are recruited to adherent leukocytes by inclusion in preformed tetraspanin nanoplatforms. *J Cell Biol.* 2008; 183(3): 527-542.

Basu S. and Broxmeyer H. E. Transforming growth factor-{beta}1 modulates responses of CD34+ cord blood cells to stromal cell-derived factor-1/CXCL12. *Blood.* 2005; 106(2): 485-493.

Baum C. M., Weissman I. L., Tsukamoto A. S., Buckle A. M. and Peault B. Isolation of a candidate human hematopoietic stem-cell population. *Proc Natl Acad Sci U S A.*

1992; 89(7): 2804-2808.

Benveniste P., Cantin C., Hyam D. and Iscove N. N. Hematopoietic stem cells engraft in mice with absolute efficiency. *Nat Immunol.* 2003; 4(7): 708-713.

Berditchevski F. Complexes of tetraspanins with integrins: more than meets the eye. *J Cell Sci.* 2001; 114(Pt 23): 4143-4151.

Berthebaud M., Rivière C., Jarrier P., Foudi A., Zhang Y., Compagno D., Galy A., Vainchenker W. and Louache F. RGS16 is a negative regulator of SDF-1-CXCR4 signaling in megakaryocytes. *Blood.* 2005; 106(9): 2962-2968.

Bhatia M., Bonnet D., Kapp U., Wang J. C., Murdoch B. and Dick J. E. Quantitative analysis reveals expansion of human hematopoietic repopulating cells after short-term ex vivo culture. *J Exp Med.* 1997; 186(4): 619-624.

Boucheix C. and Rubinstein E. Tetraspanins. *Cell Mol Life Sci.* 2001; 58(9): 1189-1205.

Bowman E. P., Campbell J. J., Druey K. M., Scheschonka A., Kehrl J. H. and Butcher E. C. Regulation of chemotactic and proadhesive responses to chemoattractant receptors by RGS (regulator of G-protein signaling) family members. *J Biol Chem.* 1998; 273(43): 28040-28048.

Broxmeyer H. E. Umbilical cord transplantation: epilogue. *Semin Hematol.* 2010; 47(1): 97-103.

Broxmeyer H. E., Orschell C. M., Clapp D. W., Hangoc G., Cooper S., Plett P. A., Liles W. C., Li X., Graham-Evans B., Campbell T. B., Calandra G., Bridger G., Dale D. C. and Srour E. F. Rapid mobilization of murine and human hematopoietic stem and progenitor cells with AMD3100, a CXCR4 antagonist. *J Exp Med.* 2005; 201(8): 1307-1318.

Byk T., Kahn J., Kollet O., Petit I., Samira S., Shivtiel S., Ben-Hur H., Peled A., Piacibello W. and Lapidot T. Cycling G1 CD34+/CD38+ cells potentiate the motility and engraftment of quiescent G0 CD34+/CD38-/low severe combined immunodeficiency repopulating cells. *Stem Cells.* 2005; 23(4): 561-574.

Cashman J. D. and Eaves C. J. High marrow seeding efficiency of human lymphomyeloid repopulating cells in irradiated NOD/SCID mice. *Blood.* 2000; 96(12): 3979-3981.

Castello S., Podestà M., Menditto V. G., Ibatici A., Pitto A., Figari O., Scarpati D., Magrassi L., Bacigalupo A., Piaggio G. and Frassoni F. Intra-bone marrow injection of bone marrow and cord blood cells: an alternative way of transplantation associated with a higher seeding efficiency. *Exp Hematol.* 2004; 32(8): 782-787.

Christopherson K. W. 2nd, Hangoc G. and Broxmeyer H. E. Cell surface peptidase CD26/dipeptidylpeptidase IV regulates CXCL12/stromal cell-derived factor-1 alpha-mediated chemotaxis of human cord blood CD34+ progenitor cells. *J Immunol.* 2002; 169(12): 7000-7008.

Christopherson K. W. 2nd, Hangoc G., Mantel C. R. and Broxmeyer H. E. Modulation of hematopoietic stem cell homing and engraftment by CD26. *Science.* 2004; 305(5686): 1000-1003.

Christopherson K. W. 2nd, Paganessi L. A., Napier S. and Porecha N. K. CD26 inhibition on CD34+ or lineage- human umbilical cord blood donor hematopoietic stem cells/hematopoietic progenitor cells improves long-term engraftment into NOD/SCID/Beta2null immunodeficient mice. *Stem Cells Dev.* 2007; 16(3): 355-360.

Chuang Y. Y., Tran N. L., Rusk N., Nakada M., Berens M. E. and Symons M. Role of synaptojanin 2 in glioma cell migration and invasion. *Cancer Res.* 2004; 64(22): 8271-8275.

Chung J., Uchida E., Grammer T. C. and Blenis J. STAT3 serine phosphorylation by ERK-dependent and -independent pathways negatively modulates its tyrosine phosphorylation. *Mol Cell Biol.* 1997; 17(11): 6508-6516.

Chute J. P. Stem cell homing. *Curr Opin Hematol.* 2006; 13(6): 399-406.

Clay D., Rubinstein E., Mishal Z., Anjo A., Prenant M., Jasmin C., Boucheix C. and Le Bousse-Kerdilès M. C. CD9 and megakaryocyte differentiation. *Blood.* 2001; 97(7): 1982-1989.

Cook G. A., Longhurst C. M., Grgurevich S., Cholera S., Crossno J. T. Jr. and

Jennings L. K. Identification of CD9 extracellular domains important in regulation of CHO cell adhesion to fibronectin and fibronectin pericellular matrix assembly. *Blood.* 2002; 100(13): 4502-4511.

Copelan E. A. Hematopoietic stem-cell transplantation. *N Engl J Med.* 2006; 354(17): 1813-1826.

Craig W., Kay R., Cutler R. L. and Lansdorp P. M. Expression of Thy-1 on human hematopoietic progenitor cells. *J Exp Med.* 1993; 177(5): 1331-1342.

Crump M. P., Gong J. H., Loetscher P., Rajarathnam K., Amara A., Arenzana-Seisdedos F., Virelizier J. L., Baggiolini M., Sykes B. D. and Clark-Lewis I. Solution structure and basis for functional activity of stromal cell-derived factor-1; dissociation of CXCR4 activation from binding and inhibition of HIV-1. *EMBO J.* 1997; 16(23): 6996-7007.

De Bruyne E., Andersen T. L., De Raeve H., Van Valckenborgh E., Caers J., Van Camp B., Delaissé J. M., Van Riet I. and Vanderkerken K. Endothelial cell-driven regulation of CD9 or motility-related protein-1 expression in multiple myeloma cells within the murine 5T33MM model and myeloma patients. *Leukemia.* 2006; 20(10): 1870-1879.

De Vries L., Zheng B., Fischer T., Elenko E. and Farquhar M. G. The regulator of G protein signaling family. *Annu Rev Pharmacol Toxicol.* 2000; 40: 235-271.

Delaney C., Heimfeld S., Brashem-Stein C., Voorhies H., Manger R. L. and Bernstein I. D. Notch-mediated expansion of human cord blood progenitor cells capable of rapid myeloid reconstitution. *Nat Med.* 2010; 16(2): 232-236.

Delaney C., Varnum-Finney B., Aoyama K., Brashem-Stein C. and Bernstein I. D. Dose-dependent effects of the Notch ligand Delta1 on ex vivo differentiation and in vivo marrow repopulating ability of cord blood cells. *Blood.* 2005; 106(8): 2693-2699.

Emerson L. J., Holt M. R., Wheeler M. A., Wehnert M., Parsons M. and Ellis J. A. Defects in cell spreading and ERK1/2 activation in fibroblasts with lamin A/C mutations. Biochim Biophys Acta. 2009; 1792(8): 810-821.

Forde S., Tye B. J., Newey S. E., Roubelakis M., Smythe J., McGuckin C. P., Pettengell R. and Watt S. M. Endolyn (CD164) modulates the CXCL12-mediated migration of umbilical cord blood CD133+ cells. *Blood.* 2007; 109(5): 1825-1833.

Frassoni F., Gualandi F., Podestà M., Raiola A. M., Ibatici A., Piaggio G., Sessarego M., Sessarego N., Gobbi M., Sacchi N., Labopin M. and Bacigalupo A. Direct intrabone transplant of unrelated cord-blood cells in acute leukaemia: a phase I/II study. *Lancet Oncol.* 2008; 9(9): 831-839.

Fritsch G., Stimpfl M., Kurz M., Printz D., Buchinger P., Fischmeister G., Hoecker P. and Gadner H. The composition of CD34 subpopulations differs between bone marrow, blood and cord blood. *Bone Marrow Transplant.* 1996; 17(2): 169-178.

Fukai J., Yokote H., Yamanaka R., Arao T., Nishio K. and Itakura T. EphA4 promotes cell proliferation and migration through a novel EphA4-FGFR1 signaling pathway in the human glioma U251 cell line. *Mol Cancer Ther.* 2008; 7(9): 2768-2778.

Ganju R. K., Brubaker S. A., Meyer J., Dutt P., Yang Y., Qin S., Newman W. and Groopman J. E. The α-chemokine, stromal cell-derived factor-1α, binds to the transmembrane G-protein-coupled CXCR-4 receptor and activates multiple signal transduction pathways. *J Biol Chem.* 1998; 273(36): 23169-23175.

Georgantas R. W., Tanadve V., Malehorn M., Heimfeld S., Chen C., Carr L., Martinez-Murillo F., Riggins G., Kowalski J. and Civin C. I. Microarray and serial analysis of gene expression analyses identify known and novel transcripts overexpressed in hematopoietic stem cells. *Cancer Res.* 2004; 64(13): 4434-4441.

Giebel B., Corbeil D., Beckmann J., Höhn J., Freund D., Giesen K., Fischer J., Kögler G. and Wernet P. Segregation of lipid raft markers including CD133 in polarized human hematopoietic stem and progenitor cells. *Blood.* 2004; 104(8): 2332-2338.

Gilman A. G. G proteins: transducers of receptor-generated signals. *Annu Rev Biochem.* 1987; 56: 615-649.

Gluckman E. and Rocha V. Cord blood transplant: strategy of alternative donor search. *Springer Semin Immunopathol.* 2004; 26(1-2): 143-154.

Gluckman E., Broxmeyer H. A., Auerbach A. D., Friedman H. S., Douglas G. W., Devergie A., Esperou H., Thierry D., Socie G., Lehn P., et al. Hematopoietic reconstitution in a patient with Fanconi's anemia by means of umbilical-cord blood from an HLA-identical sibling. *N Engl J Med.* 1989; 321(17): 1174-1178.

Gluckman E., Devergie A., Gerotta I., Hors J., Sasportes M., Boiron M. and Bernard J. Bone marrow transplantation in 65 patients with severe aplastic anemia. *Bull Cancer.* 1981; 68(1): 74-77.

Gu Y., Jasti A. C., Jansen M. and Siefring J. E. RhoH, a hematopoietic-specific Rho GTPase, regulates proliferation, survival, migration, and engraftment of hematopoietic progenitor cells. *Blood.* 2005; 105(4): 1467-1475.

Guenechea G., Segovia J. C., Albella B., Lamana M., Ramírez M., Regidor C., Fernández M. N. and Bueren J. A. Delayed engraftment of nonobese diabetic/severe combined immunodeficient mice transplanted with ex vivo-expanded human CD34(+) cord blood cells. *Blood.* 1999; 93(3): 1097-1105.

Gutman J. A., Turtle C. J., Manley T. J., Heimfeld S., Bernstein I. D., Riddell S. R. and Delaney C. Single-unit dominance after double-unit umbilical cord blood transplantation coincides with a specific CD8+ T-cell response against the nonengrafted unit. *Blood.* 2010; 115(4): 757-765.

Hall A. Rho GTPases and the actin cytoskeleton. *Science.* 1998; 279(5350): 509-514.

Han J. I., Huang N. N., Kim D. U. and Kehrl J. H. RGS1 and RGS13 mRNA silencing in a human B lymphoma line enhances responsiveness to chemoattractants and impairs desensitization. *J Leukoc Biol.* 2006; 79(6): 1357-1368.

Han S. B., Moratz C., Huang N. N., Kelsall B., Cho H., Shi C. S., Schwartz O. and Kehrl J. H. Rgs1 and Gnai2 regulate the entrance of B lymphocytes into lymph nodes and B cell motility within lymph node follicles. *Immunity.* 2005; 22(3): 343-354.

Han W., Ding P., Xu M., Wang L., Rui M., Shi S., Liu Y., Zheng Y., Chen Y., Yang T. and Ma D. Identification of eight genes encoding chemokine-like factor superfamily members 1-8 (CKLFSF1-8) by in silico cloning and experimental validation. *Genomics.* 2003; 81(6): 609-617.

Han Y., He T., Huang D. R., Pardo C.A., Ransohoff R. M. TNF-alpha mediates SDF-1 alpha-induced NF-kappa B activation and cytotoxic effects in primary astrocytes. J Clin Invest. 2001; 108(3): 425-435.

Hardin C. D. and Vallejo J. Dissecting the functions of protein-protein interactions: caveolin as a promiscuous partner. Focus on "Caveolin-1 scaffold domain interacts with TRPC1 and IP3R3 to regulate Ca2+ store release-induced Ca2+ entry in endothelial cells". *Am J Physiol Cell Physiol.* 2009; 296(3): C387-389.

Heagy W., Duca K. and Finberg R. W. Enkephalins stimulate leukemia cell migration and surface expression of CD9. *J Clin Invest.* 1995; 96(3): 1366-1374.

Hemler M. E. Targeting of tetraspanin proteins--potential benefits and strategies. *Nat Rev Drug Discov.* 2008; 7(9): 747-758.

Hemler M. E. Tetraspanin functions and associated microdomains. *Nat Rev Mol Cell Biol.* 2005; 6(10): 801-811.

Hemler M. E. Tetraspanin proteins mediate cellular penetration, invasion, and fusion events and define a novel type of membrane microdomain. *Annu Rev Cell Dev Biol.* 2003; 19: 397-422.

Heveker N., Montes M., Germeroth L., Amara A., Trautmann A., Alizon M. and Schneider-Mergener J. Dissociation of the signalling and antiviral properties of SDF-1-derived small peptides. *Curr Biol.* 1998; 8(7): 369-376.

Hirsch E., Iglesias A., Potocnik A. J., Hartmann U. and Fässler R. Impaired migration but not differentiation of haematopoietic stem cells in the absence of beta1 integrins. *Nature.* 1996; 380(6570): 171-175.

Hofmeister C. C., Zhang J., Knight K. L., Le P. and Stiff P. J. Ex vivo expansion of umbilical cord blood stem cells for transplantation: growing knowledge from the hematopoietic niche. *Bone Marrow Transplant.* 2007; 39(1): 11-23.

Hoggatt J., Singh P., Sampath J. and Pelus L. M. Prostaglandin E2 enhances hematopoietic stem cell homing, survival and proliferation. *Blood.* 2009; 113(22): 5444-5455.

Horejsí V. and Vlcek C. Novel structurally distinct family of leucocyte surface glycoproteins including CD9, CD37, CD53 and CD63. *FEBS Lett.* 1991; 288(1-2): 1-4.

Hsu H. C., Yang P., Wang J., Wu Q., Myers R., Chen J., Yi J., Guentert T., Tousson A., Stanus A. L., Le T. V., Lorenz R. G., Xu H., Kolls J. K., Carter R. H., Chaplin D. D., Williams R. W. and Mountz J. D. Interleukin 17-producing T helper cells and interleukin 17 orchestrate autoreactive germinal center development in autoimmune BXD2 mice. *Nat Immunol.* 2008; 9(2): 166-175.

Huang C. L., Liu D., Masuya D., Kameyama K., Nakashima T., Yokomise H., Ueno M. and Miyake M. MRP-1/CD9 gene transduction downregulates Wnt signal pathways. *Oncogene.* 2004; 23(45): 7475-7483.

Huang D. W., Sherman B. T. and Lempicki R. A. Systematic and integrative analysis of large gene lists using DAVID bioinformatics resources. *Nat Protoc.* 2009; 4(1): 44-57.

Ikeyama S., Koyama M., Yamaoko M., Sasada R. and Miyake M. Suppression of cell motility and metastasis by transfection with human motility-related protein (MRP-1/CD9) DNA. *J Exp Med.* 1993; 177(5): 1231-1237.

Imai K., Kobayashi M., Wang J., Ohiro Y., Hamada J., Cho Y., Imamura M., Musashi M., Kondo T., Hosokawa M. and Asaka M. Selective transendothelial migration of hematopoietic progenitor cells: a role in homing of progenitor cells. *Blood.* 1999; 93(1): 149-156.

Janowska-Wieczorek A., Marquez L. A., Dobrowsky A., Ratajczak M. Z. and Cabuhat M. L. Differential MMP and TIMP production by human marrow and peripheral blood $CD34^+$ cells in response to chemokines. *Exp Hematol.* 2000; 28(11): 1274-1285.

Jaroscak J., Goltry K., Smith A., Waters-Pick B., Martin P. L., Driscoll T. A., Howrey R., Chao N., Douville J., Burhop S., Fu P. and Kurtzberg J. Augmentation of umbilical cord blood (UCB) transplantation with ex vivo-expanded UCB cells: results of a phase 1 trial using the AastromReplicell System. *Blood.* 2003; 101(12): 5061-5067.

Katayama Y., Hidalgo A., Furie B. C., Vestweber D., Furie B. and Frenette P. S. PSGL-1 participates in E-selectin-mediated progenitor homing to bone marrow: evidence for cooperation between E-selectin ligands and alpha4 integrin. *Blood.* 2003; 102(6): 2060-2067.

Kawabata K., Ujikawa M., Egawa T., Kawamoto H., Tachibana K., Iizasa H., Katsura Y., Kishimoto T. and Nagasawa T. A cell-autonomous requirement for CXCR4 in long-term lymphoid and myeloid reconstitution. *PNAS.* 1999; 96(10): 5663-5667.

Kerre T. C., De Smet G., De Smedt M., Offner F., De Bosscher J., Plum J. and Vandekerckhove B. Both $CD34^{+}38^{+}$ and $CD34^{+}38^{-}$ cells home specifically to the bone marrow of NOD/LtSZ *scid/scid* mice but show different kinetics in expansion. *J Immunol.* 2001; 167(7): 3692-3698.

Kersey J. H., LeBien T. W., Abramson C. S., Newman R., Sutherland R. and Greaves M. P-24: a human leukemia-associated and lymphohemopoietic progenitor cell surface structure identified with monoclonal antibody. *J Exp Med.* 1981; 153(3): 726-731.

Kimura T., Boehmler A. M., Seitz G., Kuci S., Wiesner T., Brinkmann V., Kanz L. and Möhle R. The sphingosine 1-phosphate receptor agonist FTY720 supports CXCR4-dependent migration and bone marrow homing of human $CD34^{+}$ progenitor cells. *Blood.* 2004; 103(12): 4478-4486.

Köhler T., Plettig R., Wetzstein W., Schaffer B., Ordemann R., Nagels H. O., Ehninger G. and Bornhäuser M. Defining optimum conditions for the ex vivo expansion of human umbilical cord blood cells. Influences of progenitor enrichment, interference with feeder layers, early-acting cytokines and agitation of culture vessels. *Stem Cells.* 1999; 17(1): 19-24.

Kollet O., Peled A., Byk T., Ben-Hur H., Greiner D., Shultz L. and Lapidot T. beta2 microglobulin-deficient (B2m(null)) NOD/SCID mice are excellent recipients for studying human stem cell function. *Blood.* 2000; 95(10): 3102-3105.

Kollet O., Shivtiel S., Chen Y. Q., Suriawinata J., Thung S. N., Dabeva M. D., Kahn J., Spiegel A., Dar A., Samira S., Goichberg P., Kalinkovich A., Arenzana-Seisdedos F., Nagler A., Hardan I., Revel M., Shafritz D. A. and Lapidot T. HGF, SDF-1, and

MMP-9 are involved in stress-induced human CD34+ stem cell recruitment to the liver. *J Clin Invest.* 2003; 112(2): 160-169.

Kollet O., Spiegel A., Peled A., Petit I., Byk T., Hershkoviz R., Guetta E., Barkai G., Nagler A. and Lapidot T. Rapid and efficient homing of human $CD34^{+}CD38^{-/low}CXCR4^{+}$ stem and progenitor cells to the bone marrow and spleen of NOD/SCID and NOD/SCID/$B2m^{null}$ mice. *Blood.* 2001; 97(10): 3283-3291.

Komanduri K. V., St John L. S., de Lima M., McMannis J., Rosinski S., McNiece I., Bryan S. G., Kaur I., Martin S., Wieder E. D., Worth L., Cooper L. J., Petropoulos D., Molldrem J. J., Champlin R. E. and Shpall E. J. Delayed immune reconstitution after cord blood transplantation is characterized by impaired thymopoiesis and late memory T-cell skewing. *Blood.* 2007; 110(13): 4543-4551.

Kotha J., Longhurst C., Appling W. and Jennings L. K. Tetraspanin CD9 regulates beta 1 integrin activation and enhances cell motility to fibronectin via a PI-3 kinase-dependent pathway. *Exp Cell Res.* 2008; 314(8): 1811-1822.

Kovalenko O. V., Yang X. H. and Hemler M. E. A novel cysteine cross-linking method reveals a direct association between claudin-1 and tetraspanin CD9. *Mol Cell Proteomics.* 2007; 6(11): 1855-1867.

Lafleur M. A., Xu D. and Hemler M. E. Tetraspanin proteins regulate membrane type-1 matrix metalloproteinase-dependent pericellular proteolysis. *Mol Biol Cell.* 2009; 20(7): 2030-2040.

Lapidot T. and Kollet O. The essential roles of the chemokine SDF-1 and its receptor CXCR4 in human stem cell homing and repopulation of transplanted immune-deficient NOD/SCID and NOD/SCID/B2m(null) mice. *Leukemia.* 2002; 16(10): 1992-2003.

Lapidot T., Dar A. and Kollet O. How do stem cells find their way home? *Blood.* 2005; 106(6): 1901-1910.

Lapidot T., Pflumio F., Doedens M., Murdoch B., Williams D. E. and Dick J. E. Cytokine stimulation of multilineage hematopoiesis from immature human cells engrafted in SCID mice. *Science.* 1992; 255(5048): 1137-1141.

Laughlin M. J., Eapen M., Rubinstein P., Wagner J. E., Zhang M. J., Champlin R. E., Stevens C., Barker J. N., Gale R. P., Lazarus H. M., Marks D. I., van Rood J. J., Scaradavou A. and Horowitz M. M. Outcomes after transplantation of cord blood or bone marrow from unrelated donors in adults with leukemia. *N Engl J Med.* 2004; 351(22): 2265-2275.

Le Naour F., André M., Boucheix C. and Rubinstein E. Membrane microdomains and proteomics: lessons from tetraspanin microdomains and comparison with lipid rafts. *Proteomics.* 2006; 6(24): 6447-6454.

Le Naour F., Charrin S., Labas V., Le Caer J. P., Boucheix C. and Rubinstein E. Tetraspanins connect several types of Ig proteins: IgM is a novel component of the tetraspanin web on B-lymphoid cells. *Cancer Immunol Immunother.* 2004; 53(3): 148-152.

Lévesque J. P., Hendy J., Takamatsu Y., Simmons P. J. and Bendall L. J. Disruption of the CXCR4/CXCL12 chemotactic interaction during hematopoietic stem cell mobilization induced by GCSF or cyclophosphamide. *J Clin Invest.* 2003; 111(2): 187-196.

Li K., Chuen C. K., Lee S. M., Law P., Fok T. F., Ng P. C., Li C. K., Wong D., Merzouk A., Salari H., Gu G. J. and Yuen P. M. Small peptide analogue of SDF-1alpha supports survival of cord blood CD34+ cells in synergy with other cytokines and enhances their ex vivo expansion and engraftment into nonobese diabetic/severe combined immunodeficient mice. *Stem Cells.* 2006; 24(1): 55-64.

Little K. D., Hemler M. E. and Stipp C. S. Dynamic regulation of a GPCR-tetraspanin-G protein complex on intact cells: central role of CD81 in facilitating GPR56-Galpha q/11 association. *Mol Biol Cell.* 2004; 15(5): 2375-2387.

Loetscher P., Gong J. H., Dewald B., Baggiolini M., Clark-Lewis I. N-terminal peptides of stromal cell-derived factor-1 with CXC chemokine receptor 4 agonist and antagonist activities. J Biol Chem. 1998 Aug 28;273(35):22279-83.

Longo N., Yáñez-Mó M., Mittelbrunn M., de la Rosa G., Muñoz M. L., Sánchez-Madrid F. and Sánchez-Mateos P. Regulatory role of tetraspanin CD9 in tumor-endothelial cell interaction during transendothelial invasion of melanoma cells. *Blood.* 2001; 98(13): 3717-3726.

Ma Q., Jones D. and Springer T. A. The chemokine receptor CXCR4 is required for the retention of B lineage and granulocytic precursors within the bone marrow microenvironment. *Immunity.* 1999; 10(4): 463-471.

Ma Q., Jones D., Borghesani P. R., Segal R. A., Nagasawa T., Kishimoto T., Bronson R. T. and Springer T. A. Impaired B-lymphopoiesis, myelopoiesis, and derailed cerebellar neuron migration in CXCR4- and SDF-1-deficient mice. *PNAS.* 1998; 95(16): 9448-9453.

MacMillan M. L., Weisdorf D J., Brunstein C. G., Cao Q., DeFor T. E., Verneris M. R., Blazar B. R. and Wagner J. E. Acute graft-versus-host disease after unrelated donor umbilical cord blood transplantation: analysis of risk factors. *Blood.* 2009; 113(11): 2410-2415.

Maecker H. T., Todd S. C. and Levy S. The tetraspanin superfamily: molecular facilitators. *FASEB J.* 1997; 11(6): 428-442.

Majeti R., Park C. Y. and Weissman I. L. Identification of a hierarchy of multipotent hematopoietic progenitors in human cord blood. *Cell Stem Cell.* 2007; 1(6): 635-645.

Majka M., Janowska-Wieczorek A., Ratajczak J., Kowalska M. A., Vilaire G., Pan Z. K., Honczarenko M., Marquez L. A., Poncz M. and Ratajczak M. Z. Stromal-derived factor 1 and thrombopoietin regulate distinct aspects of human megakaryopoiesis. *Blood.* 2000; 96(13): 4142-4151.

Mantegazza A. R., Barrio M. M., Moutel S., Bover L., Weck M., Brossart P., Teillaud J. L. and Mordoh J. CD63 tetraspanin slows down cell migration and translocates to the endosomal-lysosomal-MIICs route after extracellular stimuli in human immature dendritic cells. *Blood.* 2004; 104(4): 1183-1190.

Martinez-Agosto J. A., Mikkola H. K., Hartenstein V. and Banerjee U. The hematopoietic stem cell and its niche: a comparative view. *Genes Dev.* 2007; 21(23): 3044-3060.

Masellis-Smith A. and Shaw A. R. CD9-regulated adhesion. Anti-CD9 monoclonal antibody induce pre-B cell adhesion to bone marrow fibroblasts through de novo recognition of fibronectin. *J Immunol.* 1994; 152(6): 2768-2777.

Matsuzaki Y., Kinjo K., Mulligan R. C. and Okano H. Unexpectedly efficient homing capacity of purified murine hematopoietic stem cells. *Immunity.* 2004; 20(1): 87-93.

McNiece I. K., Almeida-Porada G., Shpall E. J. and Zanjani E. Ex vivo expanded cord blood cells provide rapid engraftment in fetal sheep but lack long-term engrafting potential. *Exp Hematol.* 2002; 30(6): 612-616.

Merzouk A., Wong D., Salari H., Bian H., Fukuda S. and Pelus L. M. Rational design of chemokine SDF-1 analogs with agonist activity for the CXCR4 Receptor and the capacity to rapidly mobilize PMN and hematopoietic progenitor cells in mice. *Lett Drug Design Discov.* 2004; 1(2): 126-134.

Mhawech P., Herrmann F., Coassin M., Guillou L. and Iselin C. E. Motility-related protein 1 (MRP-1/CD9) expression in urothelial bladder carcinoma and its relation to tumor recurrence and progression. *Cancer.* 2003; 98(8): 1649-1657.

Miao W. M., Vasile E., Lane W. S. and Lawler J. CD36 associates with CD9 and integrins on human blood platelets. *Blood.* 2001; 97(6): 1689-1696.

Miyake M., Nakano K., Ieki Y., Adachi M., Huang C. L., Itoi S., Koh T. and Taki T. Motility related protein 1 (MRP-1/CD9) expression: inverse correlation with metastases in breast cancer. *Cancer Res.* 1995; 55(18): 4127-4131.

Möhle R., Moore M. A., Nachman R. L. and Rafii S. Transendothelial migration of CD34+ and mature hematopoietic cells: an in vitro study using a human bone marrow endothelial cell line. *Blood.* 1997; 89(1): 72-80.

Moratz C., Hayman J. R., Gu H. and Kehrl J. H. Abnormal B-cell responses to chemokines, disturbed plasma cell localization, and distorted immune tissue architecture in Rgs1-/- mice. *Mol Cell Biol.* 2004; 24(13): 5767-5775.

Mori M., Mimori K., Shiraishi T., Haraguchi M., Ueo H., Barnard G. F. and Akiyoshi T. Motility related protein 1 (MRP1/CD9) expression in colon cancer. *Clin Cancer Res.* 1998; 4(6): 1507-1510.

Nagasawa T., Hirota S., Tachibana K., Takakura N., Nishikawa S., Kitamura Y., Yoshida N., Kikutani H. and Kishimoto T. Defects of B-cell lymphopoiesis and

bone-marrow myelopoiesis in mice lacking the CXC chemokine PBSF/SDF-1. *Nature.* 1996; 382(6592): 635-638.

Nagasawa T., Kikutani H. and Kishimoto T. Molecular cloning and structure of a pre-B-cell growth-stimulating factor. *Proc Natl Acad Sci U S A.* 1994; 91(6): 2305-2309.

Nie S., Kee Y. and Bronner-Fraser M. Myosin-X is critical for migratory ability of Xenopus cranial neural crest cells. *Dev Biol.* 2009; 335(1): 132-142.

Nishida H., Yamazaki H., Yamada T., Iwata S., Dang N. H., Inukai T., Sugita K., Ikeda Y. and Morimoto C. CD9 correlates with cancer stem cell potentials in human B-acute lymphoblastic leukemia cells. *Biochem Biophys Res Commun.* 2009; 382(1): 57-62.

Ohmizono Y., Sakabe H., Kimura T., Tanimukai S., Matsumura T., Miyazaki H., Lyman S. D. and Sonoda Y. Thrombopoietin augments ex vivo expansion of human cord blood-derived hematopoietic progenitors in combination with stem cell factor and flt3 ligand. *Leukemia.* 1997; 11(4): 524-530.

Oritani K., Wu X., Medina K., Hudson J., Miyake K., Gimble J. M., Burstein S. A. and Kincade P. W. Antibody ligation of CD9 modifies production of myeloid cells in long-term cultures. *Blood.* 1996; 87(6): 2252-2261.

Orsini M. J., Parent J. L., Mundell S. J., Marchese A. and Benovic J. L. Trafficking of the HIV coreceptor CXCR4. Role of arrestins and identification of residues in the c-terminal tail that mediate receptor internalization. *J Biol Chem.* 1999; 274(43): 31076-31086.

Ovalle S., Gutiérrez-López M. D., Olmo N., Turnay J., Lizarbe M. A., Majano P., Molina-Jiménez F., López-Cabrera M., Yáñez-Mó M., Sánchez-Madrid F. and Cabañas C. The tetraspanin CD9 inhibits the proliferation and tumorigenicity of human colon carcinoma cells. *Int J Cancer.* 2007; 121(10): 2140-2152.

Page-McCaw A., Ewald A. J. and Werb Z. Matrix metalloproteinases and the regulation of tissue remodelling. *Nat Rev Mol Cell Biol.* 2007; 8(3): 221-233.

Papayannopoulou T., Priestley G. V., Nakamoto B., Zafiropoulos V. and Scott L. M.

Molecular pathways in bone marrow homing: dominant role of $\alpha_4\beta_1$ over β_2-integrins and selectins. *Blood.* 2001; 98(8): 2403-2411.

Park J. E., Lee D. H., Lee J. A., Park S. G., Kim N. S., Park B. C. and Cho S. Annexin A3 is a potential angiogenic mediator. Biochem Biophys Res Commun. 2005; 337(4): 1283-1287.

Peled A., Kollet O., Ponomaryov T., Petit I., Franitza S., Grabovsky V., Slav M. M., Nagler A., Lider O., Alon R., Zipori D. and Lapidot T. The chemokine SDF-1 activates the integrins LFA-1, VLA-4, and VLA-5 on immature human CD34(+) cells: role in transendothelial/stromal migration and engraftment of NOD/SCID mice. *Blood.* 2000; 95(11): 3289-3296.

Peled A., Petit I., Kollet O., Magid M., Ponomaryov T., Byk T., Nagler A., Ben-Hur H., Many A., Shultz L., Lider O., Alon R., Zipori D. and Lapidot T. Dependence of human stem cell engraftment and repopulation of NOD/SCID mice on CXCR4. *Science.* 1999; 283(5403): 845-848.

Peled T., Mandel J., Goudsmid R. N., Landor C., Hasson N., Harati D., Austin M., Hasson A., Fibach E., Shpall E. J. and Nagler A. Pre-clinical development of cord blood-derived progenitor cell graft expanded ex vivo with cytokines and the polyamine copper chelator tetraethylenepentamine. *Cytotherapy.* 2004; 6(4): 344-355.

Petit I., Goichberg P., Spiegel A., Peled A., Brodie C., Seger R., Nagler A., Alon R. and Lapidot T. Atypical PKC-ζ regulates SDF-1-mediated migration and development of human $CD34^+$ progenitor cells. *J Clin Invest.* 2005; 115(1): 168-176.

Pi X., Ren R., Kelley R., Zhang C., Moser M., Bohil A. B., Divito M., Cheney R. E. and Patterson C. Sequential roles for myosin-X in BMP6-dependent filopodial extension, migration, and activation of BMP receptors. *J Cell Biol.* 2007; 179(7): 1569-1582.

Qi J. C., Wang J., Mandadi S., Tanaka K., Roufogalis B. D., Madigan M. C., Lai K., Yan F., Chong B. H., Stevens R. L. and Krilis S. A. Human and mouse mast cells use the tetraspanin CD9 as an alternate interleukin-16 receptor. *Blood.* 2006; 107(1): 135-142.

Rey M., Valenzuela-Fernández A., Urzainqui A., Yáñez-Mó M., Pérez-Martínez M., Penela P., Mayor F. Jr. and Sánchez-Madrid F. Myosin IIA is involved in the endocytosis of CXCR4 induced by SDF-1alpha. *J Cell Sci.* 2007; 120(Pt 6): 1126-1133.

Rocha V. and Broxmeyer H. E. New approaches for improving engraftment after cord blood transplantation. *Biol Blood Marrow Transplant.* 2010; 16(1 Suppl): S126-132.

Rocha V., Cornish J., Sievers E. L., Filipovich A., Locatelli F., Peters C., Remberger M., Michel G., Arcese W., Dallorso S., Tiedemann K., Busca A., Chan K. W., Kato S., Ortega J., Vowels M., Zander A., Souillet G., Oakill A., Woolfrey A., Pay A. L., Green A., Garnier F., Ionescu I., Wernet P., Sirchia G., Rubinstein P., Chevret S. and Gluckman E. Comparison of outcomes of unrelated bone marrow and umbilical cord blood transplants in children with acute leukemia. *Blood.* 2001; 97(10): 2962-2971.

Rocha V., Gluckman E.; Eurocord-Netcord registry and European Blood and Marrow Transplant group. Improving outcomes of cord blood transplantation: HLA matching, cell dose and other graft- and transplantation-related factors. *Br J Haematol.* 2009; 147(2): 262-274.

Rocha V., Labopin M., Sanz G., Arcese W., Schwerdtfeger R., Bosi A., Jacobsen N., Ruutu T., de Lima M., Finke J., Frassoni F., Gluckman E.; Acute Leukemia Working Party of European Blood and Marrow Transplant Group; Eurocord-Netcord Registry. Transplants of umbilical-cord blood or bone marrow from unrelated donors in adults with acute leukemia. *N Engl J Med.* 2004; 351(22): 2276-2285.

Rocha V., Wagner J. E. Jr., Sobocinski K. A., Klein J. P., Zhang M. J., Horowitz M. M. and Gluckman E. Graft-versus-host disease in children who have received a cord-blood or bone marrow transplant from an HLA-identical sibling. Eurocord and International Bone Marrow Transplant Registry Working Committee on Alternative Donor and Stem Cell Sources. *N Engl J Med.* 2000; 342(25): 1846-1854.

Rofani C., Luchetti L., Testa G., Lasorella R., Isacchi G., Bottazzo G. F. and Berardi A. C. IL-16 can synergize with early acting cytokines to expand ex vivo CD34+ isolated from cord blood. *Stem Cells Dev.* 2009; 18(4): 671-682.

Ross E. M. and Wilkie T. M. GTPase-activating proteins for heterotrimeric G

proteins: regulators of G protein signaling (RGS) and RGS-like proteins. *Annu Rev Biochem.* 2000; 69: 795-827.

Rossi L., Manfredini R., Bertolini F., Ferrari D., Fogli M., Zini R., Salati S., Salvestrini V., Gulinelli S., Adinolfi E., Ferrara S., Di Virgilio F., Baccarani M. and Lemoli R. M. The extracellular nucleotide UTP is a potent inducer of hematopoietic stem cell migration. *Blood.* 2007; 109(2): 533-542.

Saavedra S., Jarque I., Sanz G. F., Moscardó F., Jiménez C., Martín G., Plumé G., Regadera A., Martínez J., De La Rubia J., Acosta B., Pemán J., Pérez-Bellés C., Gobernado M. and Sanz M. A. Infectious complications in patients undergoing unrelated donor bone marrow transplantation: experience from a single institution. *Clin Microbiol Infect.* 2002; 8(11): 725-733.

Sadir R., Imberty A., Baleux F. and Lortat-Jacob H. Heparan sulfate/heparin oligosaccharides protect stromal cell-derived factor-1 (SDF-1)/CXCL12 against proteolysis induced by CD26/dipeptidyl peptidase IV. *J Biol Chem.* 2004; 279(42): 43854-43860.

Saeed A. I., Sharov V., White J., Li J., Liang W., Bhagabati N., Braisted J., Klapa M., Currier T., Thiagarajan M., Sturn A., Snuffin M., Rezantsev A., Popov D., Ryltsov A., Kostukovich E., Borisovsky I., Liu Z., Vinsavich A., Trush V. and Quackenbush J. TM4: a free, open-source system for microarray data management and analysis. *Biotechniques.* 2003; 34(2): 374-378.

Sauer G., Windisch J., Kurzeder C., Heilmann V., Kreienberg R. and Deissler H. Progression of cervical carcinomas is associated with down-regulation of CD9 but strong local re-expression at sites of transendothelial invasion. *Clin Cancer Res.* 2003; 9(17): 6426-6431.

Shi G. X., Harrison K., Wilson G. L., Moratz C. and Kehrl J. H. RGS13 regulates germinal center B lymphocytes responsiveness to CXC chemokine ligand (CXCL)12 and CXCL13. *J Immunol.* 2002; 169(5): 2507-2515.

Shi W., Fan H., Shum L. and Derynck R. The tetraspanin CD9 associates with transmembrane TGF-alpha and regulates TGF-alpha-induced EGF receptor activation and cell proliferation. *J Cell Biol.* 2000; 148(3): 591-602.

Shpall E. J., Quinones R., Giller R., Zeng C., Baron A. E., Jones R. B., Bearman S. I., Nieto Y., Freed B., Madinger N., Hogan C. J., Slat-Vasquez V., Russell P., Blunk B., Schissel D., Hild E., Malcolm J., Ward W. and McNiece I. K. Transplantation of ex vivo expanded cord blood. *Biol Blood Marrow Transplant.* 2002; 8(7): 368-376.

Shultz L. D., Schweitzer P. A., Christianson S. W., Gott B., Schweitzer I. B., Tennent B., McKenna S., Mobraaten L., Rajan T. V., Greiner D. L. Multiple defects in innate and adaptive immunologic function in NOD/LtSz-scid mice. J Immunol. 1995 Jan 1;154(1):180-91.

Si Z. and Hersey P. Expression of the neuroglandular antigen and analogues in melanoma. CD9 expression appears inversely related to metastatic potential of melanoma. *Int J Cancer.* 1993; 54(1): 37-43.

Signoret N., Oldridge J., Pelchen-Matthews A., Klasse P. J., Tran T., Brass L. F., Rosenkilde M.M., Schwartz T.W., Holmes W., Dallas W., Luther M. A., Wells T. N., Hoxie J. A. and Marsh M. Phorbol esters and SDF-1 induce rapid endocytosis and down modulation of the chemokine receptor CXCR4. *J Cell Biol.* 1997; 139(3): 651-664.

Takeda Y., He P., Tachibana I., Zhou B., Miyado K., Kaneko H., Suzuki M., Minami S., Iwasaki T., Goya S., Kijima T., Kumagai T., Yoshida M., Osaki T., Komori T., Mekada E. and Kawase I. Double deficiency of tetraspanins CD9 and CD81 alters cell motility and protease production of macrophages and causes chronic obstructive pulmonary disease-like phenotype in mice. *J Biol Chem.* 2008; 283(38): 26089-26097.

Tarrant J. M., Robb L., van Spriel A. B. and Wright M. D. Tetraspanins: molecular organisers of the leukocyte surface. *Trends Immunol.* 2003; 24(11): 610-617.

Teixidó J., Hemler M. E., Greenberger J. S. and Anklesaria P. Role of beta 1 and beta 2 integrins in the adhesion of human CD34hi stem cells to bone marrow stroma. *J Clin Invest.* 1992; 90(2): 358-367.

Tse W., Bunting K. D. and Laughlin M. J. New insights into cord blood stem cell transplantation. *Curr Opin Hematol.* 2008; 15(4): 279-284.

Tudan C., Willick G. E., Chahal S., Arab L., Law P., Salari H. and Merzouk A.

C-terminal cyclization of an SDF-1 small peptide analogue dramatically increases receptor affinity and activation of the CXCR4 receptor. *J Med Chem.* 2002; 45(10): 2024-2031.

Vagima Y., Avigdor A., Goichberg P., Shivtiel S., Tesio M., Kalinkovich A., Golan K., Dar A., Kollet O., Petit I., Perl O., Rosenthal E., Resnick I., Hardan I., Gellman Y. N., Naor D., Nagler A. and Lapidot T. MT1-MMP and RECK are involved in human CD34+ progenitor cell retention, egress, and mobilization. *J Clin Invest.* 2009; 119(3): 492-503.

van der Loo J. C. and Ploemacher R. E. Marrow- and spleen-seeding efficiencies of all murine hematopoietic stem cell subsets are decreased by preincubation with hematopoietic growth factors. *Blood.* 1995; 85(9): 2598-2606.

Verfaillie C. M. Adhesion receptors as regulators of the hematopoietic process. *Blood.* 1998; 92(8): 2609-2612.

Vermeulen M., Le Pesteur F., Gagnerault M. C., Mary J. Y., Sainteny F. and Lepault F. Role of adhesion molecules in the homing and mobilization of murine hematopoietic stem and progenitor cells. *Blood.* 1998; 92(3): 894-900.

Verneris M. R., Brunstein C. G., Barker J., MacMillan M. L., DeFor T., McKenna D. H., Burke M. J., Blazar B. R., Miller J. S., McGlave P. B., Weisdorf D. J. and Wagner J. E. Relapse risk after umbilical cord blood transplantation: enhanced graft-versus-leukemia effect in recipients of 2 units. *Blood.* 2009; 114(19): 4293-4299.

Voermans C., Anthony E. C., Mul E., van der Schoot E. and Hordijk P. SDF-1-induced actin polymerization and migration in human hematopoietic progenitor cells. *Exp Hematol.* 2001a; 29(12): 1456-1464.

Voermans C., Kooi M. L., Rodenhuis S., van der Lelie H., van der Schoot C. E. and Gerritsen W. R. In vitro migratory capacity of CD34+ cells is related to hematopoietic recovery after autologous stem cell transplantation. *Blood.* 2001b; 97(3): 799-804.

Wang J. C., Bégin L. R., Bérubé N. G., Chevalier S., Aprikian A. G., Gourdeau H. and Chevrette M. Down-regulation of CD9 expression during prostate carcinoma

progression is associated with CD9 mRNA modifications. *Clin Cancer Res.* 2007; 13(8): 2354-2361.

Wang J. F., Park I. W. and Groopman J. E. Stromal cell-derived factor-1α stimulates tyrosine phosphorylation of multiple focal adhesion proteins and induces migration of hematopoietic progenitor cells: roles of phosphoinositide-3 kinase and protein kinase C. *Blood.* 2000; 95(8): 2505-2513.

Watson N., Linder M. E., Druey K. M., Kehrl J. H. and Blumer K. J. RGS family members: GTPase-activating proteins for heterotrimeric G-protein alpha-subunits. *Nature.* 1996; 383(6596): 172-175.

Willis N. D., Cox T. R., Rahman-Casañs S. F., Smits K., Przyborski S. A., van den Brandt P., van Engeland M., Weijenberg M., Wilson R. G., de Bruïne A. and Hutchison C. J. Lamin A/C is a risk biomarker in colorectal cancer. *PLoS One.* 2008; 3(8): e2988.

Wright D. E., Bowman E. P., Wagers A. J., Butcher E. C. and Weissman I. L. Hematopoietic stem cells are uniquely selective in their migratory response to chemokines. *J Exp Med.* 2002; 195(9): 1145-1154.

Wu D., Huang C. K. and Jiang H. Roles of phospholipid signaling in chemoattractant-induced responses. *J Cell Sci.* 2000; 113(17): 2935-2940.

Xia L., McDaniel J. M., Yago T., Doeden A. and McEver R. P. Surface fucosylation of human cord blood cells augments binding to P-selectin and E-selectin and enhances engraftment in bone marrow. *Blood.* 2004; 104(10): 3091-3096.

Yañez-Mó M., Barreiro O., Gonzalo P., Batista A., Megías D., Genís L., Sachs N., Sala-Valdés M., Alonso M. A., Montoya M. C., Sonnenberg A., Arroyo A. G. and Sánchez-Madrid F. MT1-MMP collagenolytic activity is regulated through association with tetraspanin CD151 in primary endothelial cells. *Blood.* 2008; 112(8): 3217-3226.

Yáñez-Mó M., Barreiro O., Gordon-Alonso M., Sala-Valdés M. and Sánchez-Madrid F. Tetraspanin-enriched microdomains: a functional unit in cell plasma membranes. *Trends Cell Biol.* 2009; 19(9): 434-446.

Yowe D., Weich N., Prabhudas M., Poisson L., Errada P., Kapeller R., Yu K., Faron L., Shen M., Cleary J., Wilkie T. M., Gutierrez-Ramos C. and Hodge M. R. RGS18 is a myeloerythroid lineage-specific regulator of G-protein-signalling molecule highly expressed in megakaryocytes. *Biochem J.* 2001; 359(Pt 1): 109-118.

Zhang C. C., Kaba M., Ge G., Xie K., Tong W., Hug C. and Lodish H. F. Angiopoietin-like proteins stimulate ex vivo expansion of hematopoietic stem cells. *Nat Med.* 2006; 12(2): 240-245.

Zhang X. F., Wang J. F., Matczak E., Proper J. A. and Groopman J. E. Janus kinase 2 is involved in stromal cell-derived factor-1alpha-induced tyrosine phosphorylation of focal adhesion proteins and migration of hematopoietic progenitor cells. *Blood.* 2001; 97(11): 3342-3348.

Zhong R., Law P., Wong D., Merzouk A., Salari H. and Ball E. D. Small peptide analogs to stromal derived factor-1 enhance chemotactic migration of human and mouse hematopoietic cells. *Exp Hematol.* 2004; 32(5): 470-475.

Zilber M. T., Setterblad N., Vasselon T., Doliger C., Charron D., Mooney N. and Gelin C. MHC class II/CD38/CD9: a lipid-raft-dependent signaling complex in human monocytes. *Blood.* 2005; 106(9): 3074-3081.

Zöller M. Tetraspanins: push and pull in suppressing and promoting metastasis. *Nat Rev Cancer.* 2009; 9(1): 40-55.

Zou Y. R., Kottmann A. H., Kuroda M., Taniuchi I. and Littman D. R. Function of the chemokine receptor CXCR4 in haematopoiesis and in cerebellar development. *Nature.* 1998; 393(6685): 595-599.